UNIVERSIDADE NOVA DE LISBOA
Faculdade de Ciências e Tecnologia
Departamento de Engenharia Civil

# Adaptive glass pane using shape-memory alloys

Por
**Mariana Portocarrero Pegado Lemos de Mendonça Oom de Sacadura**
Licenciada em Ciências da Engenharia

Dissertação para obtenção do grau de
Mestre em Engenharia Civil - Perfil Estruturas

| | |
|---|---|
| Orientador: | Doutor Filipe Pimentel Amarante dos Santos |
| Co-orientador: | Doutora Chiara Bedon |

**Júri**

| | |
|---|---|
| Presidente: | Doutor Corneliu Cismasiu |
| Vogais: | Doutor José Nuno Varandas |
| | Doutor Filipe Pimentel Amarante dos Santos |

**October 2015**

FACULDADE DE CIÊNCIAS E TECNOLOGIA
UNIVERSIDADE NOVA DE LISBOA

"Copyright" Mariana Portocarrero Pegado Lemos de Mendonça Oom de Sacadura, FCT/UNL e UNL

A Faculdade de Ciências e Tecnologia e a Universidade Nova de Lisboa têm o direito, perpétuo e sem limites geográficos, de arquivar e publicar esta dissertação através de exemplares impressos reproduzidos em papel ou de forma digital, ou por qualquer outro meio conhecido ou que venha a ser inventado, e de a divulgar através de repositórios científicos e de admitir a sua cópia e distribuição com objetivos educacionais ou de investigação, não comerciais, desde que seja dado crédito ao autor e editor.

# Acknowledgments

I would like to express my deepest acknowledgment to many people without whom I would not have been able to reach this important mark in my life.

First of all, to Professor Filipe Amarante dos Santos, not only for the opportunity and support, but also for all the wise guidance and advice. For introducing me to the themes present in this dissertation, for all the vital scientific orientation and for always have welcomed me with natural friendliness and sympathy. I also have to mention his tireless effort to help with the prototype construction and testing.

To Professor Chiara Bedon of Università degli Studi di Trieste, for introducing me to ABAQUS software and for all the incalculable precious help on clarifying all the doubts and questions that kept on emerging. For the scientific elucidations and also for the sincere warm welcoming in Trieste, it was a privilege. Also from Università degli Studi di Trieste I acknowledge Professor Claudio Amadio for the wise suggestions.

To all my friends, for the joy that always supported me with.

To my family, who made me who I am, my eternal deepest heartfelt gratefulness.

# Abstract

Glass is one of the most commonly used building materials in modern architecture around the world. Its ability to pass through natural light enabled the builders paradigm of a desire for a exterior environment connected space, but yet comfortable and protected.

New techniques and recent developments in fabrication processes made possible to use glass as a structural material.

Structural glass propelled construction in glass, turning it into the most distinctive material of modern architecture. Because of the glass design complexity, glass as a construction material, however, still represents a challenge for structural design engineers.

Glass is often associated to smart systems and active control researches, evolving shape-memory alloys or pre-stressed cables.

This dissertation's aim is to contribute to the development of a shape-memory alloys smart system, associated with a glass pane, in order to mitigate the wind action effects on the structure. The hazardous effect of the temperature on the interlayer of the laminated glass is also considered. The control action is imposed by an external system that causes an external force on the structure, enabling the system structural response to be improved.

**Keywords:**

Glass pane; Active control; Shape memory alloys; Wind action; Structural smart systems

# Resumo

**Painel de vidro adaptativo, usando ligas de memória de forma**

O vidro é um dos materiais de construção mais utilizados na arquitectura moderna por todo o Mundo. A sua característica de permitir o atravessamento de luz natural permite o equilíbrio entre a construção de espaços em contacto privilegiado com o ambiente exterior, propiciando ao mesmo tempo condições de protecção e conforto.

Recentes desenvolvimentos nos processos de fabrico e acabamento do vidro permitem que o mesmo possa desempenhar funções estruturais.

O aparecimento do vidro estrutural veio impulsionar a construção em vidro, sendo este o elemento mais marcante da arquitectura moderna. O vidro como elemento de construção representa ainda um importante desafio para os engenheiros projetistas, pela dificuldade de dimensionamento.

O vidro está muitas vezes associado a pesquisas relativas a sistemas inteligentes de controlo de ações externas, como cabos de ligas de memória de forma ou cabos de pré-esforço ativo.

A presente dissertação visa contribuir para o desenvolvimento de um sistema inteligente, composto por cabos de memória de forma associados a um painel de vidro, com o objectivo de mitigar as deformações impostas pela ação do vento na estrutura. O efeito da temperatura na degradação do material que constitui a interlayer do vidro laminado é também tida em consideração. A ação de controlo será imposta por um sistema externo que implementa uma força exterior na estrutura, permitindo uma optimização da resposta do sistema estrutural do painel.

**Palavras chave:**

Painel de vidro; Controlo ativo; Ligas de memória de forma; Ação do vento; Sistemas estruturais inteligentes

# Contents

**Contents** **ix**

**List of Figures** **xiii**

**List of Tables** **xvii**

**List of symbols and abbreviations** **xix**

**1 Introduction** **1**
1.1 Problem description . . . 1
1.1.1 Introduction . . . 1
1.2 Objectives and Scope . . . 2
1.3 Dissertation Outline . . . 4

**2 State of the art** **5**
2.1 Introduction . . . 5
2.2 Glass . . . 5
2.2.1 Use of glass through time . . . 5
2.2.2 Glass types . . . 6
2.2.2.1 Float glass . . . 6
2.2.2.2 Tempered glass . . . 7
2.2.2.3 Laminated glass . . . 8
2.2.2.4 Glass units . . . 9
2.2.3 Structure supporting system . . . 9
2.3 Shape-Memory Alloys . . . 10
2.3.1 Shape-memory alloys, a smart material . . . 10
2.3.2 Shape-memory effect and superelasticity . . . 10
2.4 Control in civil engineering structures . . . 12
2.4.1 Passive control systems . . . 12
2.4.2 Active control systems . . . 13
2.4.3 Semi-active control systems . . . 14

2.4.4 Hybrid control system . . . 14

**3 Glass pane structural behavior characterization 15**
3.1 Introduction . . . 15
3.2 The Enhanced Effective Thickness method . . . 15
3.2.1 Introduction . . . 15
3.2.2 The method . . . 17
3.3 Structural behavior characterization . . . 19
3.3.1 Introduction . . . 19
3.3.2 The cable system configuration . . . 19
3.3.3 Monolithic behavior . . . 19
3.3.3.1 Longitudinal position of the deviators . . . 19
3.3.3.2 Transversal position of the deviators . . . 22
3.3.3.3 Deviators moving along y axis, from system 2 . . . 26
3.3.3.4 Conclusion and comments . . . 29
3.3.4 Time, temperature and load duration effect on glass behavior . . . 29
3.3.4.1 System0 . . . 30
3.3.4.2 System2 . . . 32
3.3.4.3 Conclusion and comments . . . 33
3.4 ABAQUS solid model . . . 34
3.4.1 Monolithic behavior . . . 34
3.4.2 Intermediate behavior . . . 35
3.4.3 Layered 1 behavior . . . 37
3.4.4 Layered 2 behavior . . . 39
3.4.5 Comments on the results obtained . . . 41
3.4.6 Analysis of the tension within the thickness and the influence of PVB shear modulus . . . 41
3.5 Comparison between shell model with EET and solid model . . . 44

**4 Numerical implementation of an adaptive glass pane 45**
4.1 Introduction . . . 45
4.2 System's response . . . 45
4.2.1 Dynamic behavior of the glass pane . . . 45
4.2.2 Motion equation solution . . . 47
4.2.3 Characterization of the wind action . . . 48

**5 Control system implementation 51**
5.1 Introduction . . . 51
5.2 Control type . . . 51
5.2.1 Proportional control . . . 51
5.2.2 Integral control . . . 52
5.2.3 Derivative control . . . 53
5.2.4 PID control . . . 54
5.3 Algorithm to implement the control system . . . 55
5.4 Tuning of the controller . . . 55
5.5 Results . . . 56

**6 Prototype analysis 59**

6.1 Introduction . . . 59
6.2 Building and testing of the experimental prototype . . . 59
6.2.1 Prototype . . . 59
6.2.2 Static load test . . . 63
6.2.3 Dynamic suction load . . . 64
6.3 The Labview control platform . . . 66

**7 Summary, conclusions and future work** **71**
7.1 Summary and conclusions . . . 71
7.2 Future work . . . 71

**Bibliography** **73**

**A** **77**
A.1 Comparison between system0A and system2A . . . 77

**B** **81**

**C** **85**
C.1 Proportional control . . . 85
C.2 Proportional and integrative control . . . 85
C.3 Proportional, integrative and derivative control . . . 86

# List of Figures


1.1 Vittorio Emanuele galleries, Milan . . . 1
1.2 Modern glass facade, Centro de Congressos do Estoril . . . 2
1.3 Reinhold Messner Castle . . . 3
1.4 Detail of Reinhold Messner Castle's roof . . . 3

2.1 Crystal Palace, Madrid . . . 6
2.2 Float glass production process [15] . . . 7
2.3 Tempered glass production process - Adapted from [15] . . . 7
2.4 Tempered glass - Adapted from [15] . . . 8
2.5 Fracture patterns A:float glass; B:tempered glass [14] . . . 9
2.6 Examples of glass units [15] . . . 9
2.7 Stress-free martensitic transformation - Adapted from [28] . . . 11
2.8 Stress-free martensitic transformation - Adapted from [30] . . . 11
2.9 Stress-induced martensitic transformation at a - Adapted from [28] . . . 12
2.10 Feedforward control - adapted from [23] . . . 14
2.11 Feedback control - adapted from [23] . . . 14

3.1 Deflection at the central point at different temperatures - Adapted from [11] . . . 16
3.2 Glass pane dimensions . . . 18
3.3 $\psi$ values for a simply supported pane subjected to distributed load . . . 18
3.4 Initial system - System 0 . . . 20
3.5 Systems 1 to 6 . . . 20
3.6 Displacements' diagram on the different systems . . . 21
3.7 $\sigma_{11}$ and $\sigma_{22}$ on the different systems . . . 22
3.8 Systems 0 to C . . . 23
3.9 Systems 0 to C with cables connecting the deviators . . . 23
3.10 Displacements on systems 0 to C, with and without cables . . . 24
3.11 $\sigma_{11}[MPa]$ on the systems 0, A, B and C with and without cables . . . 25
3.12 $\sigma_{22}[MPa]$ on the systems 0, A, B and C with and without cables . . . 26
3.13 Displacements on the systems 0, A, B and C with and without cables . . . 27
3.14 $\sigma_{11}$ on the systems 0, A, B and C with and without cables . . . 28

3.15 $\sigma_{22}$ on the systems 0, A, B and C with and without cables . . . . . 29
3.16 Displacements [mm] . . . . . 30
3.17 $\sigma_{11}$ [MPa] . . . . . 31
3.18 $\sigma_{22}$ [MPa] . . . . . 31
3.19 Displacements [mm] . . . . . 32
3.20 $\sigma_{11}$ [MPa] . . . . . 33
3.21 $\sigma_{22}$ [MPa] . . . . . 33
3.22 Displacements [mm] . . . . . 34
3.23 $\sigma_{11}$ [MPa] . . . . . 35
3.24 $\sigma_{33}$ [MPa] . . . . . 35
3.25 Displacements [mm] . . . . . 36
3.26 $\sigma_{11}$ [MPa] . . . . . 36
3.27 $\sigma_{33}$ [MPa] . . . . . 37
3.28 Displacements [mm] . . . . . 38
3.29 $\sigma_{11}$ [MPa] . . . . . 38
3.30 $\sigma_{33}$ [MPa] . . . . . 39
3.31 Displacements [mm] . . . . . 40
3.32 $\sigma_{11}$ [MPa] . . . . . 40
3.33 $\sigma_{33}$ [MPa] . . . . . 41
3.34 Monolithic behavior - $\sigma_{33}$ within the thickness [MPa] . . . . . 42
3.35 Intermediate behavior - $\sigma_{33}$ within the thickness [MPa] . . . . . 42
3.36 Layered 1 behavior - $\sigma_{33}$ within the thickness [MPa] . . . . . 43
3.37 Layered 2 behavior - $\sigma_{33}$ within the thickness [MPa] . . . . . 43

4.1 Final mesh associated to the 1/4 of the pane . . . . . 46
4.2 FE model of the simplified system . . . . . 46
4.3 Wind pressure [kPa] . . . . . 49

5.1 Control system . . . . . 51
5.2 Proportional control - Adapted from [23] . . . . . 52
5.3 Integral control - Adapted from [23] . . . . . 53
5.4 Proportional and derivative control - Adapted from [23] . . . . . 54
5.5 Proportional, integrative and derivative control - Adapted from [23] . . . . . 54
5.6 Displacements-time history for monolithic behavior . . . . . 56
5.7 Displacements-time history for layered behavior . . . . . 57

6.1 Model's dimension . . . . . 60
6.2 Prototype construction . . . . . 60
6.3 Working principle of the experimental prototype . . . . . 61
6.4 Prototype final . . . . . 61
6.5 Detail of the prototype - Electric current feeding cables . . . . . 62
6.6 Main features of the experimental prototype . . . . . 63
6.7 Static load displacements map obtained with SAP2000 . . . . . 64
6.8 Pressure time-history . . . . . 65
6.9 Displacement time-history . . . . . 65
6.10 Cables' temperature time-history . . . . . 66
6.11 Graphical programming syntax . . . . . 67
6.12 Control action block diagram . . . . . 68

6.13 Software framework . . . . . 69
6.14 System's components overview . . . . . 69

A.1 Displacements on the systems 0 and 2 . . . . . 77
A.2 $\sigma_{11}$ on the systems 0 and 2 . . . . . 78
A.3 $\sigma_{22}$ on the systems 0 and 2 . . . . . 79

C.1 Graphic of the displacements on the center of the glass pane, action of proportional control . . . . . 85
C.2 Graphic of the displacements on the center of the glass pane, action of proportional and integral control . . . . . 86
C.3 Graphic of the displacements on the center of the glass pane, action of proportional, integral and derivative control . . . . . 86

# List of Tables


3.1 Effective thickness [mm] in terms of displacements and stresses to four distinct situations . . . 19
3.2 Distance between deviators in each system [mm] . . . 21
3.3 Distance between deviators in each system [mm] . . . 23
3.4 PVB's properties for the monolithic behavior . . . 34
3.5 PVB's properties for the intermediate behavior . . . 35
3.6 PVB's properties for the layered 1 behavior . . . 37
3.7 PVB's properties for the layered 2 behavior . . . 39
3.8 Displacements on the central point [mm] . . . 41
3.9 Comparison between the stresses obtained with Abaqus and with SAP2000 . . . 44

4.1 A,B,C,D,A',B',C' and D' parameters [7] . . . 48

5.1 $K_p$, $T_i$ and $T_d$ values . . . 56

6.1 Central point displacements comparison . . . 64

# List of symbols and abbreviations

**Abbreviations**

| | |
|---|---|
| DOF | Degree Of Freedom |
| EET | Enhaced Efective Thickness |
| PVB | Polyvinyl Butyral |
| SMA | Shape-Memory Alloys |
| TLD | Tuned Liquid Damper |
| TMD | Tuned Mass Damper |
| UNL | Universidade Nova de Lisboa |

**Symbols**

| | |
|---|---|
| $D$ | dynamic matrix |
| $D_{abs}$ | Bending stiffness relative to layered limit |
| $D_{full}$ | Bending stiffness relative to monolothic limit |
| $E$ | glass' Young module |
| $F$ | flexibility matrix |
| $G_{int}$ | shear module of the interlayer |
| $h_{int}$ | thickness of the interlayer |
| $h_1$ | thickness of the glass pane 1 |
| $h_2$ | thickness of the glass pane 2 |
| $K_{cr}$ | critical gain |
| $K_d$ | derivative gain |
| $K_i$ | integrative gain |
| $K_p$ | proportional gain |
| $M$ | mass matrix |
| $P_{cr}$ | critical period |

### Greek characters

$\nu$ glass' Poisson's ratio

$\omega$ frequency

$\omega_D$ damped frequency

$\phi$ vibration mode

# Chapter 1

# Introduction

## 1.1 Problem description

### 1.1.1 Introduction

Glass has always been a material that impassioned and impressed mankind. As one of the oldest materials ever produced by man, initially was used mainly to create simple artifacts of decoration. Over time, to take advantage of its transparency to the visible light, glass started being used in windows as a way to enlighten the interior. In Figure 1.1 are represented Vitttorio Emanuele galleries in Milan, built between 1865 and 1877, a clear example of the early days of glass in architecture.

Figure 1.1: Vittorio Emanuele galleries, Milan

Transparency and translucency are not the only advantages of glass as a construction material. Glass also provides a wide and clean environment being highly sought after by architects. Recent developments in production techniques made it possible to develop different

types of glass, with distinct appearance and improved structural behavior. The improved aesthetic effects are also a significant benefit, such as the changeable state of transparency and light reflection from translucent to mirror.

Figure 1.2: Modern glass facade, Centro de Congressos do Estoril

In contemporary architecture, glass plays an essential role, not only being present in all modern architectural icons but essentially shaping their appearance. The importance of glass in modern architecture is clearly obvious in modern cities. In Figure 1.2 is illustrated a modern glass facade.

Despite all the technological advances regarding production, the structural use of glass is still a challenge to engineers these days, because of the complexity of its design. Glass's brittle behavior makes more difficult to predict and foresee its performance along time. From one of the oldest materials made by man, to one of the most modern materials in contemporary architecture these days, how far goes the comprehension of glass as a building material and engineers design development? How much more will we be able to improve glass design? Several studies were conducted in the recent years, in an effort to answer these questions and improve glass structures behavior.

## 1.2 Objectives and Scope

The bottom line of this work is based on a scientific research of an italian article: *"Analisi strutturale di grandi lastre in vetro stratificato rinforzate con cavi in acciaio"* by Maurizio Froli and Leonardo Lani [12]. In this work, the authors propose to study the structural behavior of large size glass plates under flat bending, stiffened by a steel cable system. These glass panes were used in the reconstruction of the Reinhold Messners' castle. Figures 1.3 and 1.4 shows the aforementioned glass panes on the roof of the castle.

Figure 1.3: Reinhold Messner Castle

Figure 1.4: Detail of Reinhold Messner Castle's roof

Factors such as temperature and the load duration were discussed, as they directly affect the laminated glass behavior. These factors were considered by determining their influence on the interlayer's ability to transfer shear load.

This dissertation proposes to analyze the same glass pane presented by the authors on the

aforementioned scientific article, under the same load conditions but integrated in a smart structure. The latter is composed by a shape-memory alloy cable system with active control, in order to mitigate the wind action deformation on the glass.

The following objectives are prospected:

- Analysis of the temperature influence on the thermoplastic interlayer of laminated glass;
- Analysis of the wind action on a glass pane;
- Mitigation of the aforementioned action with an active control system.

## 1.3 Dissertation Outline

This dissertation is divided in **7 chapters**.

In the **first chapter**, the current, the problem description is presented, as well as the objectives and scope of this work.

In the **second chapter**, a brief overview of the use of glass through times is made, as well as an introduction to shape memory alloys and control systems.

In the **third chapter** is described the Enhanced Effective Thickness method, used in this work, the study of the glass pane structural behavior and the cable configuration set.

In the **fourth chapter** a case study is presented and analyzed, the results presented and commented.

In the **fifth chapter** the active control system is implemented on the case study previously presented.

In the **sixth chapter** is described the building and testing of a prototype

Finally in the **seventh chapter** the conclusions and future work are presented.

# Chapter 2

# State of the art

## 2.1 Introduction

This dissertations theme involves three distinct topics:

- Glass
- Shape-memory alloys
- Control

To better understand the dissertation outline, before presenting the work held, a brief introduction to each topic is made in this chapter.

## 2.2 Glass

### 2.2.1 Use of glass through time

As mentioned in section 1, glass is one of the oldest materials ever made by man. Initially, glass was only used for manufacturing decoration artifacts. Over time, as construction techniques were developing, glass as a construction material emerged, and increased until these days. Glass is able to respond to man's crescent necessity of creating inside the buildings a bright and exterior connected environment, but yet safe and where he feels protected. As a very versatile material, it can easily adapt these needs and still play a crucial role in aesthetics and in modern architecture.

The construction with glass had two major prime periods where its expansion was especially high:

- During the nineteenth century with the construction of many greenhouses composed by a metallic bearing system, where the glass panes were incorporated. An example of this type of glass construction is the Crystal Palace in Madrid, represented in the figure 5.2;

Figure 2.1: Crystal Palace, Madrid

- Twentieth century, with the constant advances in process techniques that made it possible to use glass as a structural element.

### 2.2.2 Glass types

Advances in process techniques made it possible to develop several types of glasses with distinct applications. In this subsection is made a brief introduction to the most relevant types of glass.

#### 2.2.2.1 Float glass

Developments in glass production processes and processing methods made possible to develop many types of glass products. Currently the *float* production process is the most common method used worldwide. This technique advantages are its low cost, its wide availability, the superior optical quality of the glass and the large size of panes that can be reliably produced [15].

The float glass production process is schematized in figure 2.2.

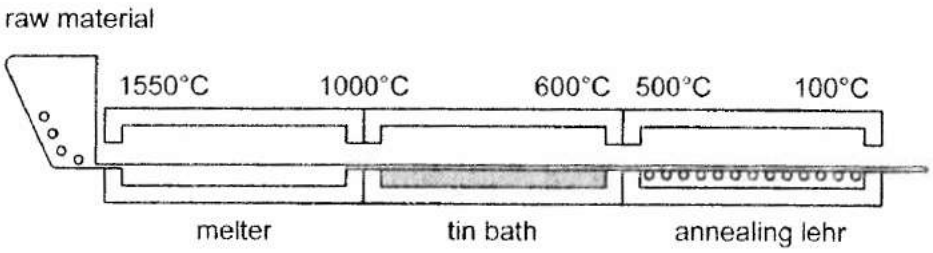


Figure 2.2: Float glass production process [15]

The float glass production process is described below: The raw materials are melted at temperatures of up to $1550^oC$. The molten glass is then poured continuously at approximately $1000^oC$ on to a shallow pool of molten tin in an atmosphere of hydrogen and nitrogen to prevent oxidation. Tin in its liquid physical state has a large temperature range ($232 - 2270^oC$), because of this and also because of its high specific weight, the glass floats on the tin and spreads outwards, forming a smooth flat surface at an equilibrium thickness of 6 to $7mm$. This surface is then gradually cooled and drawn on to rollers, and after enters a long oven at temperatures around $600^oC$. Depending on the speed of the rollers the glass thickness can be controlled within a range of 2 to $25mm$, corresponding the biggest thickness to the slowest speed and vice versa. To prevent residual stresses being induced within the glass, the annealing lehr slowly cools the glass. After the lehr the glass is ready to be cut and stored. Broken or defective pieces are sent back into the furnace and recycled. At some float plants, so called on-line coatings (hard coatings) can be applied to the hot glass surface during manufacture. As a consequence of this manufacture process, the two faces of glass sheets are not completely identical [15].

#### 2.2.2.2 Tempered glass

Tempered glass is a glass subjected to a heat treatment called tempering. This type of glass is the most important in structural applications. The tempering process is illustrated in the figure 2.3.

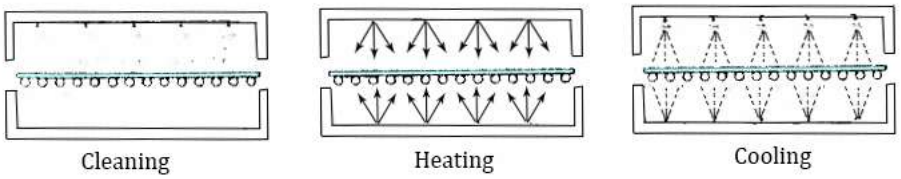


Figure 2.3: Tempered glass production process - Adapted from [15]

The treatment consists on the heating of the glass, followed by a fast cooling, provided by a cool air stream. These actions create compressive stresses on the surfaces of the glass sheet and a residual stress field in the core of the glass. This self-balanced internal tension state has a parabolic distribution within the thickness, as can be observed in figure 2.4. In the core of the glass pane, a tensile stress field is generated. This core's thickness corresponds

to approximately 60% of the glass total thickness. In the remaining 40% of the thickness, 20% on each surface, a compressive stress field is created, preventing flaws from opening on the glass surface. This state of stress enhances the glass behavior when subjected to a load action, minimizing the tensile stress on the surfaces, as schematized on the figure 2.4.

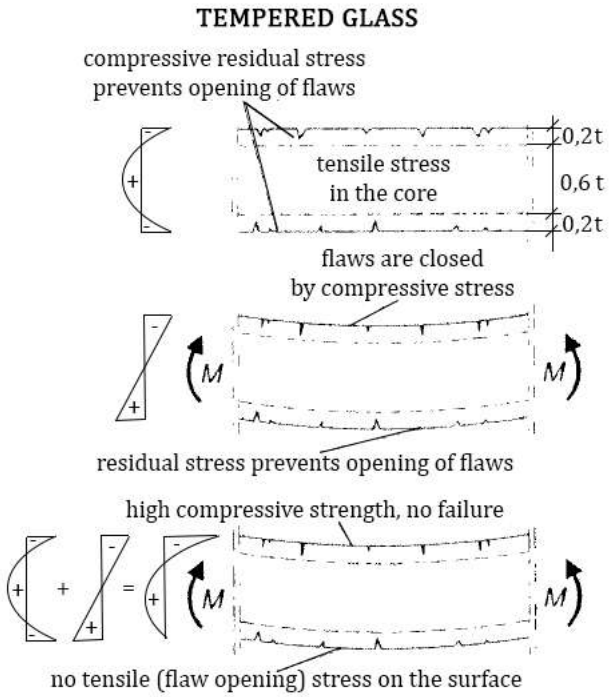


Figure 2.4: Tempered glass - Adapted from [15]

Tempering also enhances glass' behavior in what concerns to the fracture pattern. As the latter is a function of the energy stored in the glass, and tempered glass stores more energy than float glass, the fractures in tempered glass are smaller pieces, preventing large piece of glass to be projected. For this reason, tempered glass is also designed safety glass. The fracture patterns are illustrated on the figure 2.5.

#### 2.2.2.3 Laminated glass

To overcome glass' brittle behavior, laminated glass was created. It consists of two or more glass sheets, bonded together by an intermediate layer of a plastic transparent material. The combinations are infinite, as the glass panes can have different thickness or heat treatments. The interlayer is placed between the glass panes, then the whole set is compressed and heated, in order to expel the air between and merge the components. The most common material used as interlayer is polyvinyl butyral, PVB.

The presence of the interlayer enhances glass behavior in case of fracture, as it ensures the glass fragments to remain stuck after breakage. For this reason, safety tempered glass is always laminated, and it is often used in cases where accidents that compromise human lives can occur.

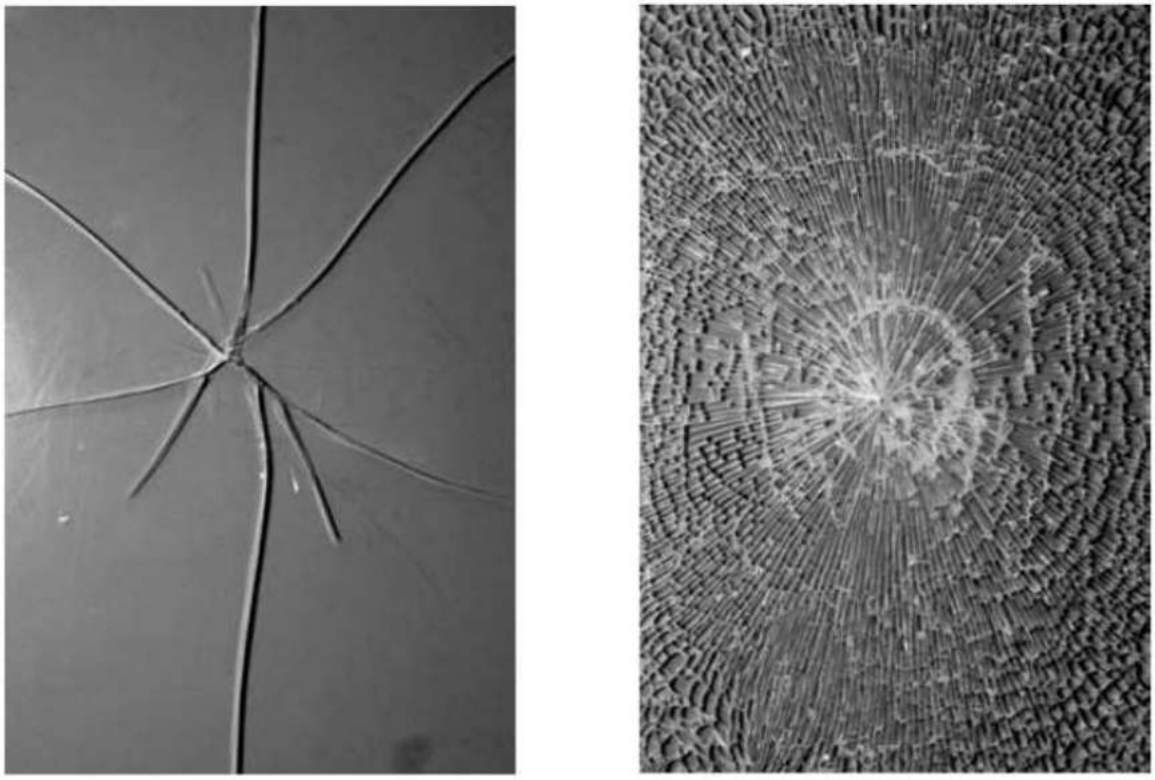


Figure 2.5: Fracture patterns A:float glass; B:tempered glass [14]

#### 2.2.2.4 Glass units

As mentioned before, a glass pane can be composed of two or more glass sheets in order to improve its structural behavior. In the figure 2.6 some examples of glass units are illustrated.

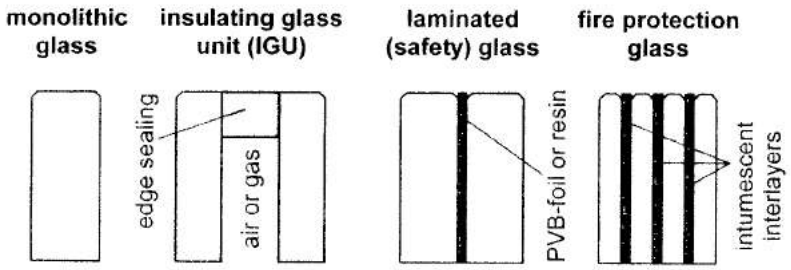


Figure 2.6: Examples of glass units [15]

### 2.2.3 Structure supporting system

The support system can be classified in three distinct categories:

- Glass facade with structural steel bearing structure - the glass panes are integrated in a steel structure;
- Cable supported spider glass facade - the glass panes are supported by metallic devices called spiders and glued at each other with silicon sealant on the edges;
- Glass facade composed by glass panes glued to each other with no structure seen from the exterior facade side. In the opposite side the bearing system can be a steel structure or a cable system.

## 2.3 Shape-Memory Alloys

### 2.3.1 Shape-memory alloys, a smart material

Shape-memory alloys (SMAs) are a functional smart new material, whose properties were first discovered around 1930 and since then is object of study of numerous researches and investigations. A smart system is defined as a system that is able to read the structure's behavior to external disturbances, and after adapt and adjust the structure characteristics in order to prevent damages [24]. Smart systems integrated in civil engineering structures made possible to provide functions such as sensing, monitoring, healing and self-adapting response to external actions. Features as durability, fatigue resistance, high power density and high damping capacity make SMAs a very interesting investigation aim. Even though this is a relatively recent material, its characteristics enable SMA to have several applications in civil engineering structures.

### 2.3.2 Shape-memory effect and superelasticity

Shape-memory alloys are a type of metallic alloys that exhibit two essential properties:

- Shape memory effect - refers to the material ability to recover its original geometry after deformed, when heated;
- Superelasticity - refers to SMAs ability to run through substantial inelastic deformations, recovering the previous configuration after the unload.

They were first discovered in 1932, when Chang and Read observed a shape memory transformation in gold-cadmium. Shape-memory effect in nickel-titanium (Nitinol) was discovered in 1962 by Buechler and co-researchers at Naval Ordnance Laboratory. There are several kind of shape memory alloys, but nitinol is still up until these days the most commonly used SMA as it possesses superior thermomechanical and thermoelectrical properties. The two aforementioned essential properties of the SMAs result from a reversible phase transformation from two crystal phases: martensite and austenite. Martensite is a weaker phase, stable in low temperature, austenite on the other hand is a high temperature stable and stronger phase.

As a crystalline structure, SMAs atoms are arranged in a symmetric twinned pattern. During the transformation from austenite to martensite, the atoms are arranged in symmetric twinned way. On the other hand, if an external stress is induced on the structure in the martensite phase, the structure responds by changing the atoms' orientation causing its detwinning. These transformations are illustrated on the diagram of the figure 2.7.

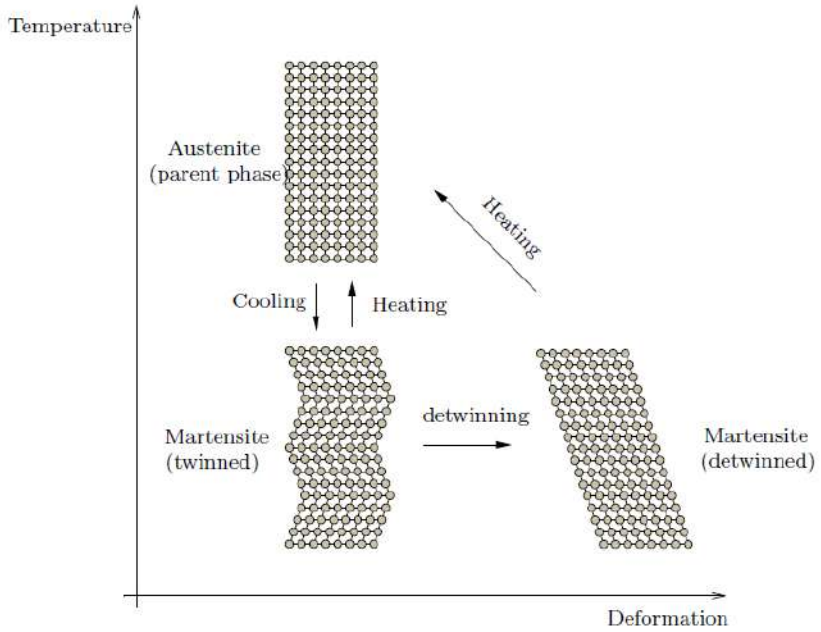


Figure 2.7: Stress-free martensitic transformation - Adapted from [28]

The transformation from a crystal phase to another can be induced by two distinct reasons: temperature gradient and mechanical loading. From a thermomechanical point of view, temperature and external stress play an equivalent role in the transformation mechanism [30]. From the two types of martensite transformations result the two essential SMAs properties: temperature-induced transformation causes SME and stress-induced transformation causes superelasticity.

A *stress-free transformation* is represented in the graphic of the figure 2.8. The loop pictured in the graphic is characterized by four transition temperatures: $M_s$, $M_f$, $A_s$ and $A_f$, described below.

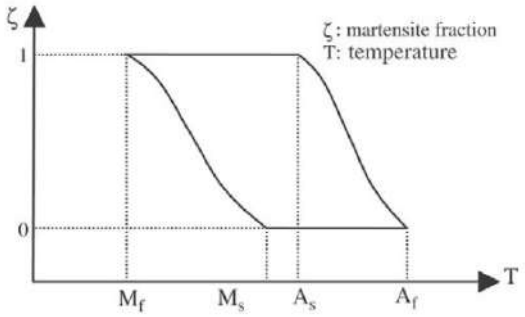


Figure 2.8: Stress-free martensitic transformation - Adapted from [30]

- $M_s$ - Martensite start temperature
- $M_f$ - Martensite finish temperature
- $A_s$ - Austenite start temperature

- $A_f$ - Austenite finish temperature, above which martensite becomes unstable

These four transition temperatures mark the start and end of the transformations phases.

A *stress-induced transformation* is represented on the stress-strain graphic of the figure 2.9. The temperature is constant and higher than $A_f$, austenitic phase.

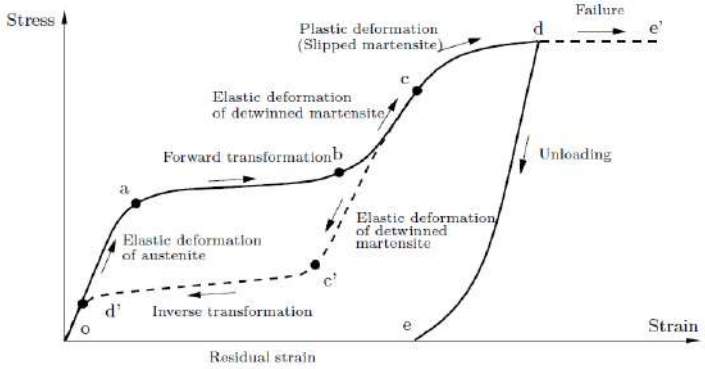


Figure 2.9: Stress-induced martensitic transformation at a - Adapted from [28]

As the stress is being applied on the structure, the elastic deformation of austenite will start to occur $(o - a)$. From the critical value $a$, the forward transformation begins, turning austenite into martensite $(a - b)$. At this point $(b)$ the structure is fully transformed into martensite. Keep straining imply the elastic deformation of detwinned martensite $(b - c)$. During this phase, if the load ceases, the elastic deformation of the detwinned martensite proceeds in the opposite direction, until a point of stress where martensite becomes unstable $(c')$. From this point on, the inverse transformation proceeds as the stress decreases, reverting back tho austenite phase $(d')$. The complete unload enables the structure to recover from all deformation, creating an hysteretical loop that allows the structure to absorb energy. This damping cycle is the superelasticity effect. If the unloading did not occur, the increasing level of stress would cause the structure to reach a point $(c)$ upon where it is enough to cause the slipping of the martensite lattices, causing plastic deformation $(c-d)$. Beyond point $d$, further loading will cause failure $(e')$, while unloading will cause significant residual deformation $(e)$.

## 2.4 Control in civil engineering structures

Recent studies and investigations are being conducted in order to develop control systems in civil engineering structures, that are able to detect and mitigate undesired effects on the aforementioned structures. There are several types of control systems, which are briefly presented in this section, to better understand the control action in structures.

### 2.4.1 Passive control systems

Passive control systems are those that don't need external energy to operate. For this reason they're the most commonly used control systems, on the other hand, if the dynamic characteristics of the structure significantly changes during the action, this control type is not recommended.

There are three types of passive control systems [21]:

- Absorbers - To absorb the structures' vibrations, a mass can be attached to the structure, connected to the latter by a spring and a damper device. This system, called Tuned Mass Damper (TMD), when correctly calibrated with the natural frequency of the structure, can absorb and mitigate dynamic actions on the structure. The TMD devices can only mitigate the response to a specific vibration mode. More than one be can be implemented on the same structure, if necessary. They're very efficient in the wind engineering area. Tuning errors reduces significantly this system's efficiency. Other type of absorber device are the Tuned Liquid Damper (TLD). These devices take advantage of the hydrodynamic characteritics of a liquid, usually water, on a reservoir, presenting a very similar behavior to the TMD, though more complex and non-linear.

- Dissipative - The dissipative devices are also known as dampers and can be viscous, visco-elastic, frictional or hysteretics. In a general way, the action of these devices consists in receiving the mechanical energy and dissipate it in order to prevent the structure to absorb it. This way, these devices have the disadvantage that they only act when the action occurs;

- Isolators - In order to prevent mainly the seismic action effects, a structure can be isolated on its base. To do this, devices of low horizontal stiffness are implemented on the base of the structure, allowing its movements to be independent from the ground's movements.

### 2.4.2 Active control systems

In contrast to passive control devices, active control devices need external power to actuate. The control system has to be able to receive data from the structure, process the latter and after that evaluate the data. To evaluate the data it is necessary to have previously defined the range of admissible values at stake. The comparison between the received data and the previously defined data will enable the system to evaluate if it is necessary to activate the control on the structure. The control can be induced by an actuator and its algorithm is carefully developed in order to be able to answer to all the structure's requirements. There are two types of active control action, differing from each other in the moment where the control occurs.

- Feedforward control - In this situation the control action is activated before the stimulus occur. Because of this particular reason, the feedforward control is generally used in situations where the structure's behaviour can be predicted. The diagram of the figure 2.10 illustrates the feedforward control action.

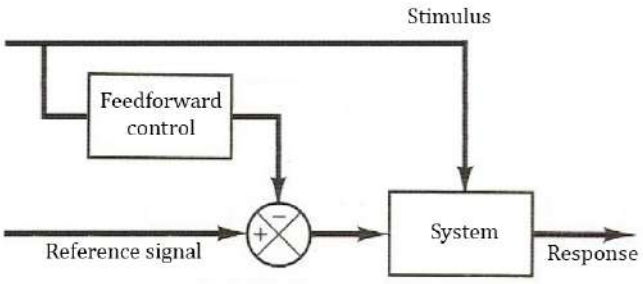


Figure 2.10: Feedforward control - adapted from [23]

- Feedback control - The control action is activated after the controller received and processed the signal, comparing it to the previously setpoint value. This action is illustrated on the figure 2.11.

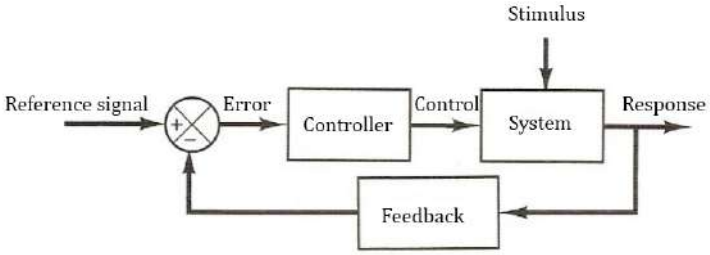


Figure 2.11: Feedback control - adapted from [23]

### 2.4.3 Semi-active control systems

Recently, several studies are being made in order to develop a control system that gather the advantages of both previously mentioned control systems. This type of control system uses a low power external source, reducing the cost associated, also using a control algorithm.

### 2.4.4 Hybrid control system

A hybrid control system is a system that combines two or more previously defined types of control. It is particularly adapted to the situation in question in order to better monitor and manage the structure's response.

# Chapter 3

# Glass pane structural behavior characterization

## 3.1 Introduction

In this section the structural behavior of the glass pane is studied in distinct cable system configurations and distinct situations along time. The enhanced effective method is applied in order to simulate the interlayer's behavior along time, that deeply affects the structural behavior of the laminated glass and is strongly dependent of factors like temperature and load duration. Several cable system configuration are studied, with shell finite elements models using the software SAP2000, so the structural behavior of the whole system is optimized. After this, a solid FE model using the software Abaqus is presented to further investigate the structural behavior and validate the results obtained with the simplified method. A comparison between the results obtained with the two software programs is made.

## 3.2 The Enhanced Effective Thickness method

### 3.2.1 Introduction

Due to the non-linear behavior of PVB, the resulting state of stress is quite difficult to exactly obtain and often requires sophisticated full three dimensional numerical analysis. Nevertheless, there are simplified methods that can be used in the design practice of laminated glass as the enhanced effective thickness (EET) method.

The developments in the production processes made in the last decades significantly enhanced glass behavior. Glass has been more and more used in modern construction, not only as a way to enlighten the interior, or even as a coating in modern buildings, but also with a structural function. The structural use of glass is not necessarily more complex or difficult than other materials, but it requires a special attention due to its intrinsic brittleness[9]. Laminated glass helps to overcome its typical brittle behavior by bonding together two or more panes of glass with intermediate polymer interlayers. The latter imposes a plastic component in the laminated glass structure and improves its post-breakage behavior, keeping the glass fragments stuck and avoiding instantaneous collapse. The interlayer PVB material characteristics depend mainly in two factors: temperature and load duration [11]. These factors strongly affect the laminated glass behavior, in fact it is shown that the interlayer's properties and thickness actually govern laminated glass behavior when subjected to bending or impact

loads [26]. The shear modulus of the interlayer is also a very important characteristic that has to be taken into account [17].

In this work, the main factor studied was the temperature influence. Being a material widely used in facades, laminated glass is frequently exposed to situations that leads to a high range of temperatures, as sun exposure, rain, wind and other weather conditions. Therefore, the behavior of laminated glass with the temperature is a subject that should be deeply investigated in order to understand and predict the structure's behavior along time.

Tests made by Reznik and Minor [27] led to the conclusion that as temperature increases, the laminated glass behavior approaches the situation where the glass sheets behave as if they are independent - layered behavior. This is due to the fact that the ability of the interlayer material to transfer shear load is reduced with the increase of the temperature. On the opposite side, laminated glass presents a monolithic behavior when the interlayer is able to transfer shear load. The temperature to which the laminated glass is subjected strongly affects its behavior. Linden et al. [20] also studied this topic and reached the conclusion that the same laminated glass sample can be weaker than a monolithic glass at high temperatures and stronger at room temperatures. El-Shami, Norville and Ibrahim [11] studied the behavior of laminated glass under a different range of temperatures. The graphic of the Figure 3.1 shows the comparison between theoretical deflections in the center of the plate at different temperatures.

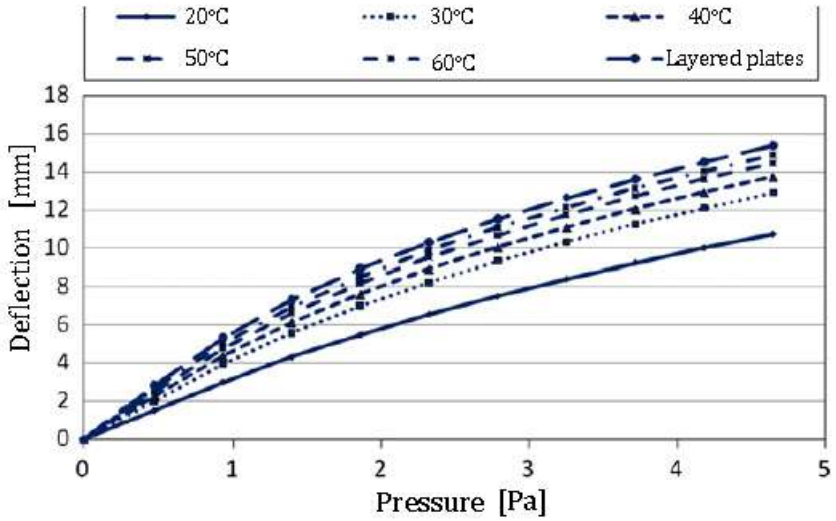


Figure 3.1: Deflection at the central point at different temperatures - Adapted from [11]

From the graphic it can be seen that as temperature increases, the deflection at the central point also increase. The curve of layered plates was obtained with the modulus of rigidity of PVB equal to zero. This graphic supports the conclusion of Reznik and Minor that as temperature increases, the laminated glass behavior migrates toward the layered glass behavior.

### 3.2.2 The method

The traditional Wölfel-Bennison formulas to determine an effective thickness are only accurate when the plate response is similar to that of a beam under uniformly distributed load [13]. The enhanced effective thickness method assumes a deformed configuration for the plate and returns an effective thickness used for estimate displacements and one other for calculate stresses. The deformed configuration assumed depends upon the boundary and load conditions. The thickness of both glass panes and the interlayer's as well as the two material properties are also taken into account.

To use this method, one first has to characterize the $\Psi$ coefficient, that depends on the boundary conditions, load and also the plate's prevailing dimensions ratio. The values that this $\Psi$ can assume are tabled [13].

After the $\Psi$ coefficient is characterized, the $\eta$ parameter should be calculated by the expression (3.1)

$$\eta = \frac{1}{1 + \frac{h_{int}E}{G_{int}(1-\nu^2)} \cdot \frac{D_{abs}}{D_{full}} \cdot \frac{h_1 h_2}{h_1 + h_2} \cdot \psi} \tag{3.1}$$

Being:
$h_{int}$ - thickness of the interlayer;
$h_1$ - thickness of the glass pane 1;
$h_2$ - thickness of the glass pane 2;
$E$ - glass' Young module;
$G_{int}$ - shear module of the interlayer;
$\nu$ - glass' Poisson's ratio;
$D_{abs}$ - Bending stiffness relative to layered limit;
$D_{full}$ - Bending stiffness relative to monolithic limit.

The $\eta$ parameter, whose value is between 0 and 1, reflects the interlayer ability to transfer shear load, when $\eta = 0$ the interlayer is not able to transfer the shear actions (layered behavior), and conversely when $\eta = 1$ we have the other limit situation where the interlayer is able to transfer all shear load (monolithic behavior).

The effective thickness in terms of displacements, $\widehat{h}_w$ should be calculated by the expression (3.2). In terms of stresses, the effective thicknesses $\widehat{h}_{1;\sigma}$ and $\widehat{h}_{2;\sigma}$ are calculated by the expressions (3.3) and (3.4)

$$\widehat{h}_w = \sqrt[3]{\frac{1}{\frac{\eta}{h_1^3 + h_2^3 + 12I_s} + \frac{1-\eta}{h_1^3 + h_2^3}}} \tag{3.2}$$

$$\widehat{h}_{1;\sigma} = \sqrt[3]{\frac{1}{\frac{2\eta d_1}{h_1^3 + h_2^3 + 12I_s} + \frac{h_1}{\widehat{h_w}^3}}} \tag{3.3}$$

$$\widehat{h}_{2;\sigma} = \sqrt[3]{\frac{1}{\frac{2\eta d_2}{h_1^3 + h_2^3 + 12I_s} + \frac{h_2}{\widehat{h_w}^3}}} \tag{3.4}$$

The glass pane used in this study is similar to the one presented in [12]. It is a rectangular pane, with the dimensions expressed on the Figure 3.2.

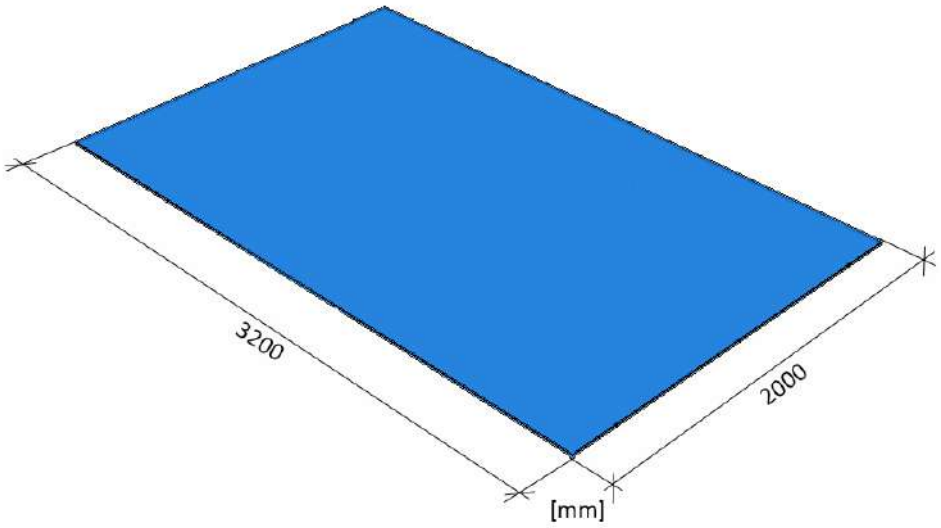


Figure 3.2: Glass pane dimensions

It is a laminated glass pane composed by two glass sheets of 8mm and 10mm of thickness and a PVB interlayer of 1,52 mm.

The $\psi$ factor is obtained by interpolation from the values of the table 3.3.

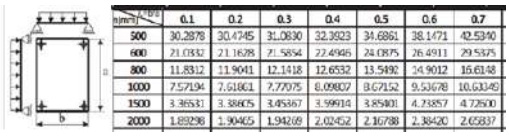

| b/a | 0.1 | 0.2 | 0.3 | 0.4 | 0.5 | 0.6 | 0.7 |
|---|---|---|---|---|---|---|---|
| 500 | 30.2878 | 30.4745 | 31.0830 | 32.1623 | 34.6861 | 38.1471 | 42.5340 |
| 600 | 21.0332 | 21.1628 | 21.5854 | 22.4946 | 24.0875 | 26.4911 | 29.5375 |
| 800 | 11.8312 | 11.9041 | 12.1418 | 12.6532 | 13.5492 | 14.9012 | 16.6148 |
| 1000 | 7.57194 | 7.61861 | 7.77075 | 8.09807 | 8.67152 | 9.53678 | 10.63349 |
| 1500 | 3.36531 | 3.38605 | 3.45367 | 3.59914 | 3.85401 | 4.23857 | 4.72600 |
| 2000 | 1.89298 | 1.90465 | 1.94269 | 2.02452 | 2.16788 | 2.38420 | 2.65837 |

Figure 3.3: $\psi$ values for a simply supported pane subjected to distributed load

To preview the interlayer's behavior degradation as the temperature increases, four distinct situations are analyzed in which each one undertakes a distinct ability to transfer shear load. To achieve this effect, in each situation is considered a different value of the shear module, from a situation that the system behaves as monolithic to a layered behavior. The four distinct situations are the following:

- G=500MPa corresponding to a short duration load - Monolithic behavior
- G=8.06MPa, 20$^{o}$C, 3sec
- G=0.2MPa, 50$^{o}$C, 10sec
- G=0.052MPa, 50$^{o}$C, 50 years corresponding to the layered behavior.

The effective thicknesses obtained to the mentioned situations are expressed on the table 3.1.

| | $\widehat{h}_w$ | $\widehat{h}_{1;\sigma}$ | $\widehat{h}_{2;\sigma}$ |
|---|---|---|---|
| **G=500MPa;Short Duration Load** | 19.487 | 18.556 | 20.566 |
| **G=8.06MPa;20ºC;3sec** | 18.805 | 18.222 | 20.206 |
| **G=0.2MPa;50ºC;10min** | 13.305 | 14.221 | 15.863 |
| **G=0.052MPa;50ºC;50years** | 12.067 | 12.950 | 14.467 |

Table 3.1: Effective thickness [mm] in terms of displacements and stresses to four distinct situations

## 3.3 Structural behavior characterization

### 3.3.1 Introduction

The configuration of the cable system is essential to understand the structural behavior of the glass pane. In this section is described a parametric study regarding the effect of the cable system in the structural behavior of the glass pane. The main results are presented, as well as some conclusions regarding the studied systems.

### 3.3.2 The cable system configuration

In order to understand the cable system's influence on the structure, various configurations were studied, differing from each other only in the deviators' position. The interlayer's properties and capacity to transfer shear load was also analyzed. A glass pane with the dimensions considered in [12] and presented in section 3.2 was considered. The load considered was also the one presented in [12], a distributed load of $1,8kN/m^2$ applied perpendicularly on the surface to simulate the wind effect on the surface. The results in terms of displacements and stresses were initially analyzed for the monolithic behavior and after that the distinct four situations described in chapter 3.2 were compared.

### 3.3.3 Monolithic behavior

#### 3.3.3.1 Longitudinal position of the deviators

Starting from a configuration with only one deviator in the center of the longest edge on both sides of the pane as shown in Figure 3.4, the deviator's position was gradually moved along the edge, as can be seen in Figure 3.5. The distance between the deviators in each system are reported on table 3.3.3.1.

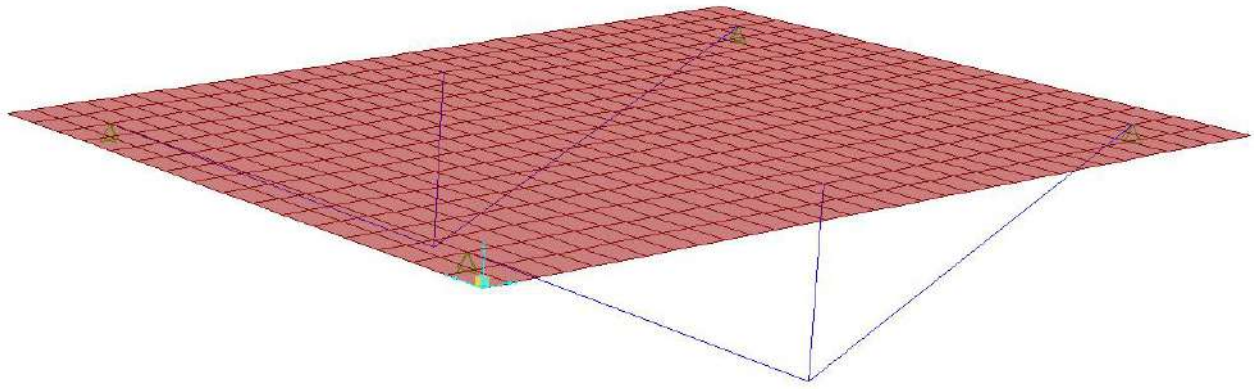

Figure 3.4: Initial system - System 0

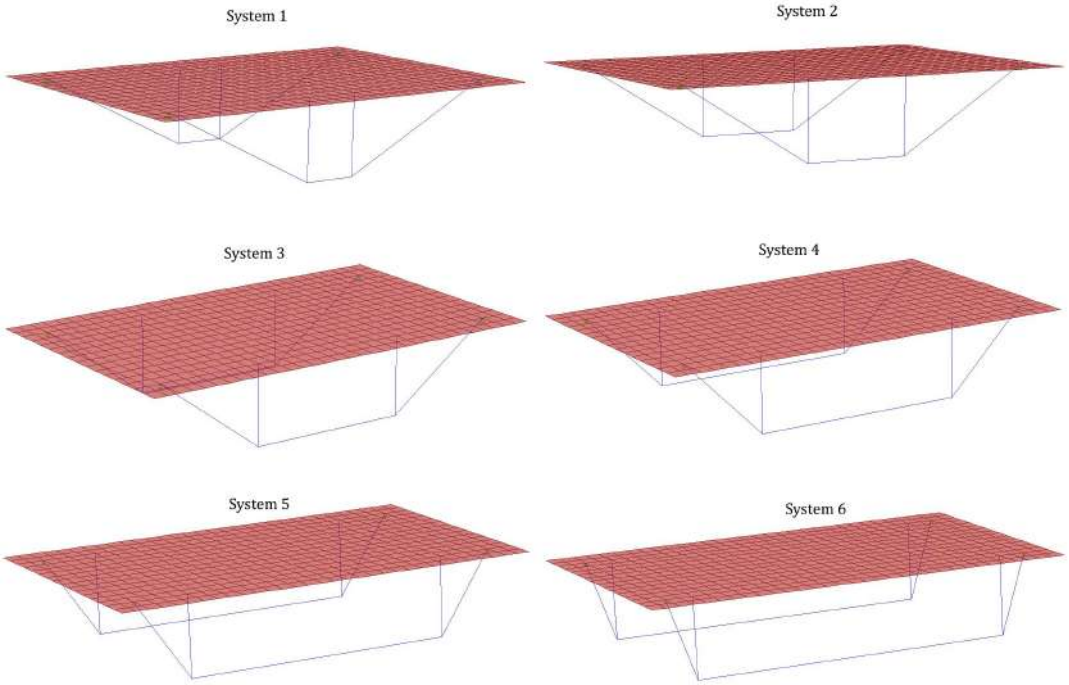


Figure 3.5: Systems 1 to 6

| System | Distance between deviators [mm] |
|---|---|
| 0 | - |
| 1 | 400 |
| 2 | 800 |
| 3 | 1200 |
| 4 | 1600 |
| 5 | 2000 |
| 6 | 2400 |

Table 3.2: Distance between deviators in each system [mm]

The displacements obtained with the systems 0 to 6 are expressed on the diagrams of the figure 3.6.

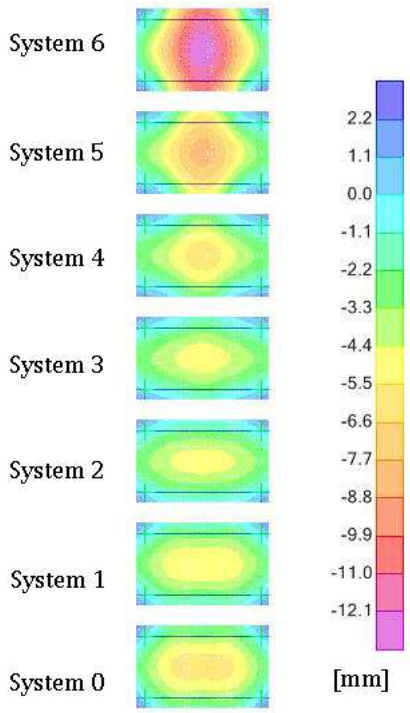


Figure 3.6: Displacements' diagram on the different systems

The stresses obtained are expressed on the diagrams of the Figures 3.7.

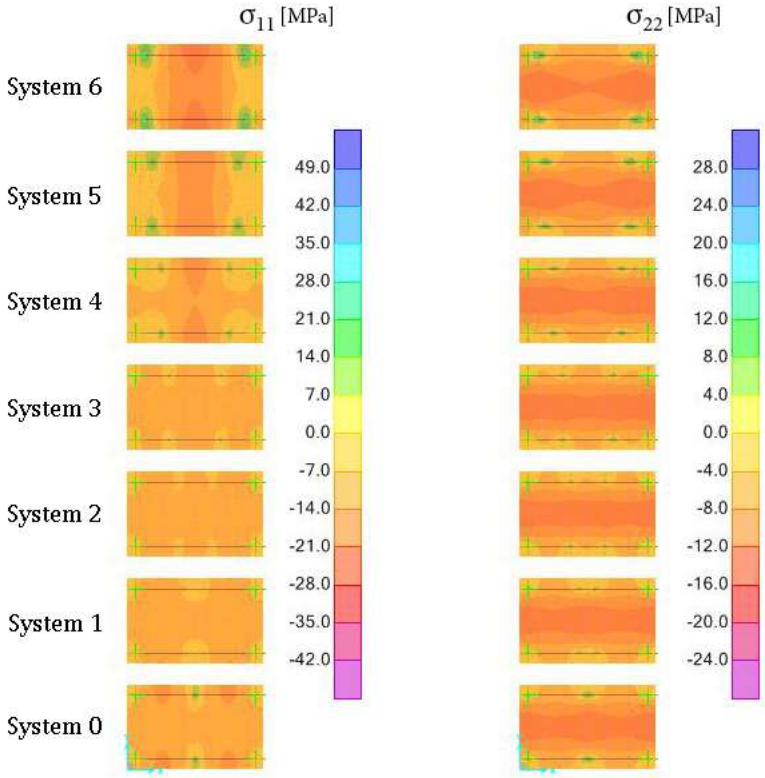


Figure 3.7: $\sigma_{11}$ and $\sigma_{22}$ on the different systems

From the results obtained, one can observe that the most efficient system in terms of displacements and stresses is the system 2, correspondent to 800mm between deviators.

#### 3.3.3.2 Transversal position of the deviators

The deviators' position was also analyzed along the y axis. Starting, once again, from the initial configuration of the system 0 shown on Figure 3.4 (system 0), both deviators were moved towards the central point of the pane, as shown in Figure 3.8. The distances between the deviators are indicated on table 3.3.3.2. To prevent the deviators' rotation in the xz plane, the same systems here represented were also analyzed with an additional transversal cable connecting the deviators transversally as shown in Figure 3.9.

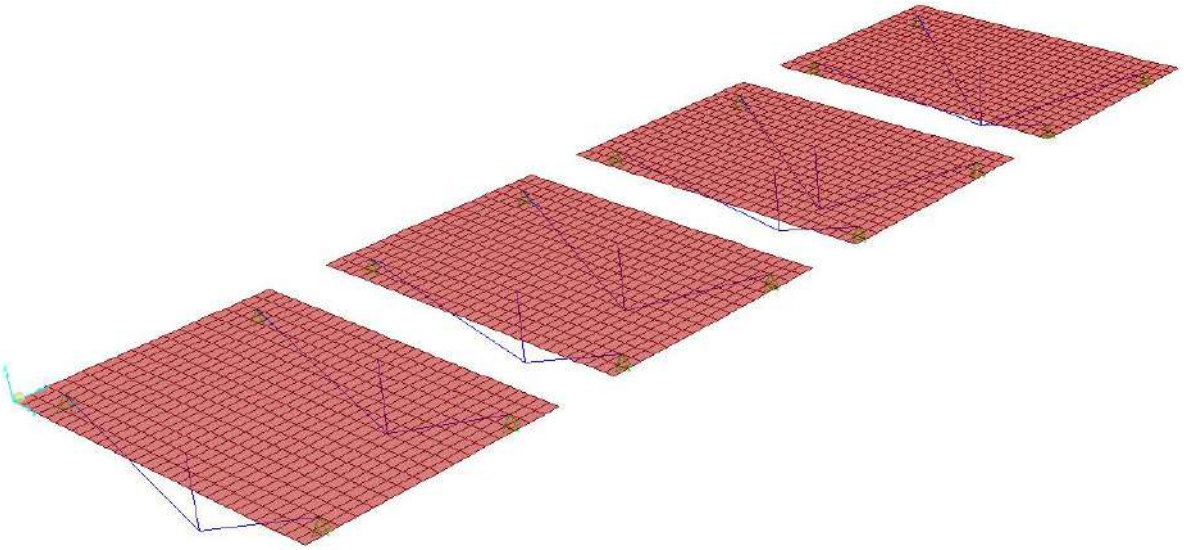

Figure 3.8: Systems 0 to C

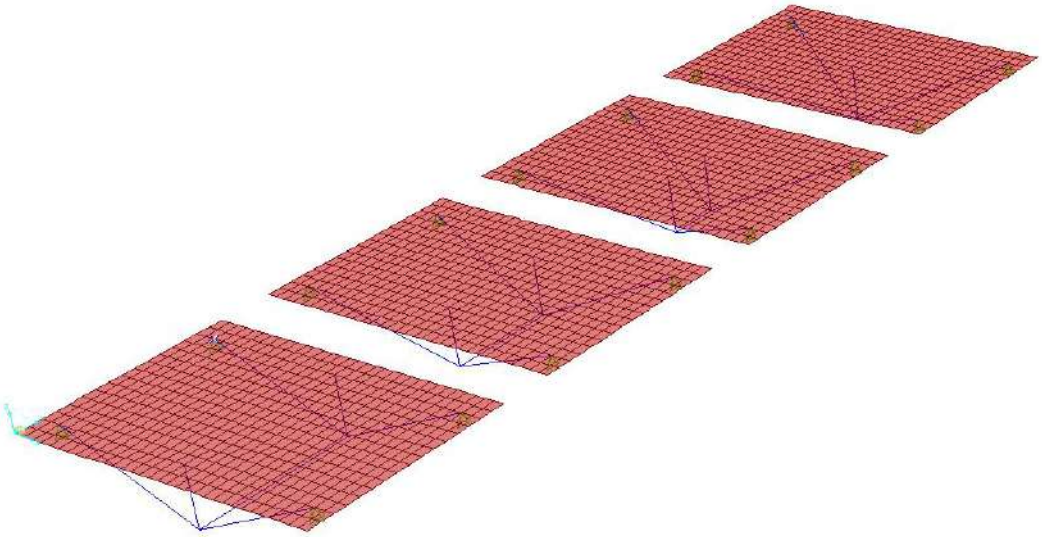

Figure 3.9: Systems 0 to C with cables connecting the deviators

| System | Distance between deviators [mm] |
|---|---|
| 0 | 1500 |
| A | 1000 |
| B | 500 |
| C | - |

Table 3.3: Distance between deviators in each system [mm]

The displacements obtained on the different systems are expressed in the diagrams of the Figure 3.10.

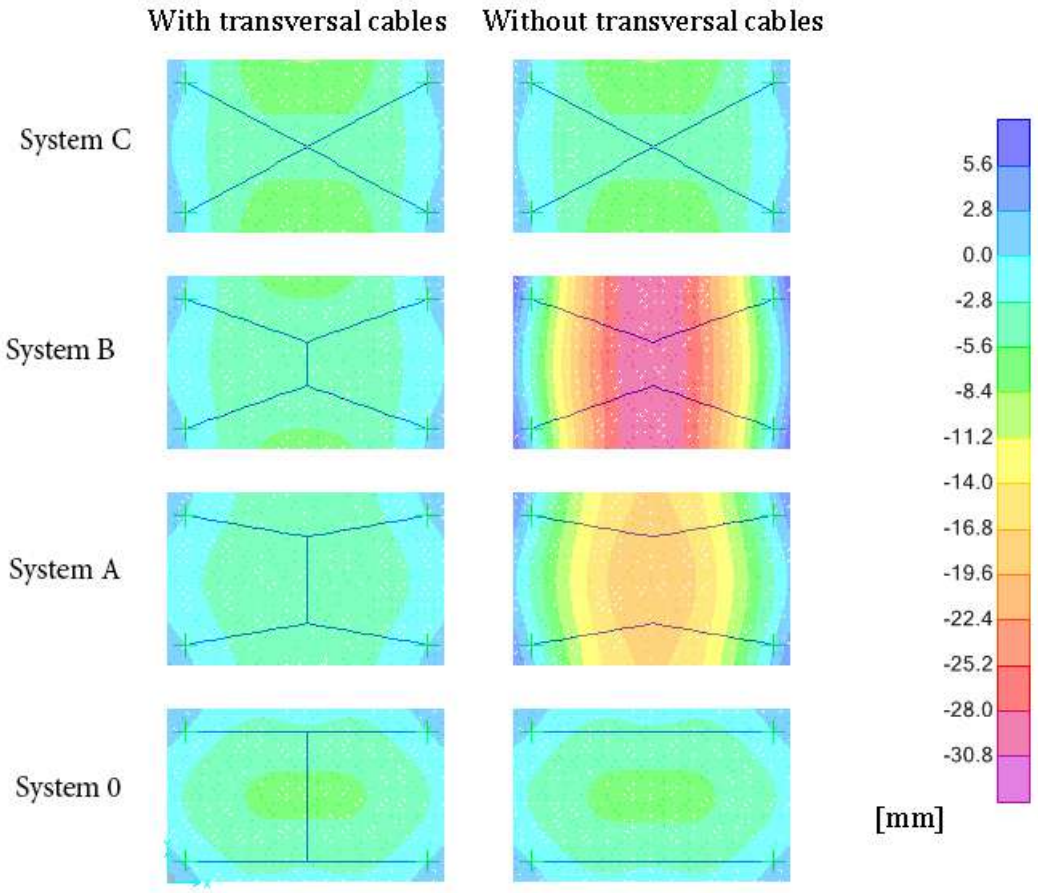


Figure 3.10: Displacements on systems 0 to C, with and without cables

The stresses $\sigma_{11}$ and $\sigma_{22}$ obtained in the same previous systems are expressed on the diagrams of the Figures 3.11 and 3.12.

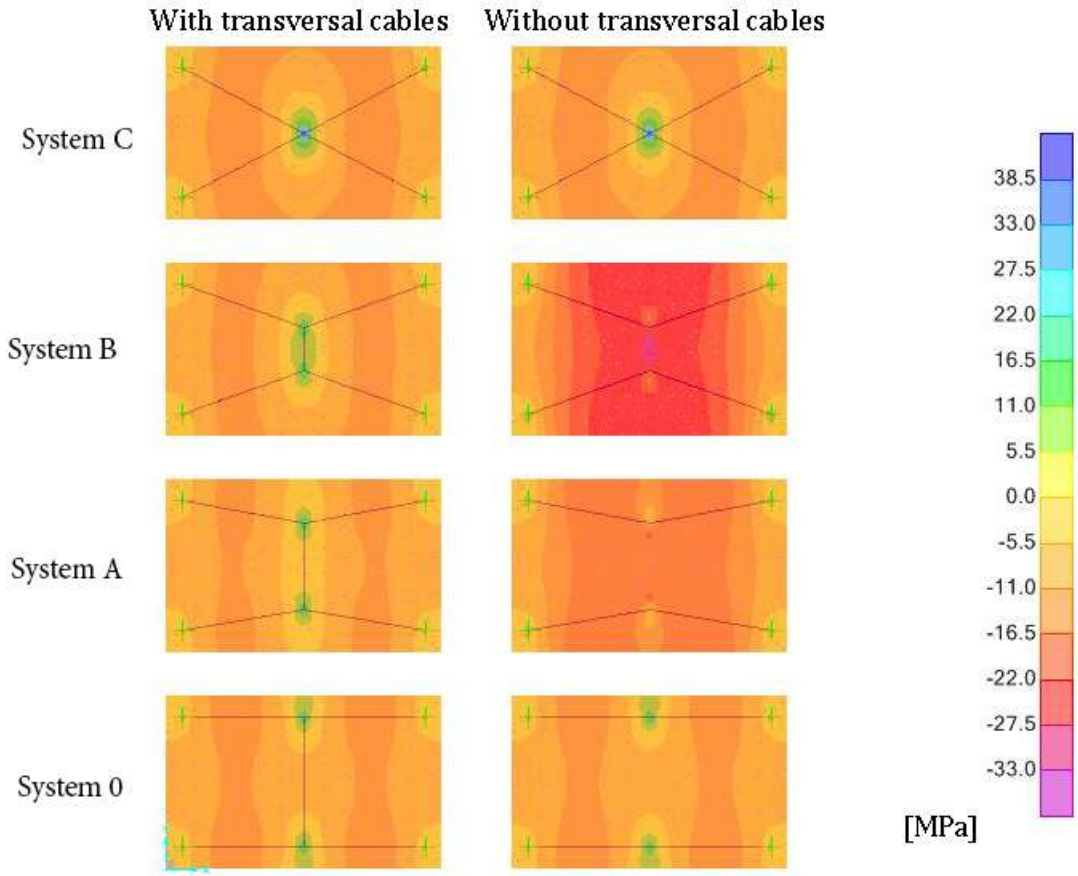


Figure 3.11: $\sigma_{11}[MPa]$ on the systems 0, A, B and C with and without cables

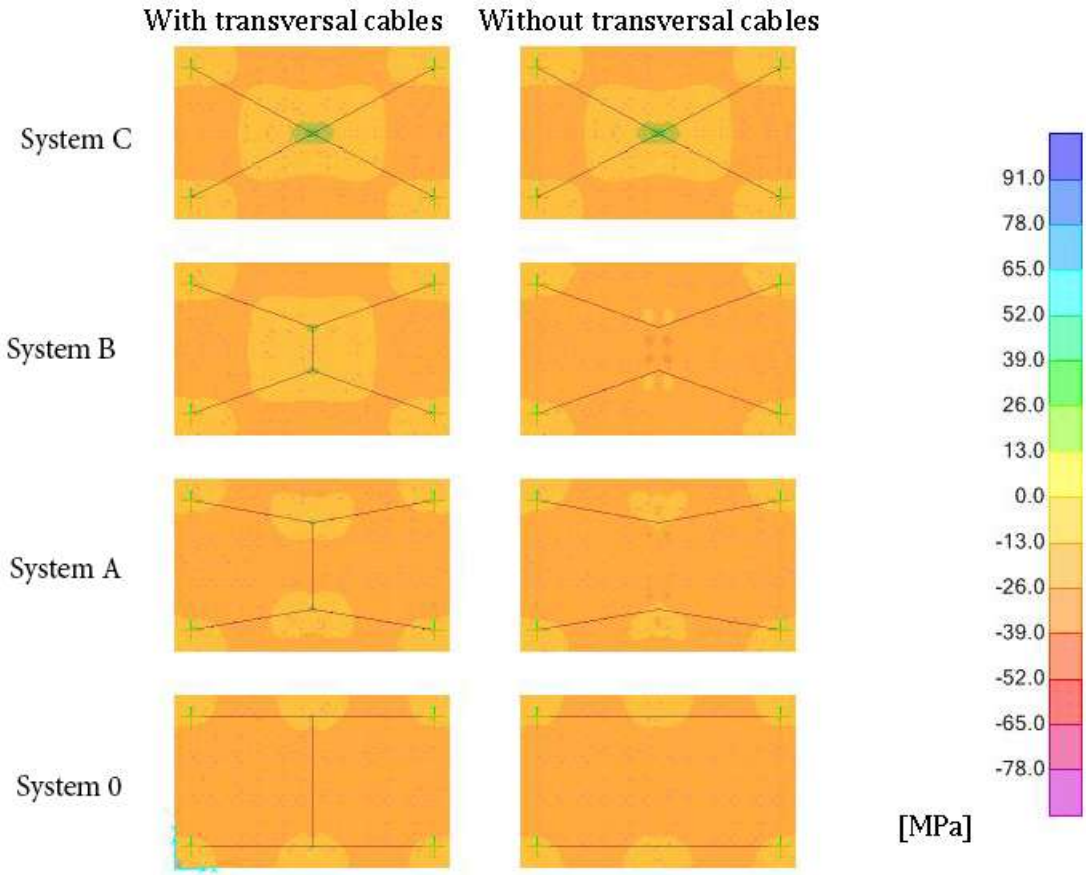


Figure 3.12: $\sigma_{22}[MPa]$ on the systems 0, A, B and C with and without cables

The results obtained show, as expected, that the extra cable connecting the deviators in the plane z=-600mm has a remarkable effect, perceptible specially in terms of displacements, as can be seen on the diagram of the Figure 3.10. Analyzing the results obtained, it can be observed that the most efficient system in terms of displacements and stresses is the system A, correspondent to 1000 mm between deviators.

#### 3.3.3.3 Deviators moving along y axis, from system 2

Since system 2 was proved to be the best cables' configuration system in section 3.3.3.1, the panel's behavior moving deviators along y axis starting from system 2 was also analyzed. The diagrams of the obtained displacements can be consulted on the Figure 3.13.

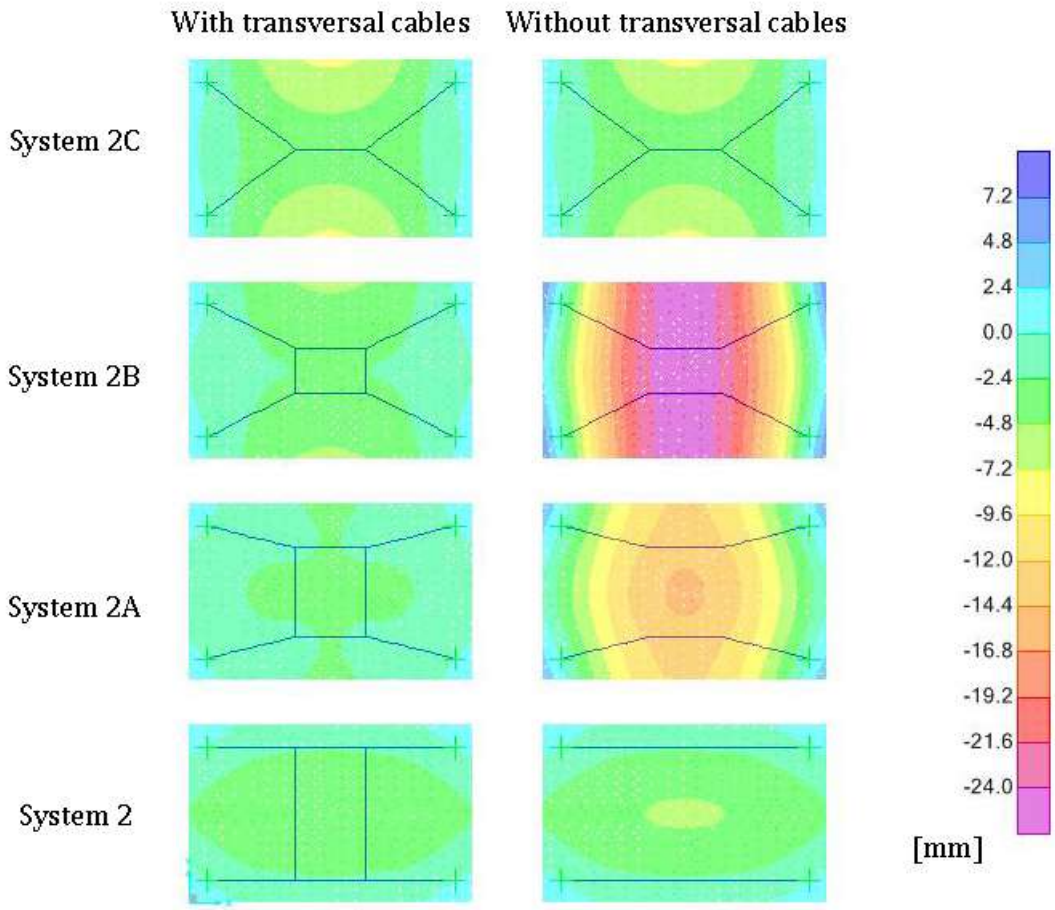


Figure 3.13: Displacements on the systems 0, A, B and C with and without cables

The stresses $\sigma_{11}$ and $\sigma_{22}$ obtained in the same previous systems are expressed on the maps of the Figures 3.14 and 3.15.

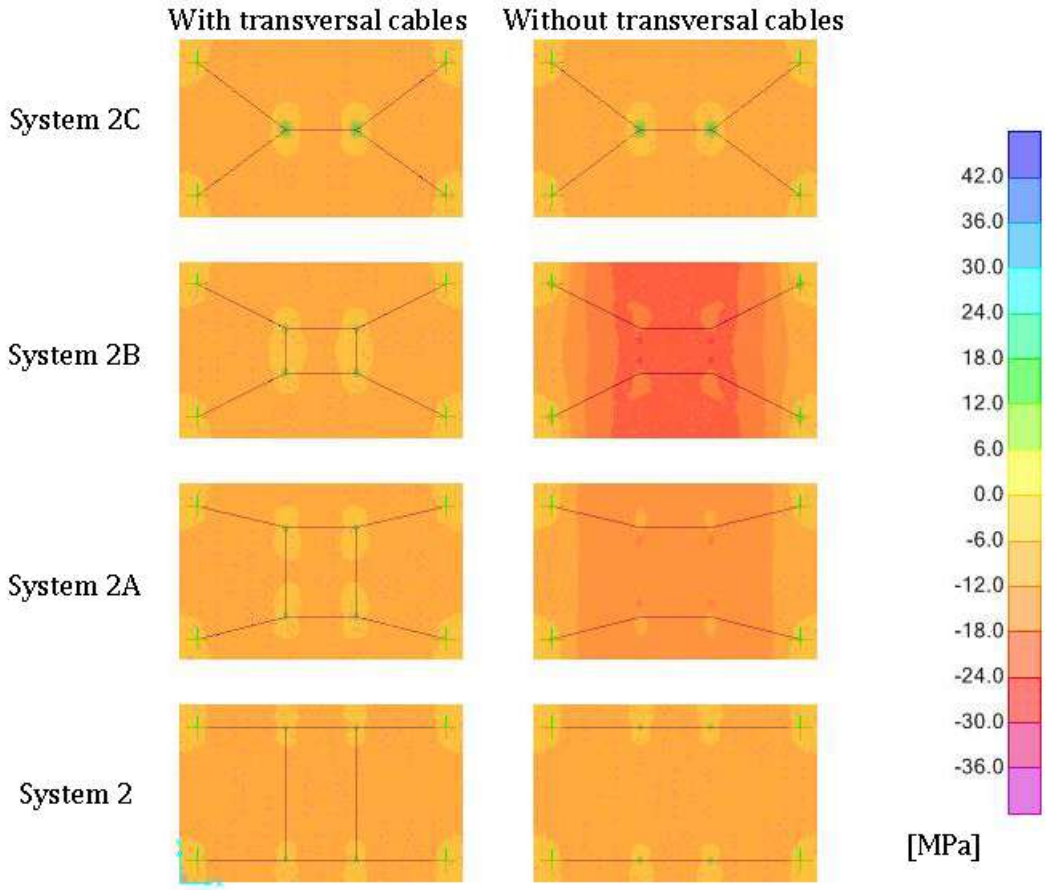


Figure 3.14: $\sigma_{11}$ on the systems 0, A, B and C with and without cables

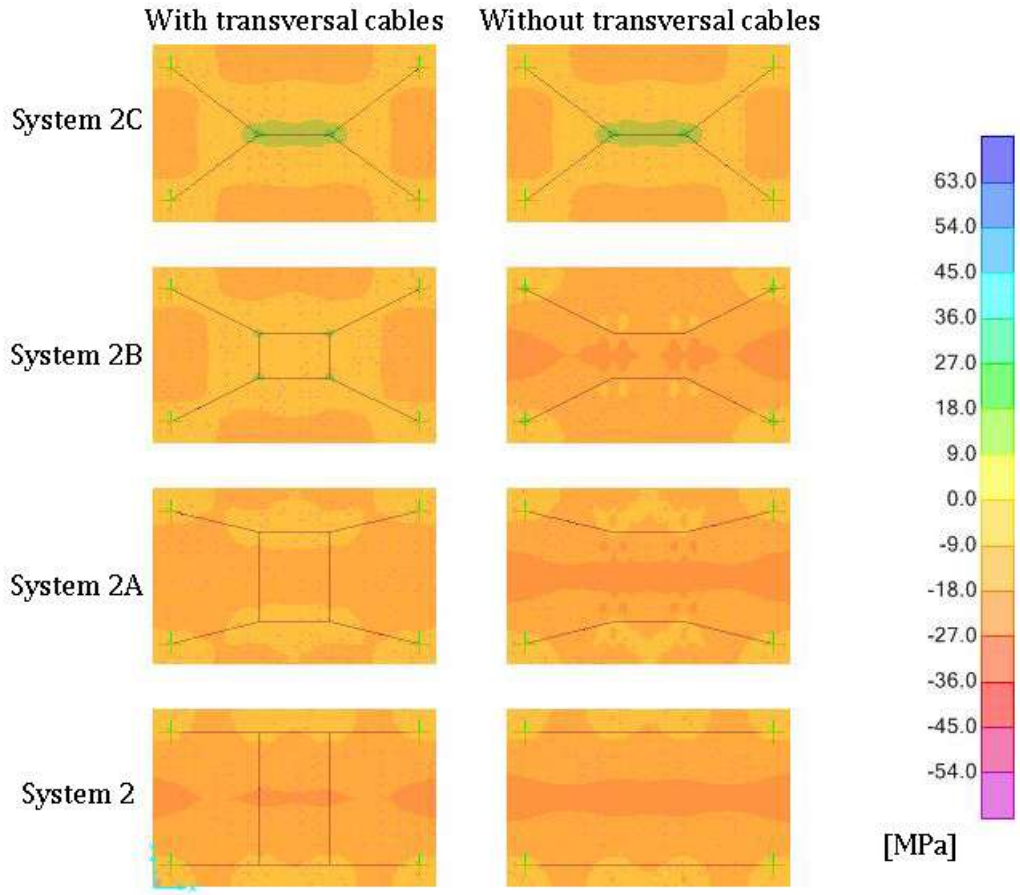


Figure 3.15: $\sigma_{22}$ on the systems 0, A, B and C with and without cables

#### 3.3.3.4 Conclusion and comments

The results of the displacements and stresses obtained in the performed studies lead to the following conclusions:

- The optimized deviators' distance in x direction is 800mm correspondent to system 2;
- The optimized deviators' distance in y direction is 1000mm correspondent to system A;
- The systems with the aditional transversal cables exhibit a significant improved behavior compared to the systems without the extra cables;

A comparison between system0A and system2A was also studied, and is presented in Appendix A.

### 3.3.4 Time, temperature and load duration effect on glass behavior

As mentioned before, the PVB material characteristics depends on time, temperature and load duration. By varying the PVB's shear modulus, the structural behavior of glass along time can be foreseen. Therefore, four distinct situations were considered:

- G=500MPa corresponding to a short duration load - Monolithic behavior

- G=8.06MPa, 20°C, 3sec

- G=0.2MPa, 50°C, 10sec

- G=0.052MPa, 50°C, 50 years corresponding to the layered behavior.

The results obtained are shown in the following diagrams.

#### 3.3.4.1 System0

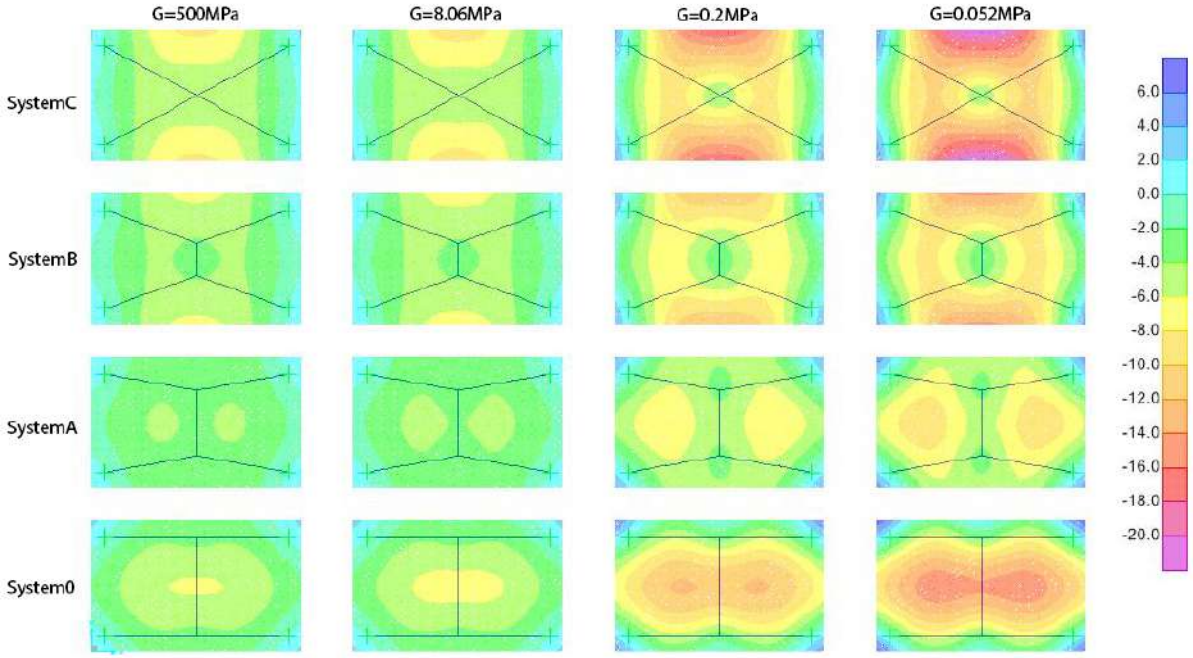


Figure 3.16: Displacements [mm]

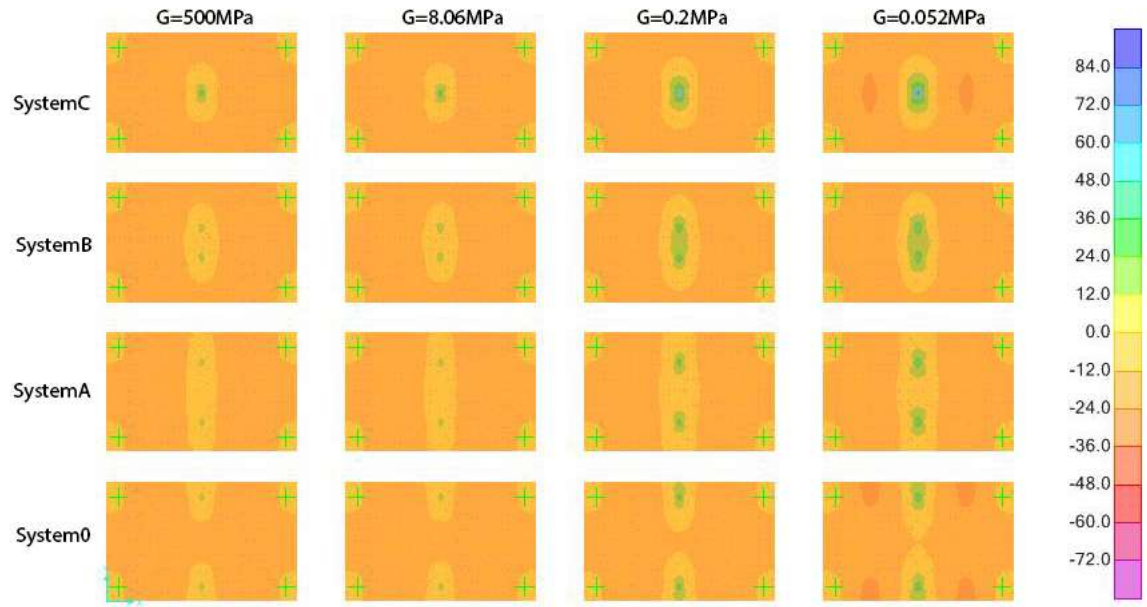


Figure 3.17: $\sigma_{11}$ [MPa]

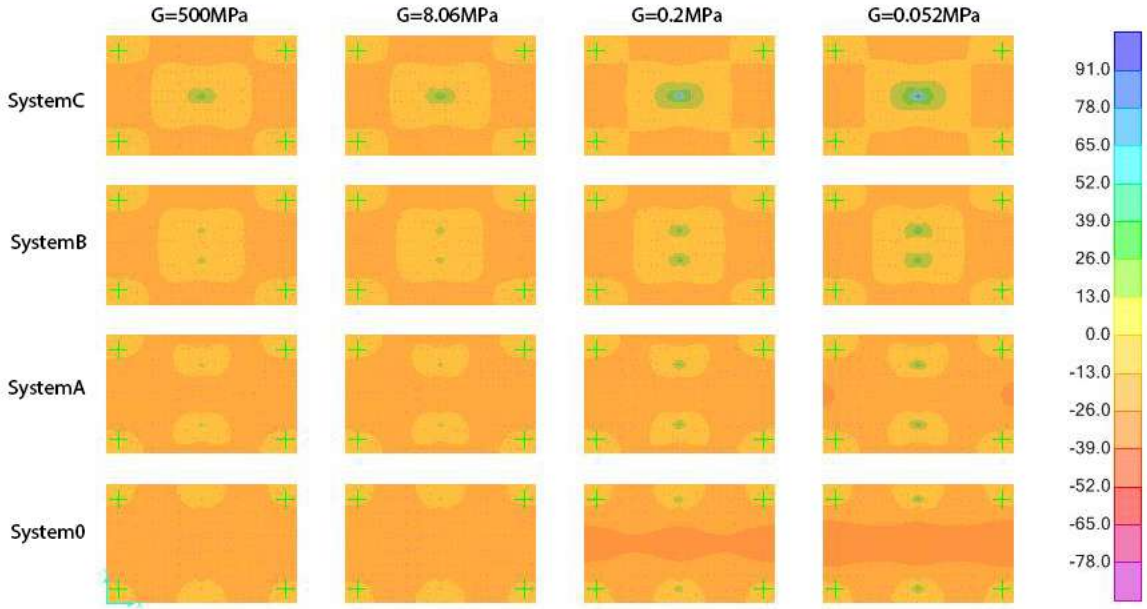


Figure 3.18: $\sigma_{22}$ [MPa]

#### 3.3.4.2 System2

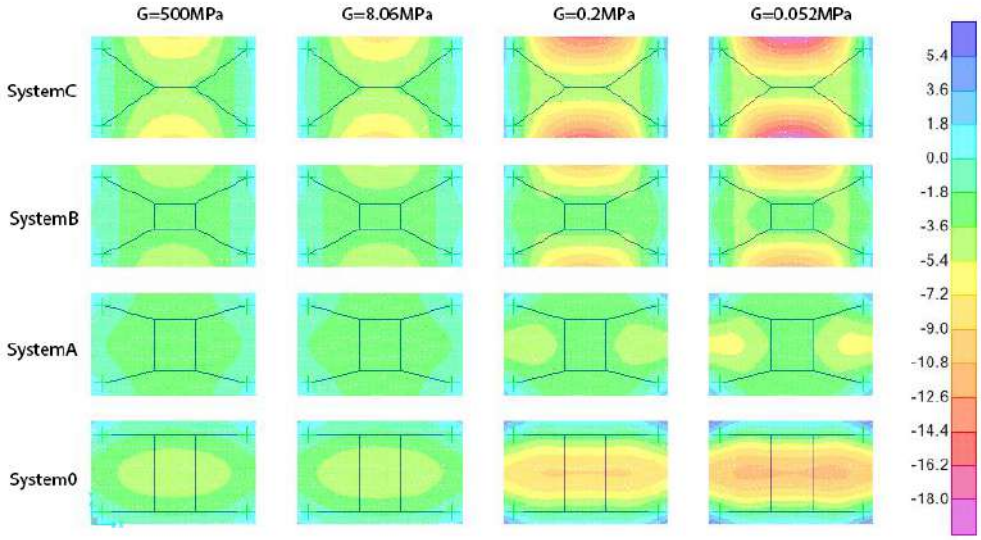


Figure 3.19: Displacements [mm]

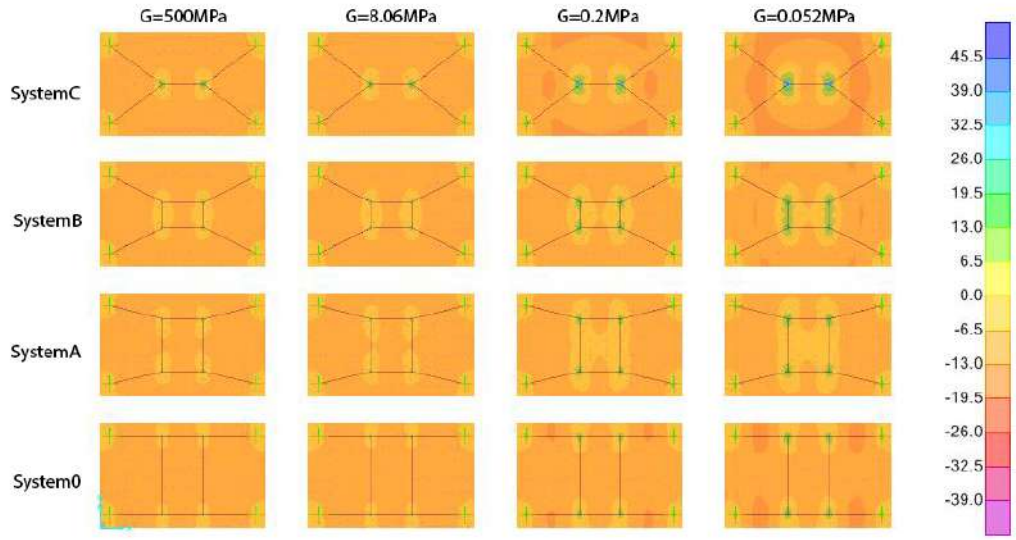


Figure 3.20: $\sigma_{11}$ [MPa]

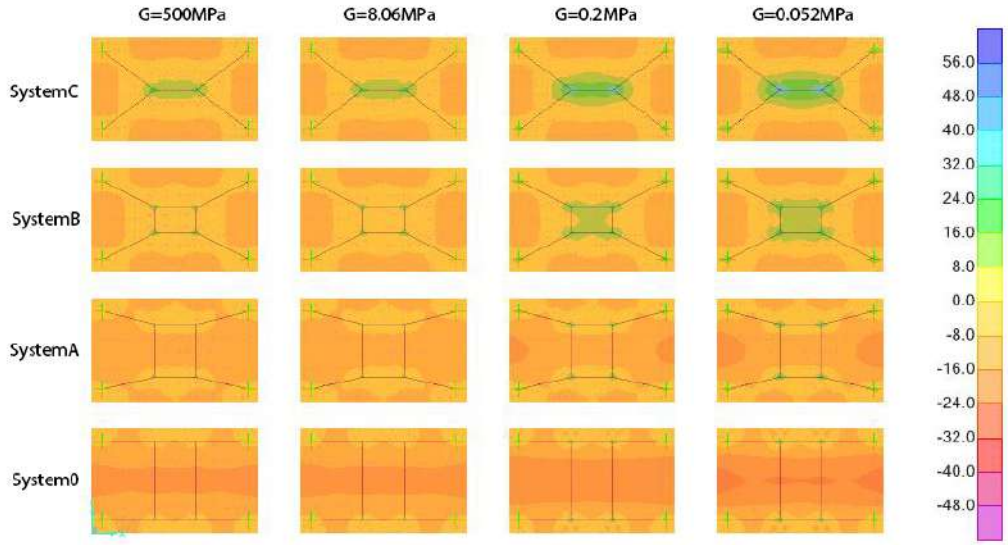


Figure 3.21: $\sigma_{22}$ [MPa]

#### 3.3.4.3 Conclusion and comments

With the EET method it is possible to preview the structure behavior along time. The results confirm that the system A is the one that exhibit better behavior along time.

## 3.4 ABAQUS solid model

A solid model analysis was performed in the ABAQUS software. The interlayer's PVB properties were adapted to simulate the four distinct situations mentioned on section 3.2. The stresses obtained are expressed below:

### 3.4.1 Monolithic behavior

When a short duration load is applied on the pane, The PVB's characteristic are expressed on the table 3.4

| G | E |
|---|---|
| 500MPa | 1490 MPa |

Table 3.4: PVB's properties for the monolithic behavior

The displacements obtained are expressed on the Figure 3.22 and the stresses are expressed in Figures 3.23 and 3.24.

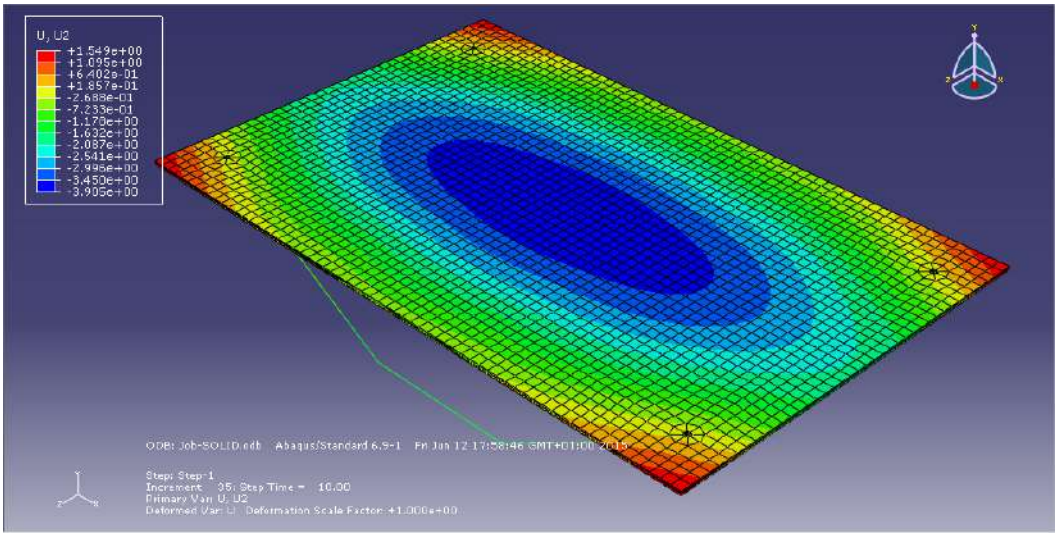


Figure 3.22: Displacements [mm]

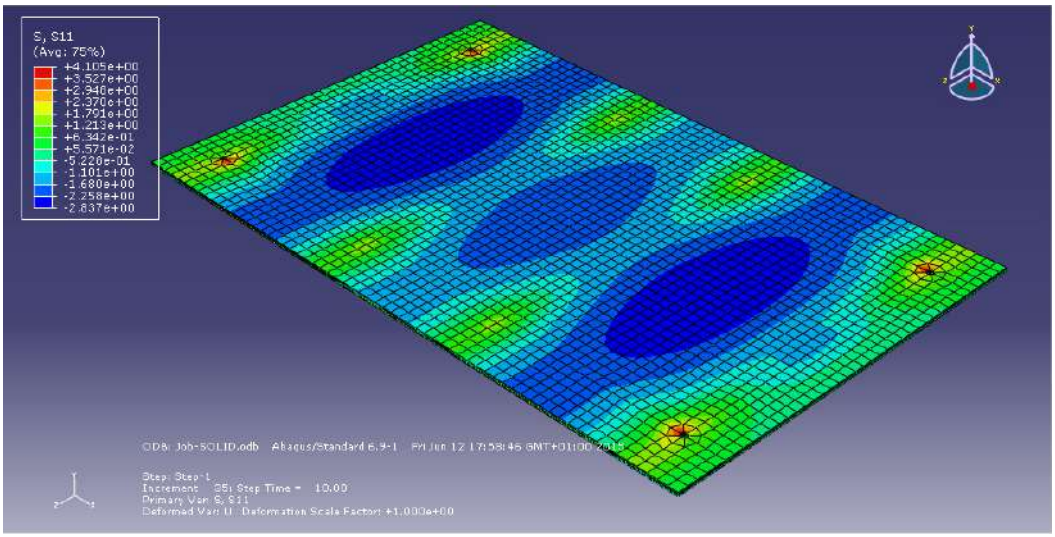


Figure 3.23: $\sigma_{11}$ [MPa]

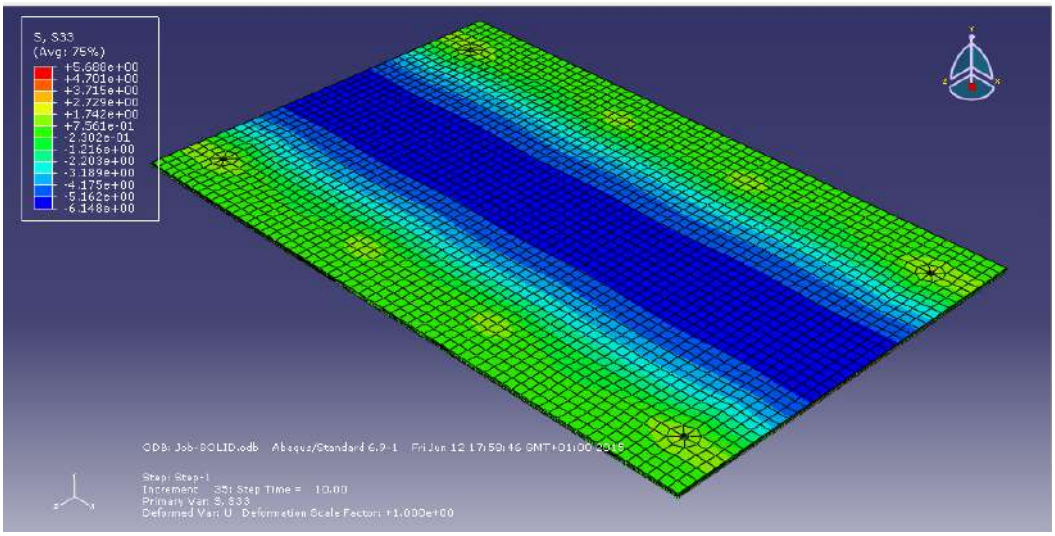


Figure 3.24: $\sigma_{33}$ [MPa]

### 3.4.2 Intermediate behavior

In the intermediate situation the load duration considered was 3 seconds and the temperature 20$^{o}$C. The PVB's characteristics are expressed on table 3.5

| G | E |
|---|---|
| 8.06MPa | 24.02 MPa |

Table 3.5: PVB's properties for the intermediate behavior

The displacements obtained are expressed on the Figure 3.25 and the stresses are expressed in Figures 3.26 and 3.27.

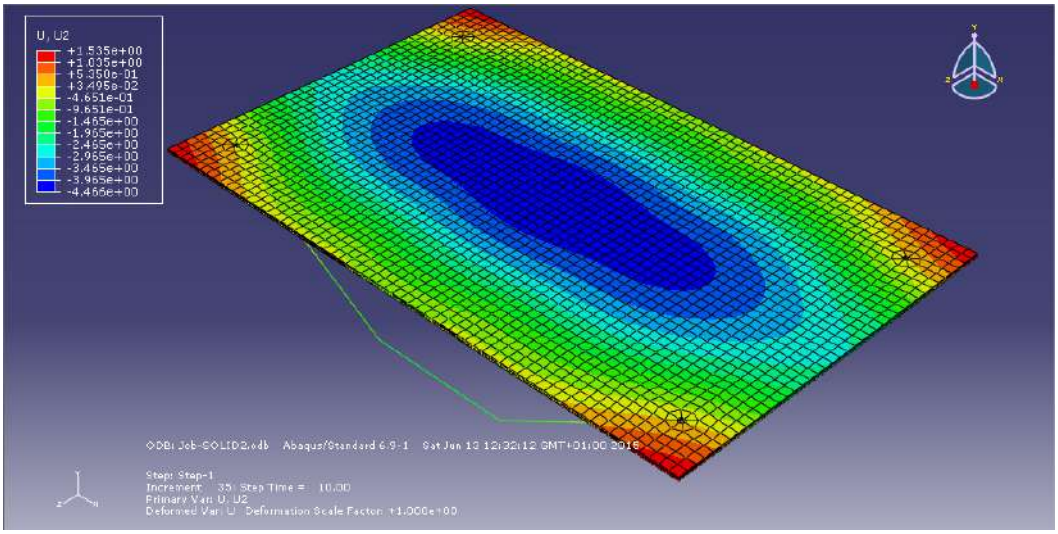


Figure 3.25: Displacements [mm]

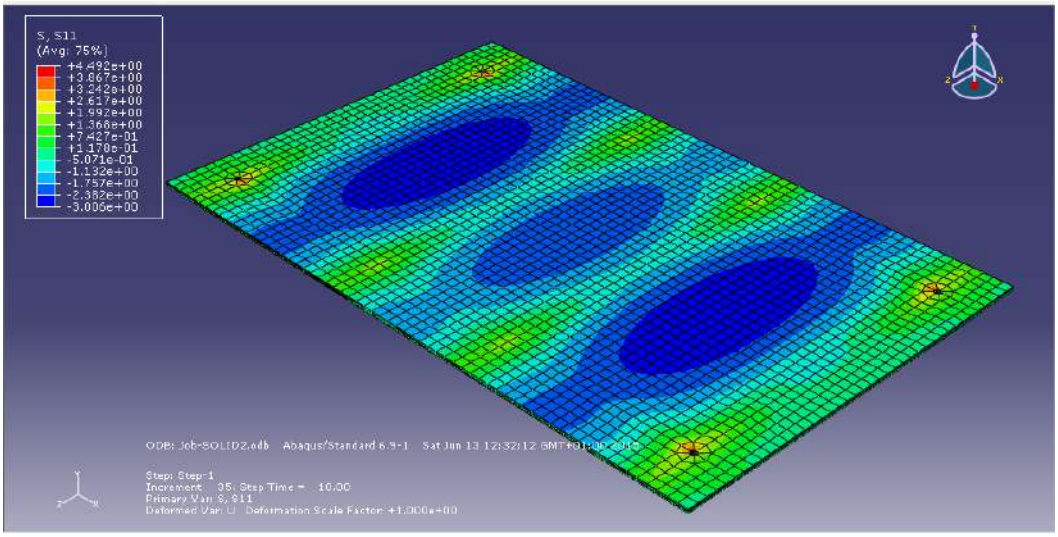


Figure 3.26: $\sigma_{11}$ [MPa]

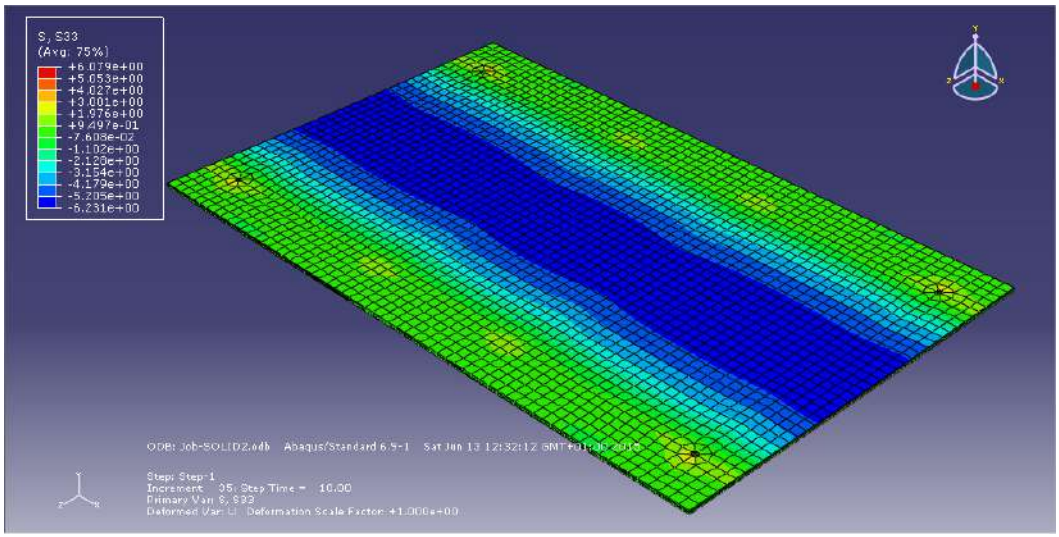


Figure 3.27: $\sigma_{33}$ [MPa]

### 3.4.3 Layered 1 behavior

In the layered 1 situation the load duration considered was 10 minutes and the temperature 50$^{o}$C. The PVB's characteristics are expressed on table 3.6

| G | E |
|---|---|
| 0.2 MPa | 0.596 MPa |

Table 3.6: PVB's properties for the layered 1 behavior

The displacements obtained are expressed on the Figure 3.28 and the stresses are expressed in Figures 3.29 and 3.30.

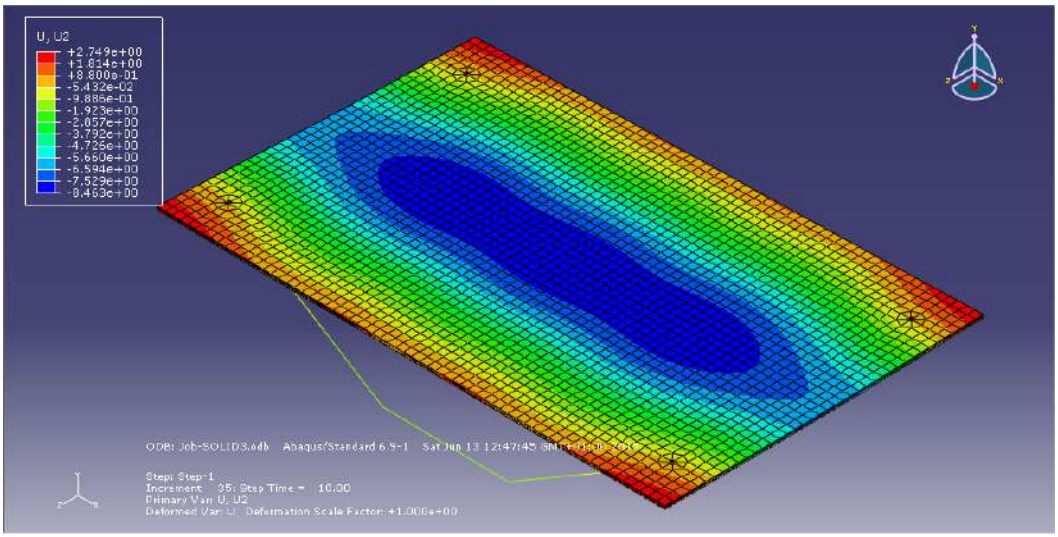


Figure 3.28: Displacements [mm]

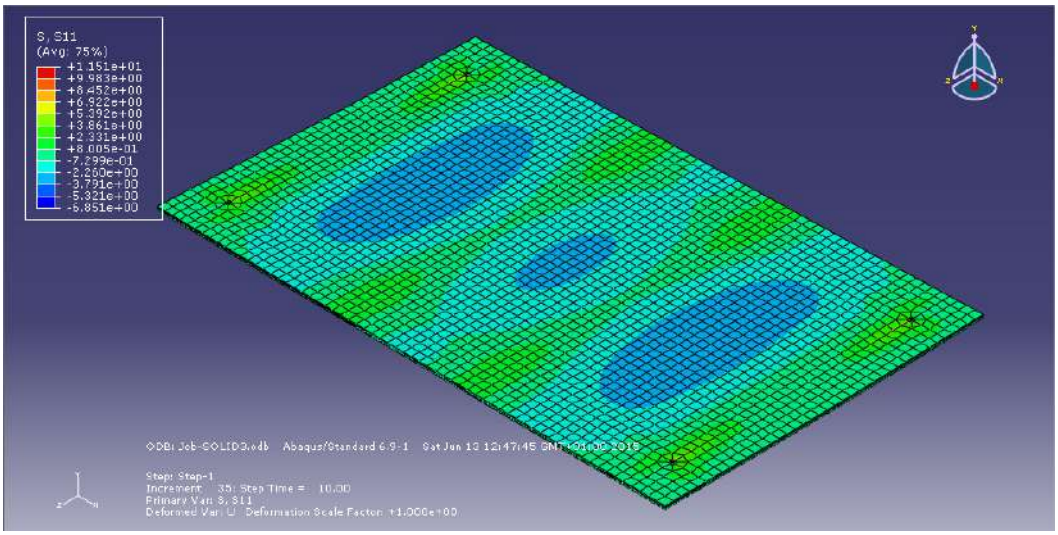


Figure 3.29: $\sigma_{11}$ [MPa]

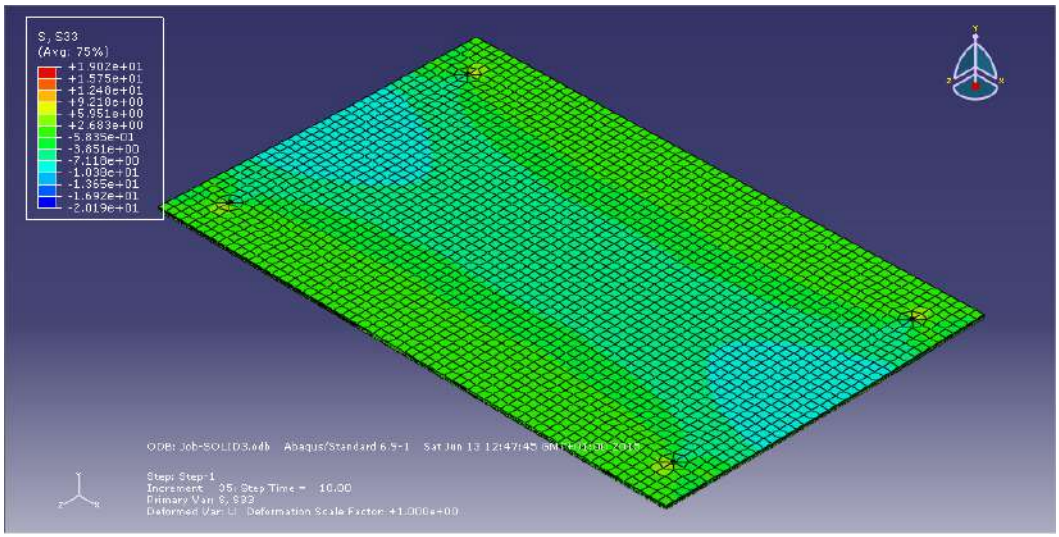


Figure 3.30: $\sigma_{33}$ [MPa]

### 3.4.4 Layered 2 behavior

In the layered 2 situation the load duration considered was 50 years and the temperature 50$^{o}$C. The PVB's characteristics are expressed on table 3.7

| G | E |
|---|---|
| 0.052 MPa | 0.155 MPa |

Table 3.7: PVB's properties for the layered 2 behavior

The displacements obtained are expressed on the Figure 3.31 and the stresses are expressed in Figures 3.32 and 3.33.

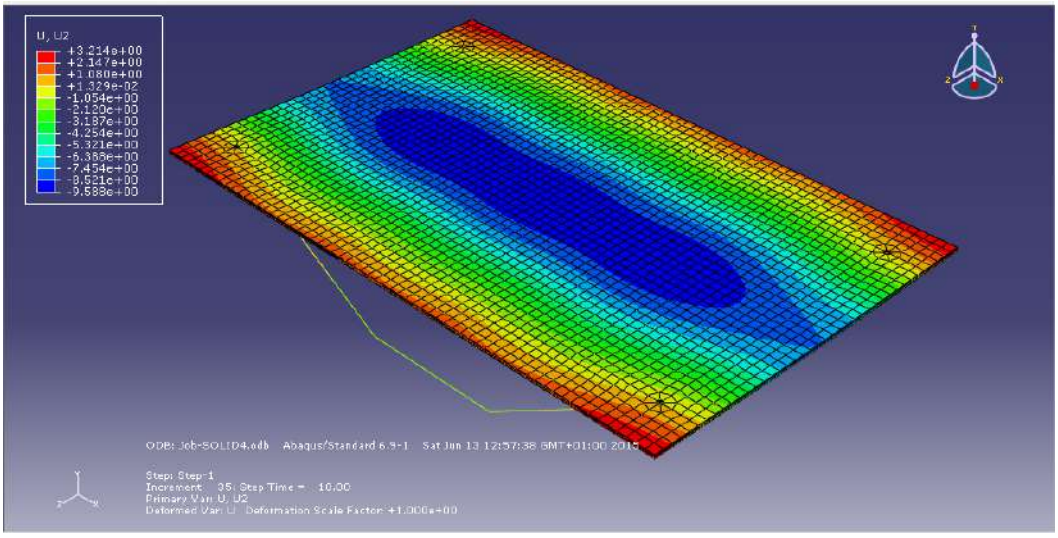


Figure 3.31: Displacements [mm]

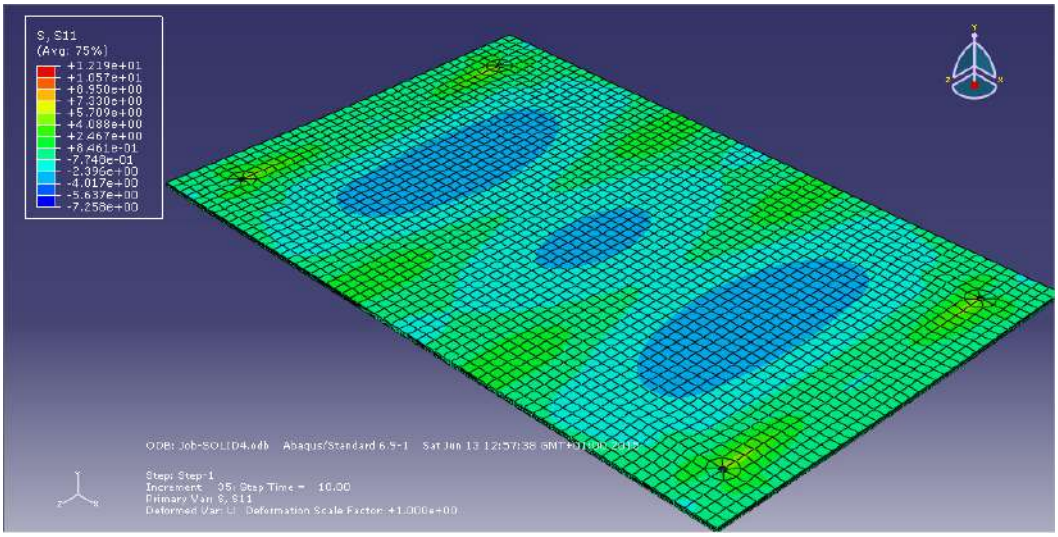


Figure 3.32: $\sigma_{11}$ [MPa]

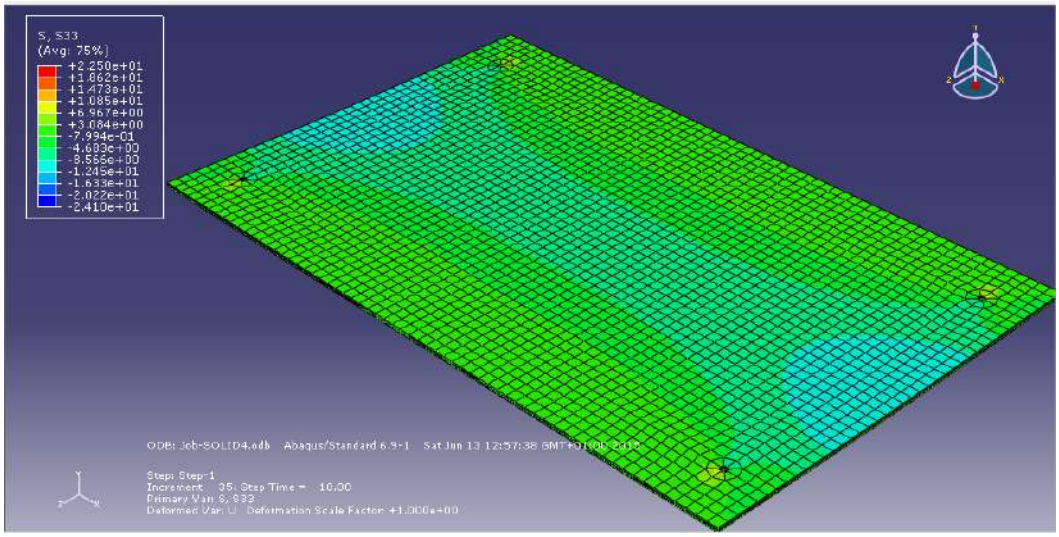


Figure 3.33: $\sigma_{33}$ [MPa]

### 3.4.5 Comments on the results obtained

*Displacements*
From the displacements diagrams obtained in the four different situations, represented in Figures 3.22, 3.25, 3.28 and 3.31, it can be observed that, as expected, the deformed shape of the pane is gradually increasing. The central point displacements in all the four situations are expressed on the table 3.8. It can be noted that the displacement increases $2,5$ times from monolithic to layered.

Apart from the increasing magnitude of the displacements, it can also be noted that the pane's behavior changes gradually to a situation similar to cylindrical bending.

| | U2 [mm] |
|---|---|
| Monolithic | -3.9045 |
| Intermediate | -4.46532 |
| Layered 1 | -8.46128 |
| Layered 2 | -9.58516 |

Table 3.8: Displacements on the central point [mm]

*Stresses*
Except for the magnitude, the stresses distributions are similar in all the four situations. Note that the scale isn't the same in all the images. The stress magnitude increases from monolithic to layered.

### 3.4.6 Analysis of the tension within the thickness and the influence of PVB shear modulus

The tensions within the thickness depends upon PVB's capacity to transfer shear load. As the pane behavior goes from monolithic to layered, the tensions distribution have distinct configurations. When the shear modulus value is high, the structure behaves as monolithic,

as the two glass sheets and PVB behave as a single element. This is illustrated on the graphic of the Figure 3.34. On the other hand, when the shear modulus is low the glass sheets act individually, and the interlayer is not able to transfer the shear load, as can be seen on the graph of the Figure 3.37. In between these two limit situation, the structure behavior is intermediate, as can be seen on the graphs in Figures 3.35 and 3.36.

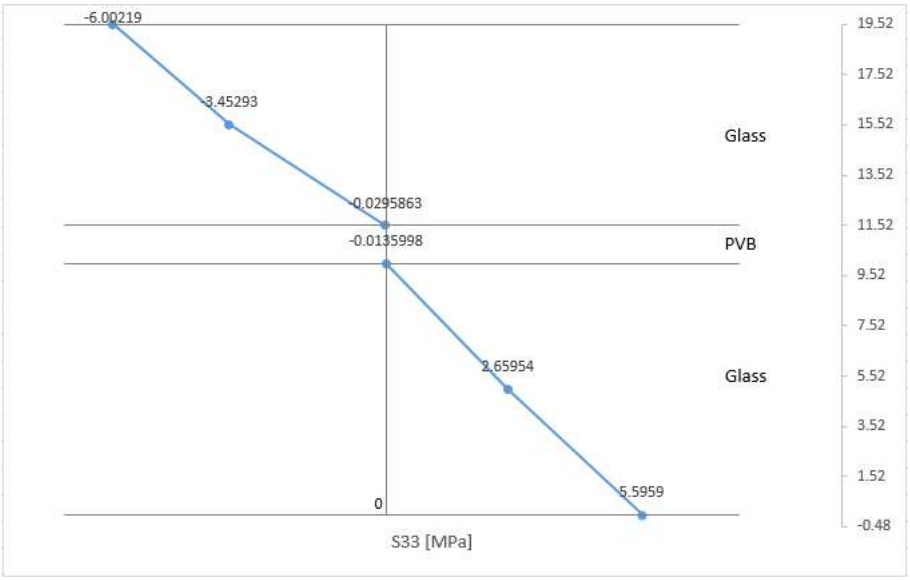


Figure 3.34: Monolithic behavior - $\sigma_{33}$ within the thickness [MPa]

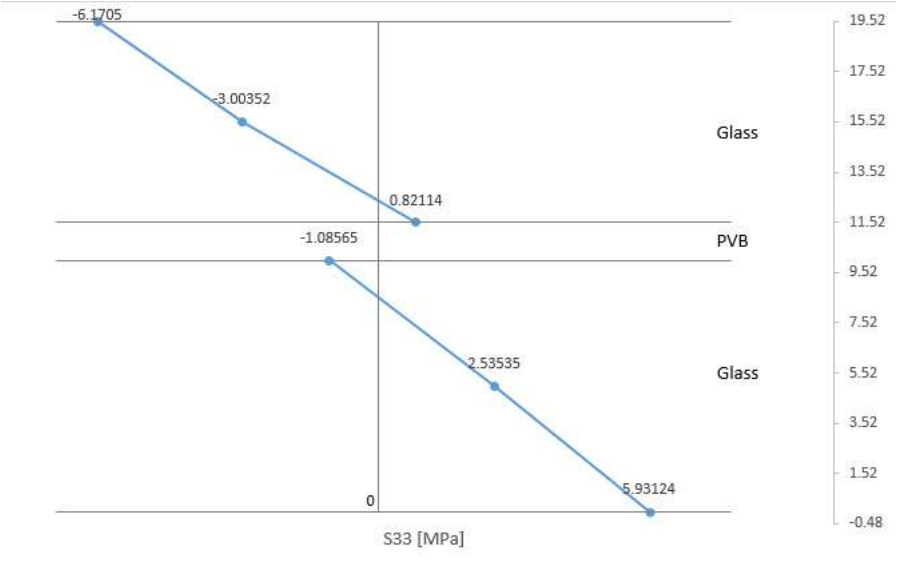


Figure 3.35: Intermediate behavior - $\sigma_{33}$ within the thickness [MPa]

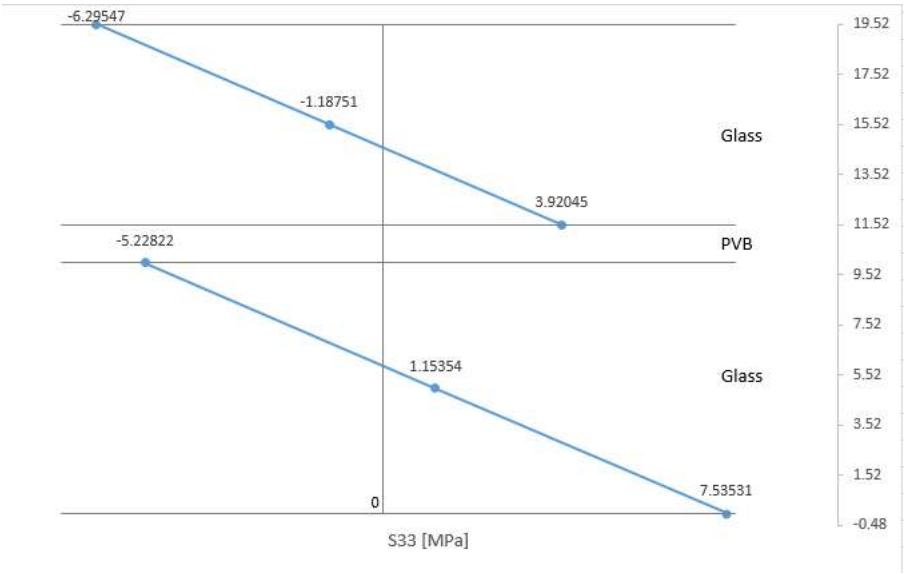


Figure 3.36: Layered 1 behavior - $\sigma_{33}$ within the thickness [MPa]

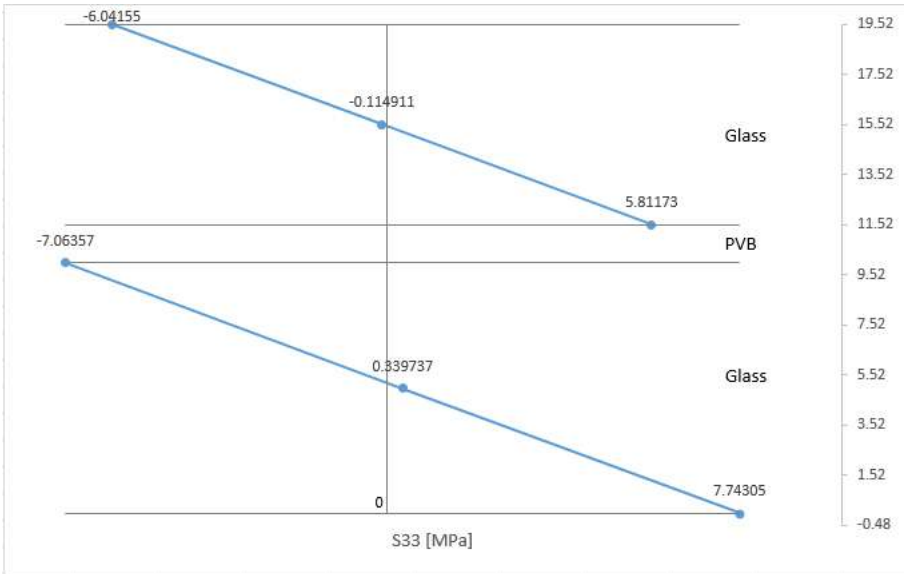


Figure 3.37: Layered 2 behavior - $\sigma_{33}$ within the thickness [MPa]

## 3.5 Comparison between shell model with EET and solid model

| | S11 | | S33 | |
|---|---|---|---|---|
| | ABAQUS | SAP2000 | ABAQUS | SAP2000 |
| G=500MPa;Short Duration Load | -2.18426 | -3.002762121 | -6.00219 | -9.859225727 |
| G=8.06MPa;20$^{o}$C;3sec | -2.35067 | -3.017388431 | -6.1705 | -10.19242012 |
| G=0.2MPa;50$^{o}$C;10min | -2.58257 | -3.472483179 | -6.29547 | -16.07492231 |
| G=0.052MPa;50$^{o}$C;50years | -2.80099 | -3.798391842 | -6.04155 | -19.11950193 |

Table 3.9: Comparison between the stresses obtained with Abaqus and with SAP2000

# Chapter 4

# Numerical implementation of an adaptive glass pane

## 4.1 Introduction

In this chapter is presented the numerical implementation of an adaptive glass pane, subjected to a wind dynamic loading. The flexibility and mass matrices were used to compute the dynamic matrix and the dynamic parameters were characterized. The dynamic wind action was also characterized. A solid model of the system was created on Abaqus software, and the obtained results are presented. At last, a comparison between the solid model and the shell models with EET previously analyzed is presented.

## 4.2 System's response

The dynamic study of a glass pane was performed using a simulation in the software MatLab. The implementation of a control routine to mitigate the mean wind action was developed, and is presented in the following sections.

### 4.2.1 Dynamic behavior of the glass pane

The dynamic behavior of the pane was analyzed, using a finite-element model made with the software SAP2000. The mode shapes were obtained as well as the corresponding vibration frequencies. The natural frequency of the glass pane yielded $17.92Hz$. A sensibility analysis was conducted in order to simplify the structure, reducing the number of degrees of freedom (DOF), keeping the frequency as close as possible to the initial. Taking advantage of its double symmetry, it was possible to obtain a system corresponding to a $1/4$ of the total pane, with 19 DOF and frequency of $17.36Hz$. The mesh is represented in Figures 4.1 and 4.2.

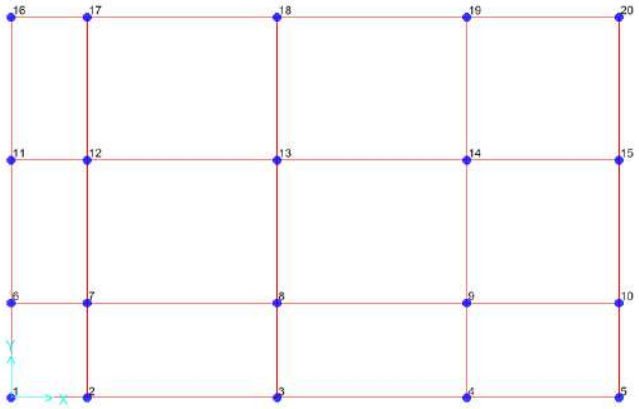


Figure 4.1: Final mesh associated to the 1/4 of the pane

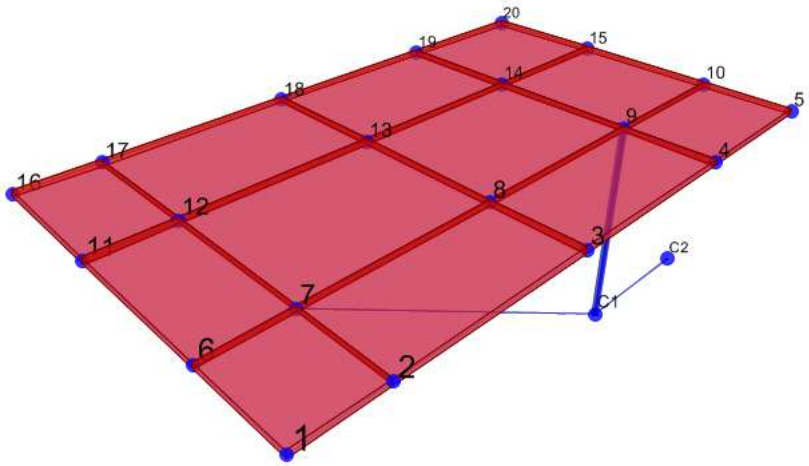


Figure 4.2: FE model of the simplified system

It should be noted that the node 7 of the represented FE model corresponds to the point of support. The node 9 corresponds to the point where the deviator meets the pane and where the control force will act.

By applying an unitary force in each DOF and obtaining the displacements induced by that force, the flexibility matrix can be constructed.

The flexibility matrix obtained, in $[m/kN]$ is represented in appendix B, as well as the mass matrix.

Assuming in a simplified way that to each DOF corresponds a lumped mass, the mass matrix was obtained by assigning to each DOF an influence area which was then multiplied by the thickness and density of each material (PVB and glass).

From the flexibility and mass matrices the dynamic matrix can be determined by the expression: $D = F \cdot M$. The dynamic matrix is represented in appendix B.

Knowing the dynamic matrix, the modal frequencies and vibration modes can be characterized by the expressions:

Modal frequencies, $\omega$:

$$\omega = \frac{1}{\sqrt{eigenvalues(D)}}$$

Vibration modes, $\phi$:

$$\phi = eigenvectors(D)$$

### 4.2.2 Motion equation solution

For a discrete action, the system's response can be achieved in a numerical way by interpolating the action in time steps [7]. For a multiple degrees of freedom system, the final response is given by a modal superposition. In a damped system, the motion equation is given by the expression:

$$m\ddot{u} + c\dot{u} + ku = p_i + \frac{\Delta p_i}{\Delta t_i} \tag{4.1}$$

The system response is given by the following expression [7]:

$$\begin{aligned} u(\tau) = u_i e^{-\zeta\omega_n\tau}\left(\frac{\zeta}{\sqrt{1-\zeta^2}}\sin\omega_D\tau + \cos\omega_D\tau\right) + \dot{u}_i e^{-\zeta\omega_n\tau}\left(\frac{1}{\omega_D}\sin\omega_D\tau\right) + \\ \frac{p_i}{K_n}\left[1 - e^{-\zeta\omega_n\tau}\left(cos\omega_D\tau + \frac{\zeta}{\sqrt{1-\zeta^2}}\sin\omega_D\tau\right)\right] + \\ \frac{\Delta p_i}{K_n}\left[\frac{\tau}{\delta t_i} - \frac{2\zeta}{\omega_n\Delta t_i} + e^{-\zeta\omega_n\tau}\left(\frac{2\zeta^2-1}{\omega_D\delta t_i}\sin\omega_D\tau + \frac{2\zeta}{\omega_n\delta t_i}\cos\omega_D\tau\right)\right] \end{aligned} \tag{4.2}$$

While the response's velocity is given by [7]:

$$\begin{aligned} \dot{u}(\tau) = -u_i e^{-\zeta\omega_n\tau}\left(\frac{\omega_n}{\sqrt{1-\zeta^2}}\sin\omega_D\tau\right) + \dot{u}_i e^{-\zeta\omega_n\tau}\left(\cos\omega_D\tau - \frac{\zeta}{\sqrt{1-\zeta^2}}\sin\omega_D\tau\right) + \\ \frac{p_i}{K_n}e^{-\zeta\omega_n\tau}\left(\frac{\omega_n}{\sqrt{1-\zeta^2}}\sin\omega_D\tau\right) + \frac{\Delta p_i}{K_n\Delta t_i}\left[1 - e^{-\zeta\omega_n\tau}\left(\frac{\zeta}{\sqrt{1-\zeta^2}}\sin\omega_D\tau + \cos\omega_D\tau\right)\right] \end{aligned} \tag{4.3}$$

The previous expressions with $\tau = \Delta t_i$, return respectively the structure's response $u_{i+1}$ and the structure response's velocity $u_{i+1}^{\cdot}$ in the instant $t_{i+1}$. The aforementioned expressions can be simplified replacing the parameters A, B, C, D, A', B', C' and D' presented on the table XXX, obtaining the following expressions:

$$u_{i+1} = Au_i + B\dot{u}_i + Cp_i + Dp_{i+1} \tag{4.4}$$

$$u_{i+1}^{\cdot} = A'u_i + B'\dot{u}_i + C'p_i + D'p_{i+1} \tag{4.5}$$

| | |
|---|---|
| A | $e^{-\zeta\omega_n\Delta t}\left(\frac{\zeta}{\sqrt{1-\zeta^2}}\sin\omega_D\Delta t + \cos\omega_D\Delta t\right)$ |
| B | $e^{-\zeta\omega_n\Delta t}\left(\frac{1}{\omega_D}\sin\omega_D\Delta t\right)$ |
| C | $\frac{1}{K_n}\left\{\frac{2\zeta}{\omega_n\Delta t} + e^{-\zeta\omega_n\Delta t}\left[\left(\frac{1-2\zeta^2}{\omega_D\Delta t} - \frac{\zeta}{\sqrt{1-\zeta^2}}\right)\sin\omega_D\Delta t - \left(1+\frac{2\zeta}{\omega_n\Delta t}\right)\cos\omega_D\Delta t\right]\right\}$ |
| D | $\frac{1}{K_n}\left[1 - \frac{2\zeta}{\omega_n\Delta t} + e^{-\zeta\omega_n\Delta t}\left(\frac{2\zeta^2-1}{\omega_D\Delta t}\sin\omega_D\Delta t + \frac{2\zeta}{\omega_n\Delta t}\cos\omega_D\Delta t\right)\right]$ |
| A' | $e^{-\zeta\omega_n\Delta t}\left(\frac{\omega_n}{\sqrt{1-\zeta^2}}\sin\omega_D\Delta t\right)$ |
| B' | $e^{-\zeta\omega_n\Delta t}\left(\cos\omega_D\Delta t - \frac{\zeta}{\sqrt{1-\zeta^2}}\sin\omega_D\Delta t\right)$ |
| C' | $\frac{1}{K_n}\left\{-\frac{1}{\Delta t} + e^{-\zeta\omega_n\Delta t}\left[\left(\frac{\omega_n}{\sqrt{1-\zeta^2}} + \frac{\zeta}{\Delta t\sqrt{1-\zeta^2}}\right)\sin\omega_D\Delta t + \frac{1}{\Delta t}\cos\omega_D\Delta t\right)\right\}$ |
| D' | $\frac{1}{K_n\Delta t}\left[1 - e^{-\zeta\omega_n\Delta t}\left(\frac{\zeta}{\sqrt{1-\zeta^2}}\sin\omega_D\Delta t + \cos\omega_D\Delta t\right)\right]$ |

Table 4.1: A,B,C,D,A',B',C' and D' parameters [7]

Being $\omega_D$ the damped structure's frequency, given by the expression:

$$\omega_D = \omega_n\sqrt{1-\zeta^2} \tag{4.6}$$

As mentioned before, in a system with multiple degrees of freedom, the final structure's response is given by a modal superposition. To each degree of freedom corresponds a vibration mode defined by an expression and the solution of each expression represents a modal coordinate. The modal superposition is given by the following expression:

$$u = \sum \phi_i q_i \tag{4.7}$$

### 4.2.3 Characterization of the wind action

The mean wind velocity series were retrieved from the portuguese wunderground (http://portuguese.wundergrounc database. The latter provides the daily variation of wind velocity with a 30 minutes interval.

The velocity values were adjusted in order to set the value prescribed in Eurocode 1-4, $30m/s$. The mean wind pressure was subsequently calculated using the following expression:

$$q_p = 1/2 \cdot \rho \cdot v^2$$

in which $\rho$ represents the air's density and $v$ the wind velocity.

To characterize the wind force in each degree of freedom, the following relation was used:

$$F_w = C_{pe} \cdot q_p \cdot A$$

in which:
$C_{pe}$ represents the exterior pressure coefficient;
$q_p$ is the wind pressure previously calculated;
$A$ is the influence area of each DOF.

Thus, the graphic of the Figure 4.3 is obtained, which represents the wind pressure in the pane, throughout the day.

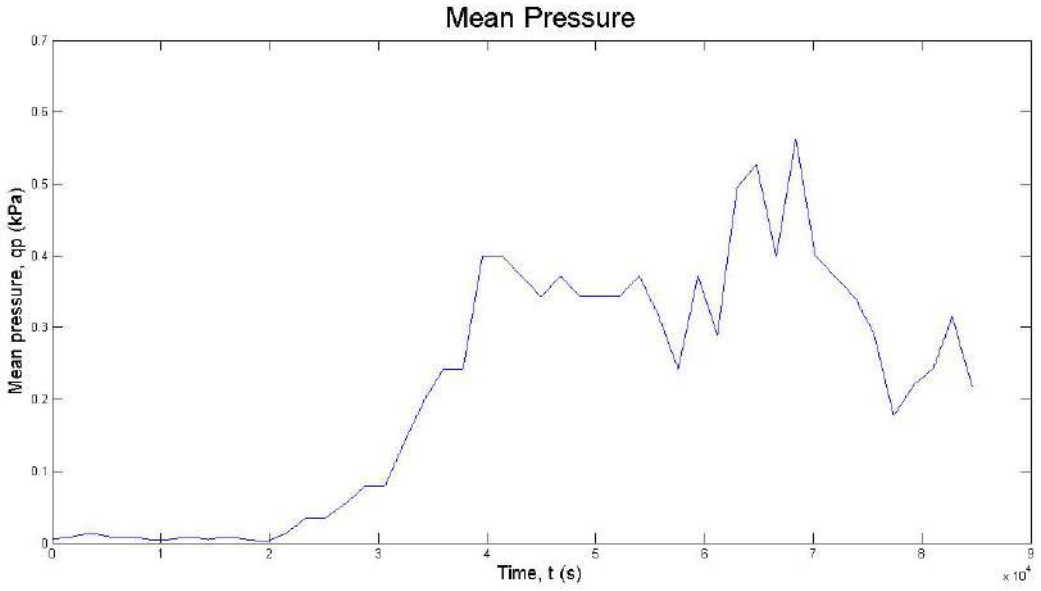


Figure 4.3: Wind pressure [kPa]

# Chapter 5

# Control system implementation

## 5.1 Introduction

In this chapter the active control system is analyzed and subsequently implemented in the studied structure. The system is implemented in order to control a variable, measuring its value and forcing it to comply with a previously set value. In this particular case, the variable to control is the displacement in the central point of the pane. This input signal is afterwards subjected to a control function that relates the input and the output signal. The block diagram of the figure 6.12 illustrates this simple action.

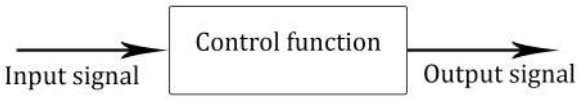


Figure 5.1: Control system

## 5.2 Control type

The control action considered in this study was the PID system, in which three control actions are combined in order to improve the system response:

### 5.2.1 Proportional control

With this control action, the output of the controller is proportional to the error signal. The response of this action can be described as:

$$u(t) = K_p \cdot e(t);$$

in which $K_p$ is a adjustable constant called proportional gain.

When an error proportional force is being generated is as though a displacement proportional force is being introduced [21]. This effect in an mechanical system involves a stiffness

increase. Therefore, through the proportional gain action it is possible to modify a system's natural frequency.

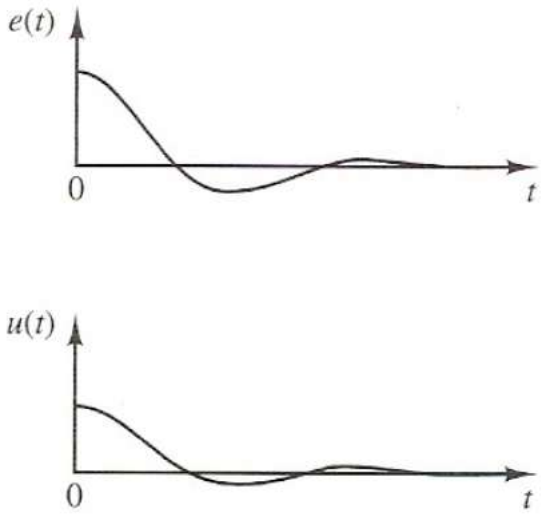


Figure 5.2: Proportional control - Adapted from [23]

### 5.2.2 Integral control

With integral control, the output of the controller is proportional to the integral of the error signal, the response being generally described as:

$$u(t) = K_i \cdot \int_0^t e(t)dt.$$

in which $K_i$ is a adjustable constant called integrative gain.

As the controller response is defined by the integral of the error signal, it should be noted that being the error null at a certain instant it does not mean that the system's response also is null, in contrast with what happens with the proportional control. This behavior is illustrated by the graphics of the figure 5.3.

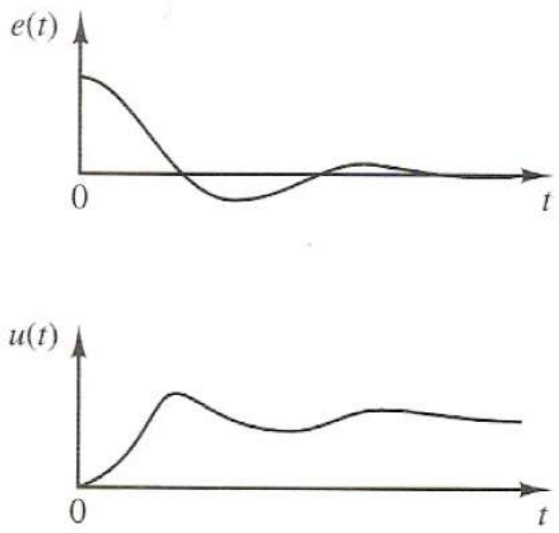


Figure 5.3: Integral control - Adapted from [23]

### 5.2.3 Derivative control

The derivative control response is proportional to the rate of change of the error signal. This way, the response is generally described as:

$$u(t) = K_d \cdot \frac{de(t)}{dt};$$

in which $K_d$ is a adjustable constant called derivative gain.

As in the proportional controller case, the derivative controller's action on a mechanical system also modifies the dynamic properties. As mentioned above, the derivative control action outcome is proportional to the rate of change of the error signal, that corresponds to the application of a force proportional to the velocity. This is equivalent to the introduction of an additional damping on the system. This control action is never implemented isolated. It's usual to combine the action of a derivative controller with a proportional controller. The control response is described as:

$$u(t) = K_p \cdot e(t) + K_d \cdot \frac{de(t)}{dt};$$

where $K_p$ and $K_d$ are adjustable constants.

The PD control action can be observed in the graphics of the Figure 5.4.

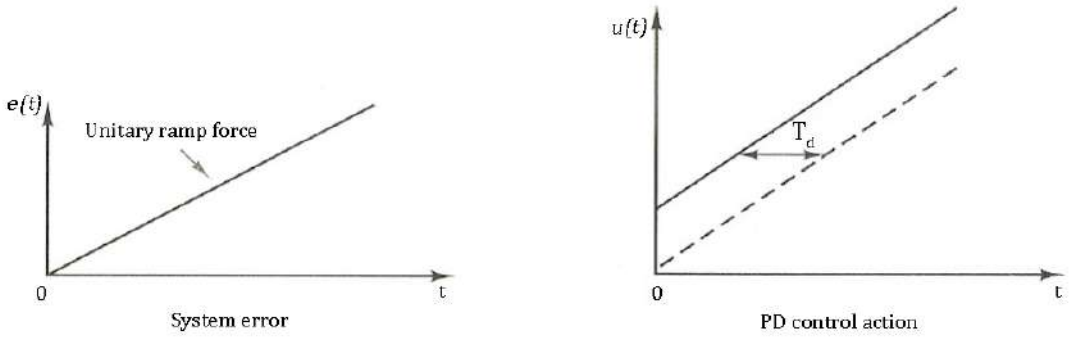


Figure 5.4: Proportional and derivative control - Adapted from [23]

From the graphic exposed above, it can be observed an error anticipation of $T_d$.

### 5.2.4 PID control

A PID control system is a system that combines all the types of control previously described: proportional, integral and derivative. The controller response is given by the following expression:

$$u(t) = K_p \cdot e(t) + K_i \cdot \int_0^t e(t)dt + K_d \cdot \frac{de(t)}{dt};$$

Knowing that $K_i = \frac{K_p}{T_i}$ and $K_d = K_p \cdot T_d$ and replacing on the controller's response expression:

$$u(t) = K_p \cdot e(t) + \frac{K_p}{T_i} \cdot \int_0^t e(t)dt + K_p \cdot T_d \cdot \frac{de(t)}{dt};$$

where $K_p$ is the proportional gain; $T_i$ is the integral time and $T_d$ is the derivative time.

The PID controller response is represented on the graphic of the Figure 5.5.

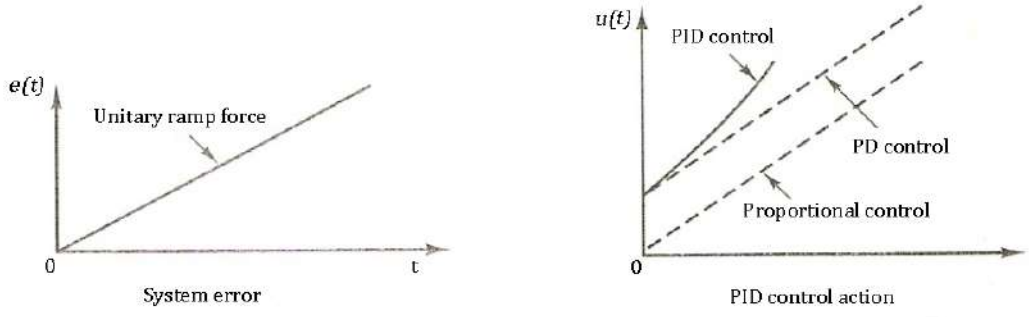


Figure 5.5: Proportional, integrative and derivative control - Adapted from [23]

From the graphic presented, it can be observed that the PID response not only presents an error anticipation as in the PD control, but also the control action velocity is increased by the integral action.

## 5.3 Algorithm to implement the control system

To impose the PID action and control the displacements on the central point an algorithm was implemented with the procedure described below:

- A dynamic study was performed on the system, defining the mass and dynamic matrices. After defining the damping, the modal frequencies, vibration modes and damped frequencies can be calculated. The time is also set, in accordance with the time defined on the wind characterization.
- The wind force is defined, in accordance with the procedure previously described on section 4.2.3.
- The generalized forces for each vibration mode are defined by the expression:

$$F_n = \phi_n^T \cdot f(t) \tag{5.1}$$

- After, the A, B, C, D, A', B', C' and D' parameters are defined, according to the expressions described on section 4.2.2 and the structure's response and its velocity to each vibration mode are respectively given by the following expressions:

$$u_{i+1} = Au_i + B\dot{u}_i + Cp_i + Dp_{i+1} \tag{5.2}$$

$$\dot{u_{i+1}} = A'u_i + B'\dot{u}_i + C'p_i + D'p_{i+1} \tag{5.3}$$

  A modal superposition gives the structure's final response:

$$u = \sum \phi_i q_i \tag{5.4}$$

Until this phase, the system's response is being defined with no type of control. The outcome is the passive system's behavior to the defined action.

Then the proportional, integrative and derivative gains are defined, the control node and the node in which the results are consulted are set.

Afterwards the structure's response with control is defined:

$$u(t) = K_p e(t) + K_i \int_0^t e(t) + K_d \frac{de(t)}{dt} \tag{5.5}$$

After the system's response with control is defined, the same steps are set as before, and the two situations are compared in terms of a superposed graphic with the two responses.

## 5.4 Tuning of the controller

The proportional, integrative and derivative constants, $K_p, K_i$ and $K_d$ have to be adequately tuned in order to grant the appropriate behavior of the control system. The method used to tune the PID controller was the second method of Ziegler-Nichols in which is considered initially only the proportional action, being $K_i = K_d = 0$. The integral time, $T_i = K_p/K_i$, and derivative time, $T_d = K_d/K_p$, are respectively $\infty$ and 0 in this phase. By increasing the

proportional gain from 0 to a critical value, $K_{cr}$, the system returns a harmonic oscillatory response. When the critical value is exceeded the system becomes unstable. When the eminent instability is achieved, the critical value $K_{cr}$ and critical period $P_{cr}$ can be known and the proportional gain, integrative and derivative time can be calculated by the expressions presented on table 5.1

| | $K_p$ | $T_i$ | $T_d$ |
|---|---|---|---|
| **P** | $0.5K_{cr}$ | $\infty$ | 0 |
| **PI** | $0.45K_{cr}$ | $\frac{P_{cr}}{1.2}$ | 0 |
| **PID** | $0.6K_{cr}$ | $0.5P_{cr}$ | $0.125P_{cr}$ |

Table 5.1: $K_p$, $T_i$ and $T_d$ values

The process of tuning the controller is further developed in C.

## 5.5 Results

Two distinct analysis were conducted, one for the situation of monolithic behavior and other for the situation of layered behavior of the glass pane. The results obtained are expressed in the graphs of the Figures 5.6 and 5.7.

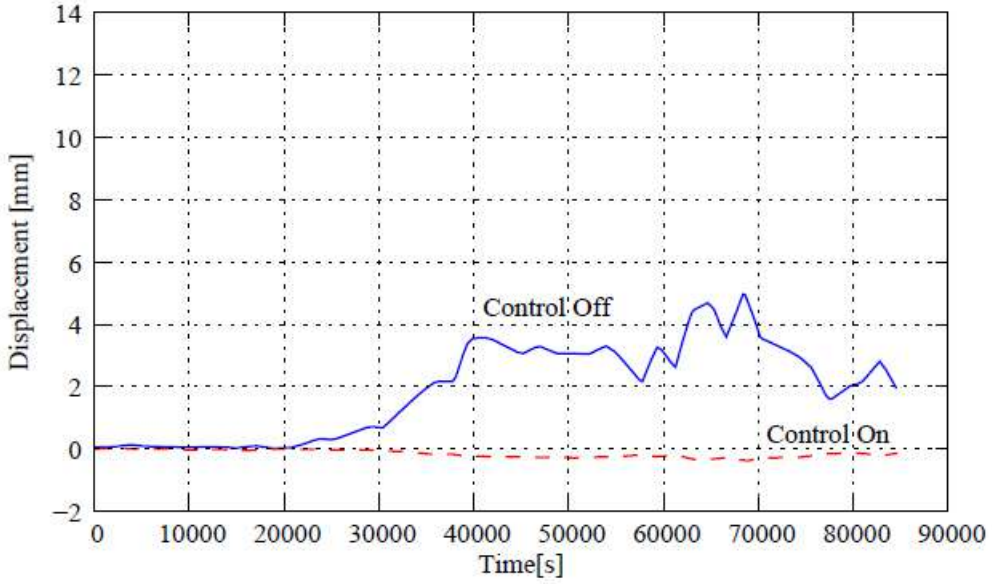


Figure 5.6: Displacements-time history for monolithic behavior

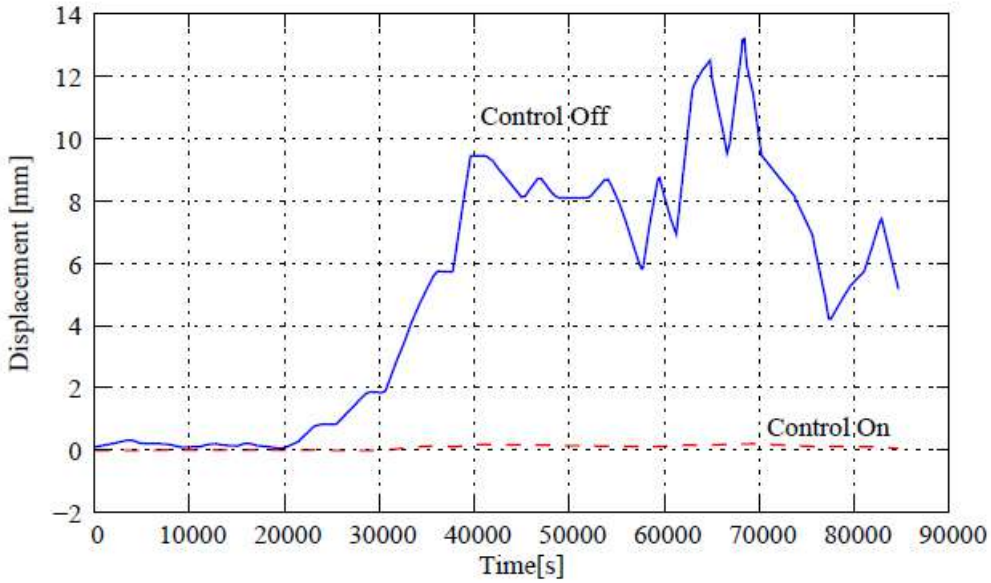


Figure 5.7: Displacements-time history for layered behavior

Both analysis present satisfying results in terms of the controlled solution, as in both situations the displacements obtained in the analysis with the active control solution are approximately null. The results are significantly distinct however when it comes to the analysis without control. This proves once again the importance of the interlayer ability to transfer shear load. The graph of the Figure 5.7 is particularly enlightening of the efficiency of the proposed system, decreasing the maximum displacement to approximately 2% of the obtained without the control system.

# Chapter 6

# Prototype analysis

## 6.1 Introduction

In this section is described the procedure of building and testing a prototype with the scaled configuration of model System 2 described on section 3.

## 6.2 Building and testing of the experimental prototype

### 6.2.1 Prototype

The prototype is composed by a $5101 \times 320 mm^2$ plexiglass plate with $2.5mm$ of thickness. The plate is pinned at four steel struts with $5mm$ diameter, which are also the points from where a cable system is set. Four additional steel struts with $3mm$ of diameter and $93mm$ of length are set on the following configuration: each pair is set in between two points of support along the longest edge, allowing the cables to take the configuration of the Figure 6.1. These two cables are SMA wires which actuates through temperature modulation by Joule effect. The whole system is assembled within a $550 \times 350 \times 200[mm^3]$ wooden box enfolding it, topped by the aforementioned plexiglass plate, and sealed along its edges. By applying a suction force within the wooden box the wind force is simulated and the system can be tested. Figure 6.2 represents a prototype construction phase.

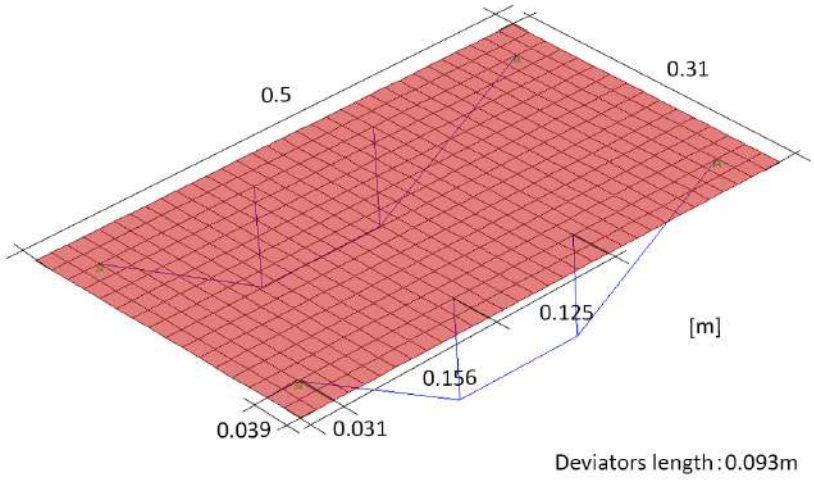


Figure 6.1: Model's dimension

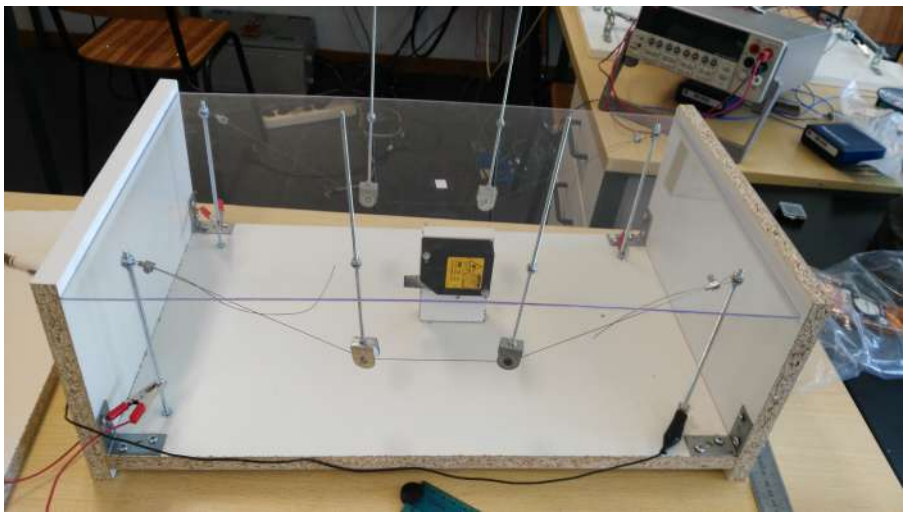

Figure 6.2: Prototype construction

The system is able to adapt its behavior to the action by compensate in real time the displacements obtained due to the external action. The control algorithm is based on a PID control approach, in which the displacements of the pane are reduced by defining a vertical reference position for the mid-section of the acrylic pane. As the suction is introduced and the pane starts to deform, the system increases the stress in the restraining wires in order to compensate for this displacement. Figure 6.3 illustrates the working principle of the experimental prototype.

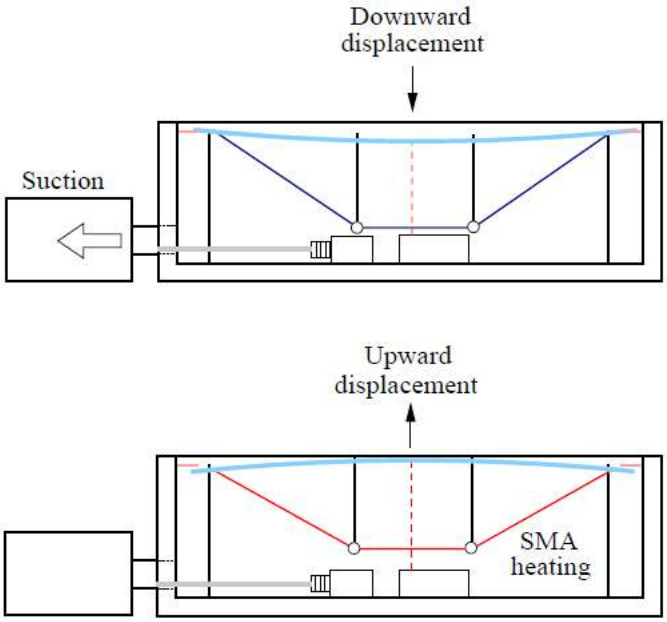


Figure 6.3: Working principle of the experimental prototype

The stress in the wires is applied to the system by temperature induced phase transformations,in NiTi SMA, martensitic actuator wires. The finalized prototype is represented in the Figure 6.4.

Figure 6.4: Prototype final

After building the prototype, the control sensors were set, from which the input is read and sent to the system. To measure the displacement of the central point, a laser measurement device was set on the framebox bottom. The SMA cables are straight and oxide-free, provided

by Dynalloy, Inc., and have a 0.51 mm diameter circular cross section .A cables' detail can be observed on the Figure 6.5.

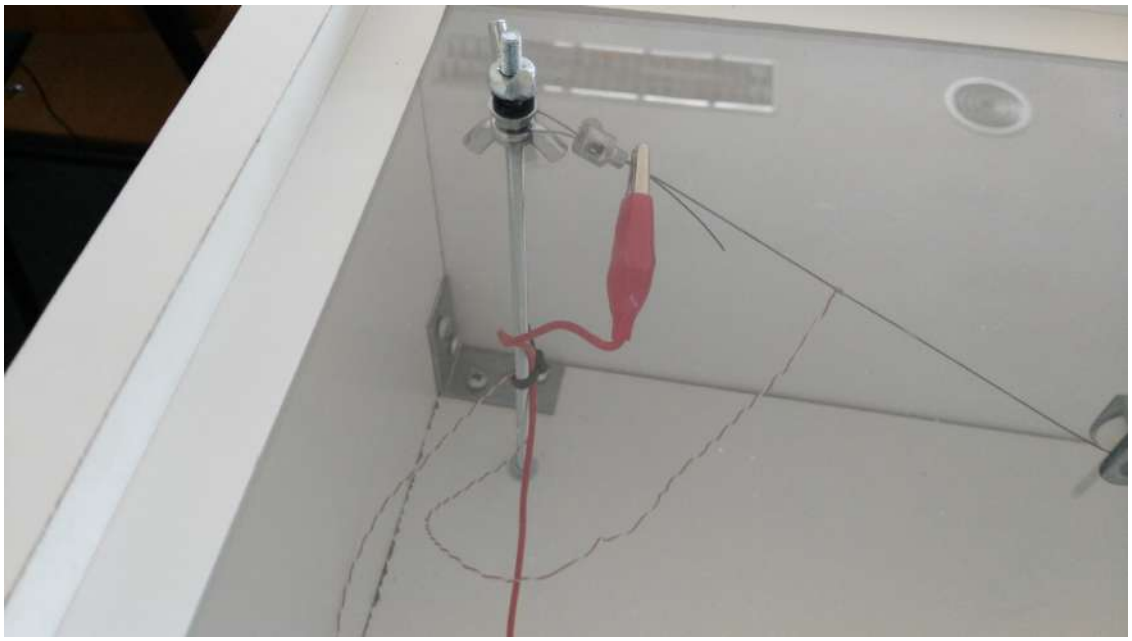

Figure 6.5: Detail of the prototype - Electric current feeding cables

To allow the Joule heating of the SMA wire actuators, a Sorensen programmable DC power supply (PPS), model XHR 40-25, was connected to the system. The control of the SMA actuator was performed in a voltage control mode, with a maximum input current of 2A. The temperature of the NiTi wires was monitored by a T-type thermocouple (Copper-Constantan), with a temperature reading range of -40?C to 100?C, connected to a NI SCXI-1112 8 channel thermocouple amplifier. To create, edit and run the analog inputs corresponding to the voltage measurement tasks was used a DAQ assistant express VI, using NI-DAQmx software. To attenuate the noise of the readings, a sample compression of the data points was performed. The system and its main features is represented in Figure 6.6.

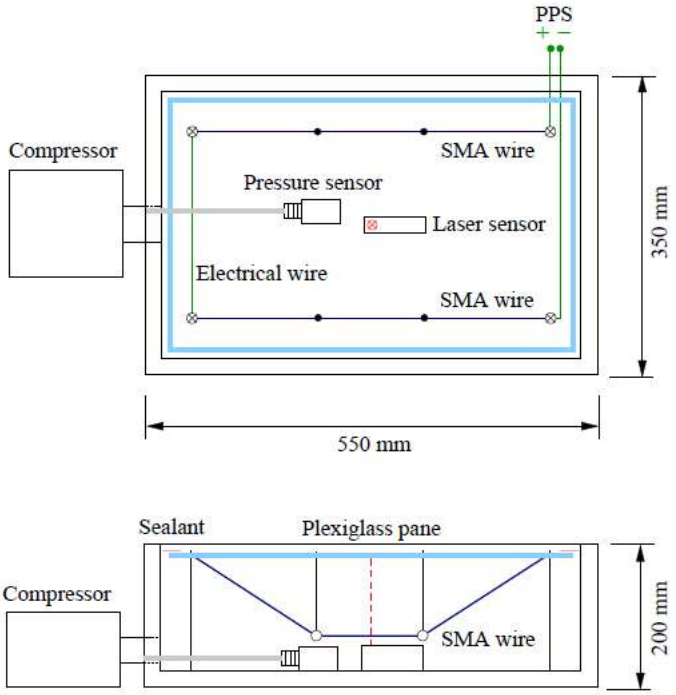


Figure 6.6: Main features of the experimental prototype

### 6.2.2 Static load test

The prototype was first tested with a static load, positioned at the center of the pane. The load values tested were 8N, 16N and 24N. The same load was simulated at software SAP2000, the displacements map obtained is shown in figure 6.7. The comparison of the displacements obtained with the two tests are expressed on table 6.1.

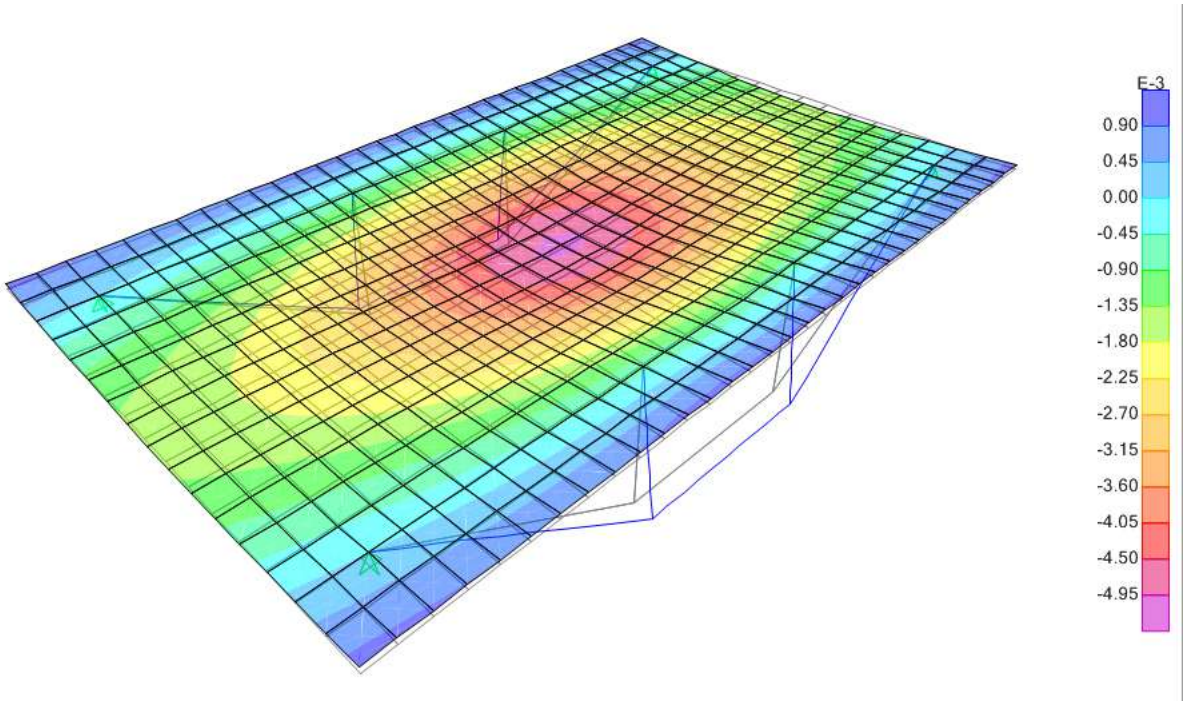


Figure 6.7: Static load displacements map obtained with SAP2000

| **Load [N]** | **Central point displacement [mm]** | |
|---|---|---|
| | **Static load test** | **SAP2000** |
| **8** | 1,9 | 1,7 |
| **16** | 3,3 | 3,4 |
| **24** | 5,1 | 5,1 |

Table 6.1: Central point displacements comparison

The obtained results shows a good conformity between the two tests.

### 6.2.3 Dynamic suction load

In order to better simulate the dynamic action of the wind load, a dynamic suction load was applied on the structure. This was achieved by isolating the wood frame and applying a suction inside it. This proved to be a easier way to apply the load than applying pressure outside it. Five separate tests were conducted, two of them without control action, the other three with control. A overlap of two tests, one without control and other with control, was made in order to better illustrate the benefit of the system. The graphs of the Figures 6.8. 6.9 and 6.10 represent respectively the pressure, displacements and cables' temperature along time.

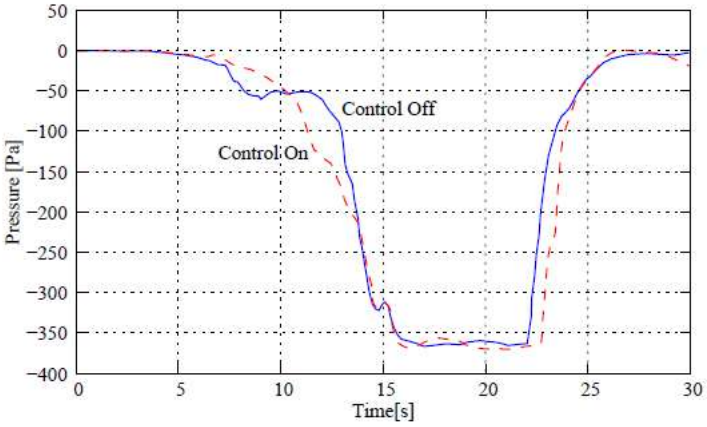


Figure 6.8: Pressure time-history

The graph of the Figure 6.8 represents the overlap of the pressure along time in the two situations tested: with control and without. Here it is desirable that the two situations are the more even possible in order to validate the comparison between the following obtained results.

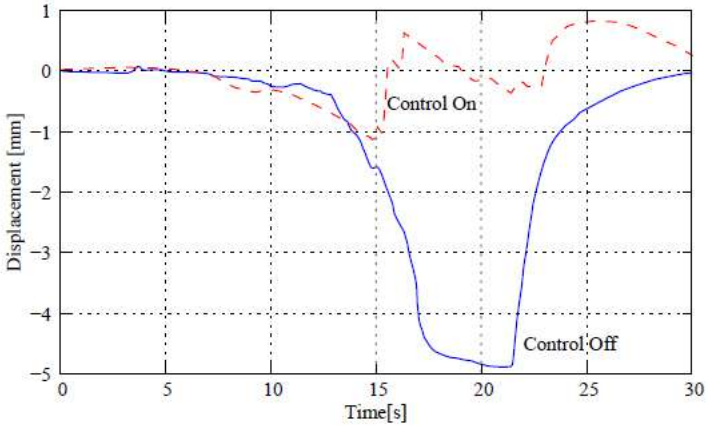


Figure 6.9: Displacement time-history

The graph of the Figure 6.9 represents the overlap of the displacements obtained in the test with control and without. Here it is visible the difference between the two situations, with the maximum displacement going from $-5mm$ in the system without control to $0.8mm$ in the controlled system. This represents an overall reduction of 85% in absolute value of the original displacement.

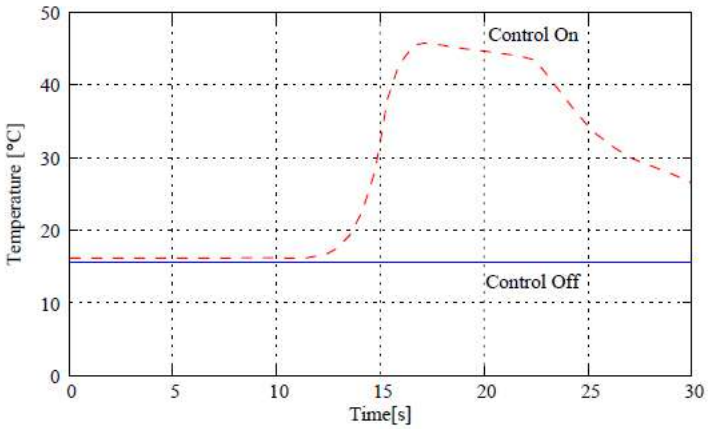


Figure 6.10: Cables' temperature time-history

The graph of the Figure 6.10 shows the overlap of the cables temperature readings, along the test. While the temperature remains constant in the test without control, in the controlled test the activation of the wires causes a considerable variation of the temperature, from approximately $18C$ up to $46C$.

## 6.3 The Labview control platform

The LabView control platform is a National Instruments development environment that allows the user to program a control code by a graphical programming syntax. The user defines the inputs and set the limits from which the control will start. The block diagram of the figure 6.11 represents the control action implemented on the prototype structure.

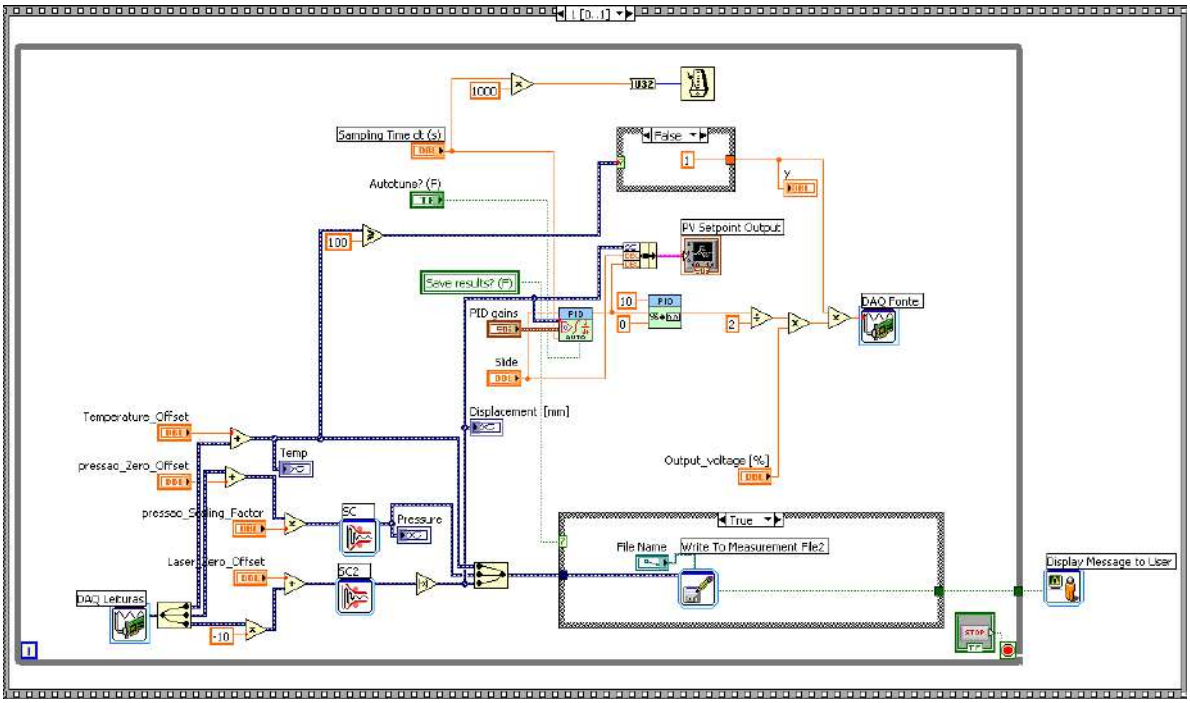


Figure 6.11: Graphical programming syntax

The system receives three inputs: the pressure inside the prototype box, the temperature on the cables and the central point displacement measured by a laser. The input that activates the control system is the midpoint displacement. When the value read reaches the setpoint previously defined, the PID control system starts reacting by sending an electric current through the cables, causing them to contract and pushing the deviators upwards. This action will force the glass pane to rise, counteracting the wind pressure effect. The PID gains are automatically calculated and adjusted by the software. The actions' sequence outline is represented on the figure6.12.

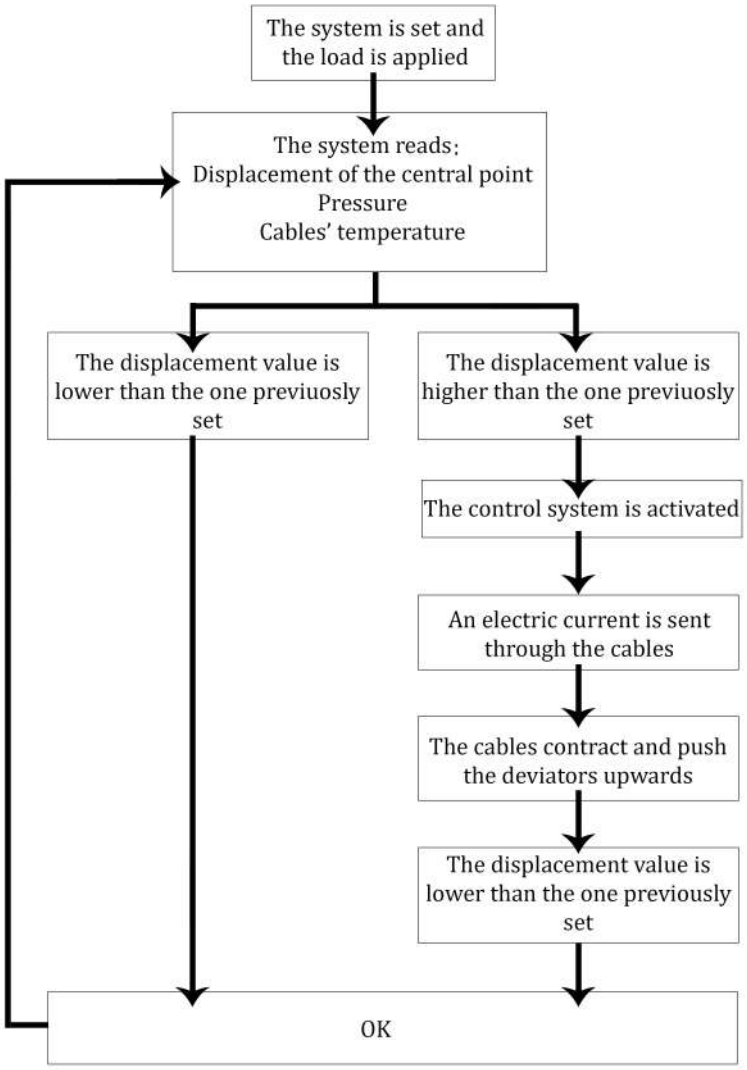


Figure 6.12: Control action block diagram

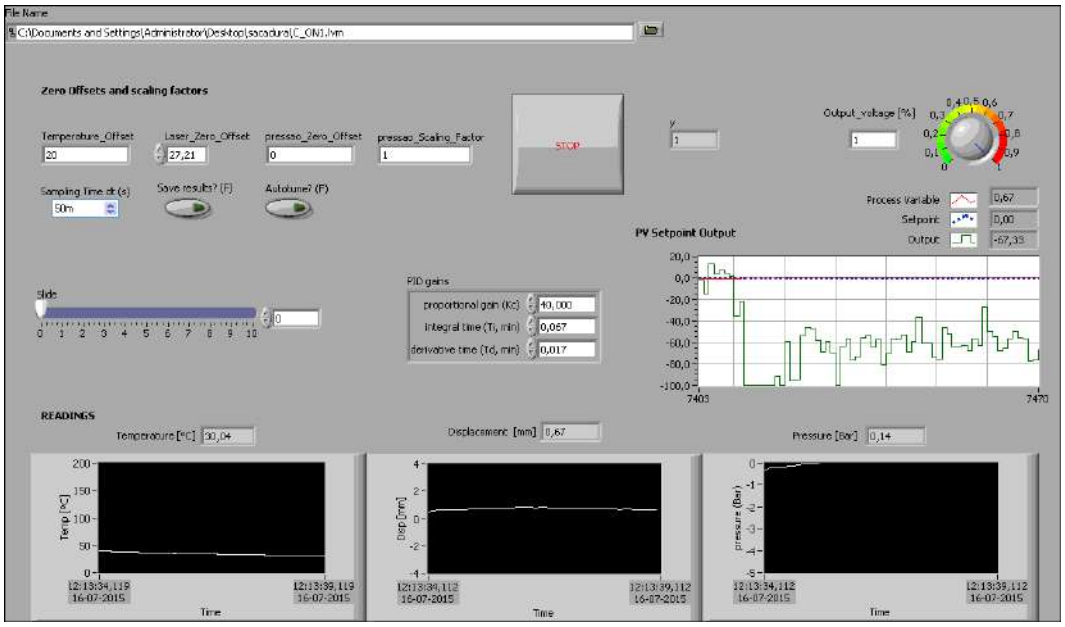


Figure 6.13: Software framework

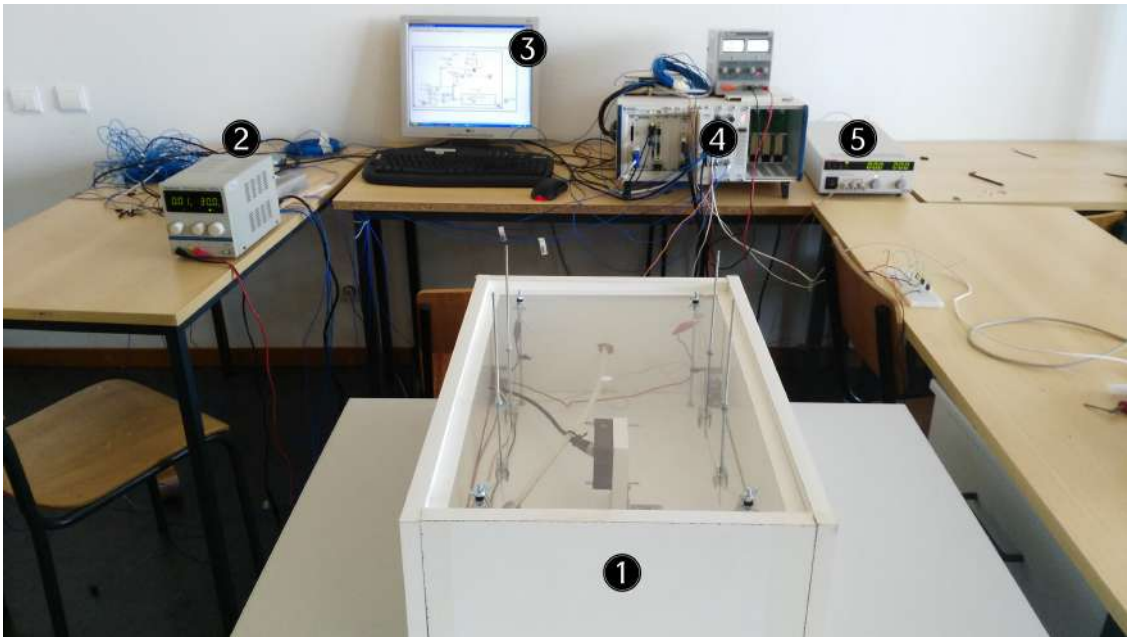


Figure 6.14: System's components overview

Legend:

1. Prototype
2. Power supply feeder
3. Monitor

4. CPU
5. Reader

# Chapter 7

# Summary, conclusions and future work

## 7.1 Summary and conclusions

The present work aimed to develop and study a smart system with active control, composed of a glass pane and a shape-memory alloys cable system. The aforementioned system would be able to process the structure reaction to an external action and implement a response in order to mitigate the deformation on the glass due to the external action.

The system here proposed presents in fact an enhanced structural behavior when compared with the same structure without the active control action.

The proposed system is able to decrease the maximum displacement to approximately 2% of the obtained without the control system.

The influence of the temperature in the layered glass structural behavior proofed to be a key point that has to be properly considered. Due to the temperature action the interlayer's ability to transfer shear load is seriously affected, going from a monolithic to layered behavior, and increasing $2,5$ times the displacements obtained with the same load condition.

The active control system implemented allows the structural engineers to develop projects in a more efficient and economic way.

The tests performed on the experimental prototype were able to implement an overall reduction of 85% in absolute value of the original displacement, due to the control action.

Being an active control system, it is important to refer its requirement of an external source of power.

This type of solution to mitigate the effects of external actions should be investigated particularly in each specific case, adapting the control system to the actual structure characteristics.

## 7.2 Future work

In order to improve this dissertation in a more comprehensively way, the control system could be implemented in more systems with other cables' configuration. In the same way, the shape

and size of the glass pane could be further developed, as well as the glass constitution: to mention some examples the thickness of the layers, interlayer material, interlayer thickness, among others.

The application of the aforementioned system to a real glass pane with the dimensions referred in this work and the comparison with other types of glass would be advantageous to understand the influence on the final behavior.

# Bibliography


[1] Alsop, D.J.A., Colvin, J., Desai, S.B., Gilder, P.J., Ledbetter, S.R., Otlet, M., Parke, G.A.R., Pike, D., Saunders, R.J., Smith, J.G. and Taylor, S.N. *Structural Use of Glass in Buildings.* SETO for The Institution of Structural Engineers, 1999. ISBN 1 874266 51 4.

[2] Amadio, C. and Bedon, C. *Elastoplastic dissipative devices for the mitigation of blast resisting cable-supported glazing facades* Engineering Structures, vol. 39, pp. 103?115, 2012.

[3] Balkow, D., Schittich, C., Schuler, M., Sobek, W. and Staib, G. *Glass Construction Manual* 1999 Birkhäuser - Publishers for Architecture ISBN 3-7643-6077-1; ISBN 0-8176-6077-1

[4] Bedon, C., Cismasiu, C. and Santos, F.A. *Smart glazed cable facade subjected to a blast loading* 2014

[5] Bedon, C. *Buckling and Post?buckling analysis of a laminated glass column* Workshop on numerical modeling of glass components February 2014 Lausanne, Switzerland.

[6] CEN, 2005. *EN 1991-1-4 Eurocode 1: Actions on structures, Part 1-4: Wind Actions.* European Committee for Standardization, Brussels, Belgium.

[7] Chopra, A.K. *Dynamics of structures: theory and applications to earthquake engineering.* Prentice-Hall international series in civil engineering and engineering mechanics. Prentice-Hall, Inc., 1995. ISBN 0-13-855214-2.

[8] Cismasiu, C., Gamboa-Marrufo, M., Gonçalves, P. and Santos, F. *Smart glass facade subjected to wind loading* Institution of Civil Engineers, 2013.

[9] CNR*Istruzioni per la Progettazione, l?Esecuzione ed il Controllo di Costruzioni con Elementi Strutturali di Vetro* Consiglio Nazionale delle Ricerche, 2013.

[10] Dispersyn, J. and Santarsiero, M. *Exercise on numerical modelling of adhesive joints with cohesive elements* Workshop on numerical modeling of glass components February 2014 Lausanne, Switzerland.

[11] El-Shami, M. M., Norville, S. and Ibrahim, Y. E. *Stress analysis of laminated glass with different interlayer materials*, Alexandria Engineering Journal August 2012 Faculty of Engineering, Alexandria University

[12] Froli, M. and Lani, L. *Analisi strutturale di grandi lastre in vetro stratificato rinforzate con cavi in acciaio* Costruzioni Metalliche, 2007.

[13] Galuppi, L. and Royer-Carfagni, G. *The Effective Thickness of Laminated Glass Plates* Department of Civil-Environmental Engineering and Architecture University of Parma, Italy, November 2011.

[14] Gonçalves, P. *Fachada de Vidro Inteligente* MSc thesis, Faculdade de Ciências e Tecnologia da Universidade Nova de Lisboa, December 2012.

[15] Haldimann, M., Luible, A. and Overend, M. *Structural Use of Glass* International Association for Bridge and Structural Engineering, 2008. ISBN 978-3-85748-119-2.

[16] Holmes, J.D. *Wind Loading of Structures* Spon Press, 2001.

[17] Hooper,J.A. *On the bending of architectural laminated glass*, International Journal of Mechanical Sciences (Great Britain) 15 (1973) 309?333.

[18] Jagota, A., Bennison, S.J., Smith, C.A., Foss, R.V. and Van Duser, A. Mechanical Deformation and Fracture of Glass/PVB Laminates Glass Processing Days, 1999, ISBN 952-91-0885-0.

[19] Linden,M.P., Minor,J.E., Behr,R.A. and Vallabhan,C.V.G. *Evaluation of Laterally Loaded Glass Units by Theory and Experiment*, Glass Research and Testing Laboratory, Texas Tech University, Lubbock, Texas, 1983 (NTIS Accession No. PB84-216423).

[20] Linden,M.P., Minor,J.E., Behr,R.A. and Vallabhan,C.V.G *Evaluation of Laterally Loaded Glass Unites by Theory and Experiment, Supplemental Report No. 1.* Glass Research and Testing Laboratory, Texas Tech University, Lubbock, Texas, 1984 (NTIS Accession No. PB85-111532).

[21] Moutinho, C. *Controlo de vibrações em estruturas de engenharia civil.* Ph.D. thesis, Faculdade de Engenharia da Universidade do Porto, Agosto 2007.

[22] Norville,H.S. *Breakage Tests of Du Pont Laminated Glass Units*, Glass Research and Testing Laboratory, Texas Tech University, Lubbock, Texas, 1990.

[23] Ogata, K. *Modern Control Engineering.* Prentice-Hall, $3^{rd}$ edition, 1997. ISBN 0-13-261389-1.

[24] Otani, S., Hiraishi, H. and Midorikawa, M. *Development of smart systems for building structures* Proceedings of SPIE 2000;3988:2-9.

[25] Pereira, S. *Estudo do comportamento estrutural de fachadas em vidro* MSc. thesis, Faculdade de Ciências e Tecnologia da Universidade Nova de Lisboa, March 2012.

[26] Quenett, R. *The Mechanical Behavior of Laminated Safety Glass under Bending and*

*Impact Stresses*, Forgetragen auf dem DVM-Tag, Wurzburg (Germany), Manuskript-Eing., 1967.

[27] Reznik,P.L. and Minor, J.E. *Failure Strengths of Laminated Glass Units*, Glass Research and Testing Laboratory, Texas Tech University, Lubbock, Texas, 1986 (NTIS Accession No. PB87-118873/AS).

[28] Santos, F.A. *Vibration control with shape-memory alloys in civil engineering structures.*Ph.D. thesis, Faculdade de Ciências e Tecnologia da Universidade Nova de Lisboa, March 2011.

[29] Serafim, P. *Controlo de vibrações em Engenharia Civil* MSc. thesis, Faculdade de Ciências e Tecnologia da Universidade Nova de Lisboa, September 2011

[30] Song, G., Ma, N. and Li, H.-N. *Applications of shape-memory alloys in civil structures.* Engineering Structures 28 (2006) 1266-1274.

[31] Vallabhan, C.V.G.,. Das, Y.C, Magdi, M., Asik, M., and Bailey, J.R. *Analysis of laminated glass units*, Journal of Structural Engineering, ASCE 119 (5) (1993) 1572?1585.

[32] Wurm, J. *Glass Structures- Design and construction of self-supporting skins.* Birkhäuser Verlag AG, 2007. ISBN 978-3-7643-7608-6

# Appendix A

## A.1 Comparison between system0A and system2A

To conclude the study of the cables' configuration an analysis between the system0 and system2 was made. The results obtained are expressed on the following diagrams.

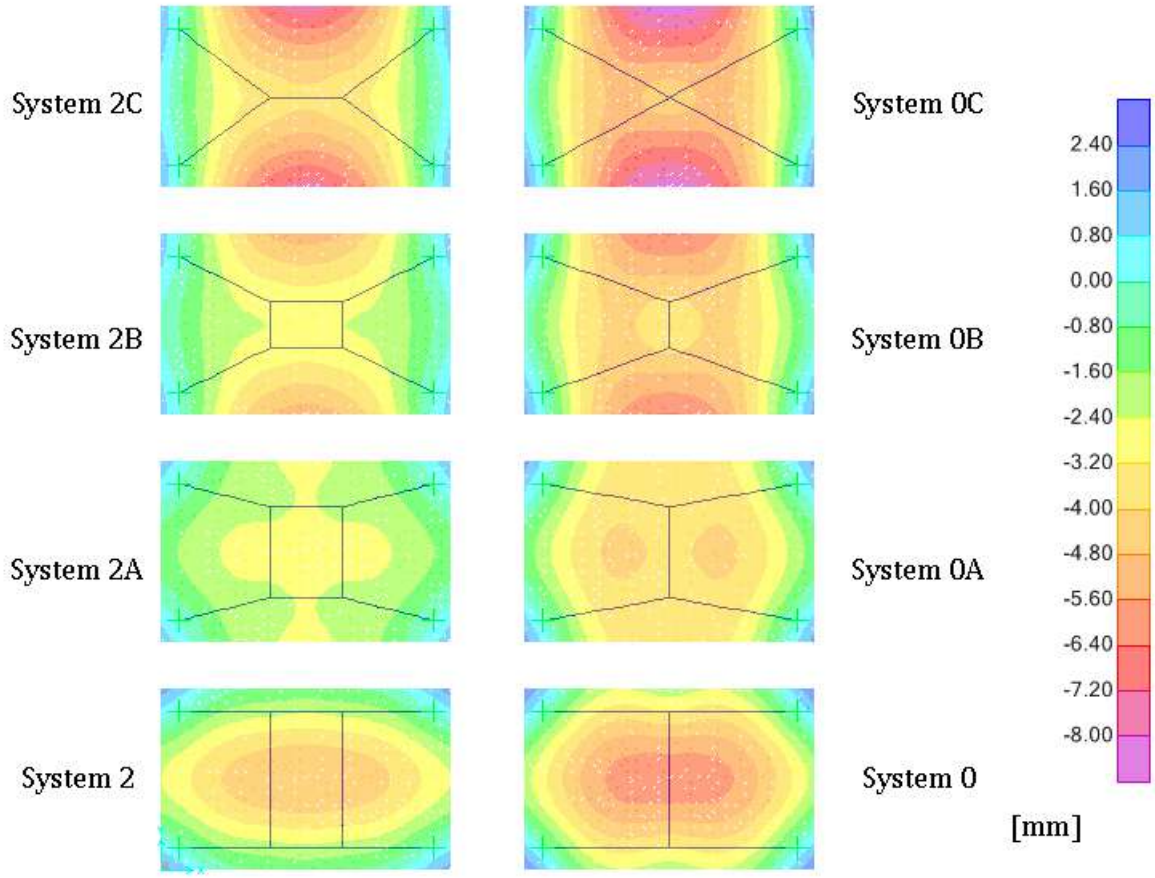


Figure A.1: Displacements on the systems 0 and 2

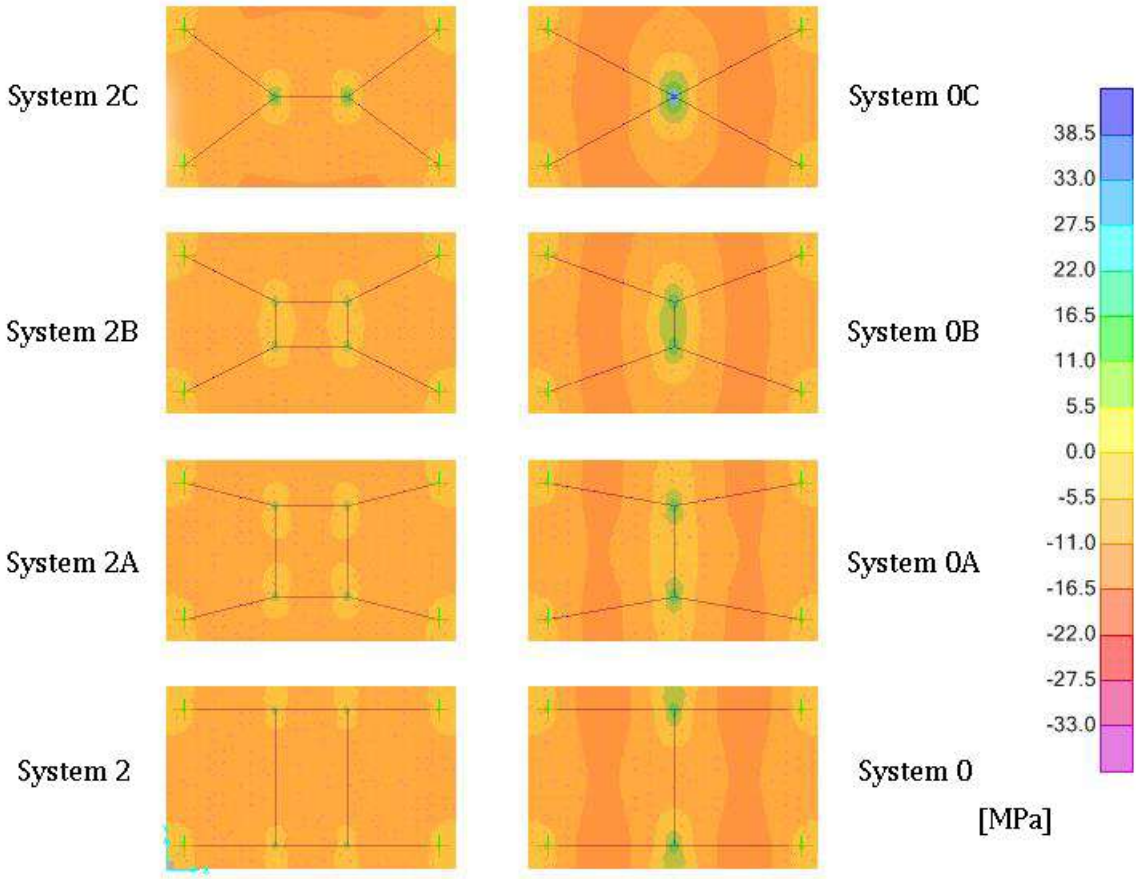


Figure A.2: $\sigma_{11}$ on the systems 0 and 2

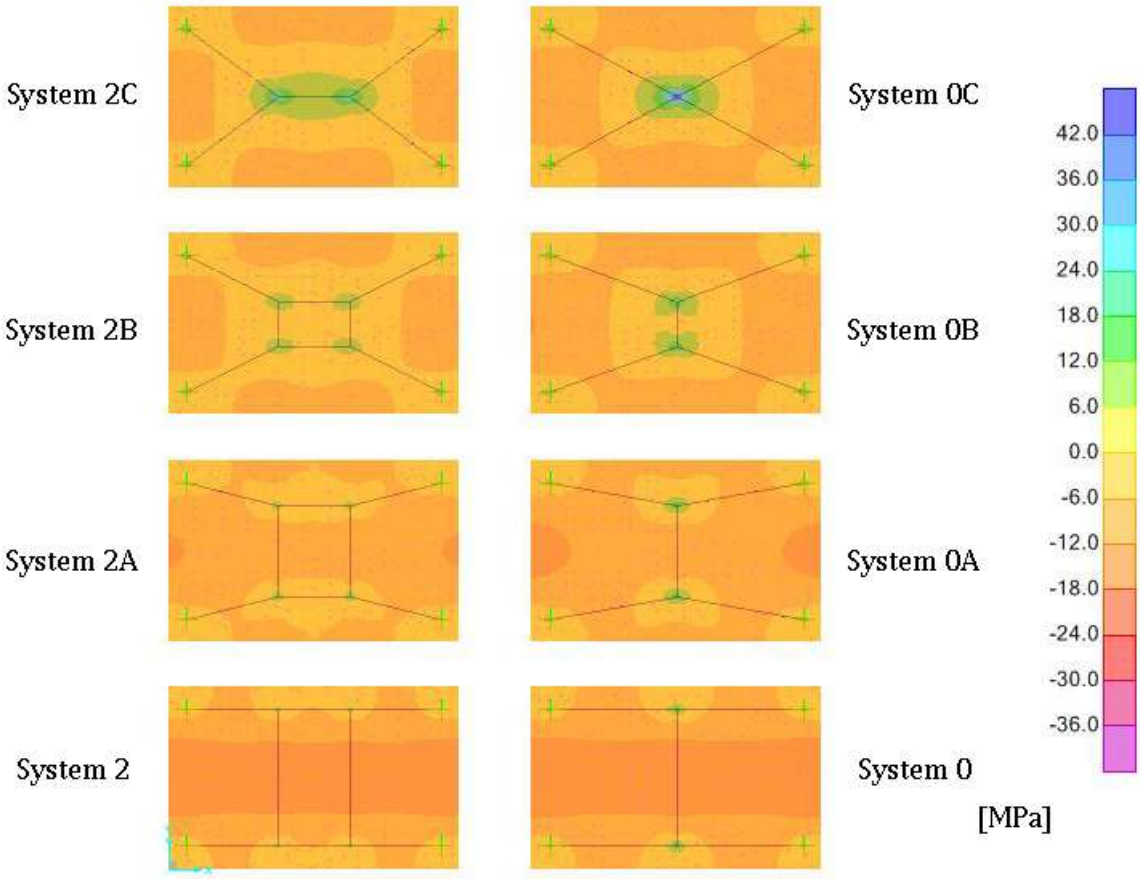


Figure A.3: $\sigma_{22}$ on the systems 0 and 2

# Appendix B

$$
F = \begin{bmatrix}
8.34 & 5.04 & 1.41 & 1.48 & 1.61 & 1.60 & -0.99 & -0.24 & -0.04 & -4.32 & -4.37 & -3.76 & -2.48 & -2.07 & -5.99 & -5.69 & -4.72 & -3.36 & -2.88 \\
5.04 & 5.36 & 3.23 & 1.87 & 1.57 & -0.27 & 0.32 & 0.01 & -0.07 & -5.25 & -4.49 & -2.98 & -2.20 & -2.04 & -6.72 & -5.84 & -4.11 & -3.04 & -2.78 \\
1.41 & 3.23 & 6.77 & 3.29 & 1.97 & -1.54 & 2.49 & 0.61 & -0.05 & -4.56 & -3.36 & -1.66 & -2.04 & -2.36 & -5.58 & -4.51 & -2.97 & -2.96 & -3.15 \\
1.48 & 1.87 & 3.29 & 5.52 & 5.23 & -0.31 & 0.69 & 1.03 & 1.34 & -2.43 & -2.26 & -2.29 & -2.69 & -2.74 & -3.24 & -3.12 & -3.32 & -3.82 & -4.01 \\
1.61 & 1.57 & 1.97 & 5.23 & 9.32 & 0.08 & -0.10 & 1.13 & 2.98 & -1.84 & -2.01 & -2.56 & -2.65 & -2.44 & -2.61 & -2.79 & -3.45 & -3.86 & -3.95 \\
1.60 & -0.27 & -1.54 & -0.31 & 0.08 & 2.26 & -1.19 & -0.24 & 0.00 & 1.68 & 0.55 & -0.77 & -0.37 & -0.15 & 1.50 & 0.67 & -0.58 & -0.44 & -0.25 \\
-0.99 & 0.32 & 2.49 & 0.69 & -0.10 & -1.19 & 2.33 & 0.58 & 0.08 & -1.00 & -0.02 & 1.53 & 0.84 & 0.41 & -0.85 & -0.03 & 1.21 & 0.94 & 0.62 \\
-0.24 & 0.01 & 0.61 & 1.03 & 1.13 & -0.24 & 0.58 & 0.98 & 1.07 & -0.23 & 0.01 & 0.55 & 0.92 & 1.02 & -0.22 & 0.01 & 0.54 & 0.90 & 1.00 \\
-0.04 & -0.07 & -0.05 & 1.34 & 2.98 & 0.00 & 0.08 & 1.07 & 3.06 & -0.03 & 0.00 & 0.27 & 1.30 & 2.06 & -0.07 & -0.01 & 0.39 & 1.33 & 1.71 \\
-4.32 & -5.25 & -4.56 & -2.43 & -1.84 & 1.68 & -1.00 & -0.23 & -0.03 & 11.01 & 7.76 & 3.27 & 2.18 & 2.05 & 13.89 & 10.66 & 5.00 & 3.06 & 2.79 \\
-4.37 & -4.49 & -3.36 & -2.26 & -2.01 & 0.55 & -0.02 & 0.01 & 0.00 & 7.76 & 6.76 & 4.09 & 2.70 & 2.39 & 10.54 & 9.09 & 5.75 & 3.74 & 3.28 \\
-3.76 & -2.98 & -1.66 & -2.29 & -2.56 & -0.77 & 1.53 & 0.55 & 0.27 & 3.27 & 4.09 & 5.79 & 4.45 & 3.83 & 4.98 & 5.75 & 7.13 & 6.01 & 5.30 \\
-2.48 & -2.20 & -2.04 & -2.69 & -2.65 & -0.37 & 0.84 & 0.92 & 1.30 & 2.18 & 2.70 & 4.45 & 6.34 & 6.51 & 3.15 & 3.75 & 5.91 & 8.15 & 8.63 \\
-2.07 & -2.04 & -2.36 & -2.74 & -2.44 & -0.15 & 0.41 & 1.02 & 2.06 & 2.05 & 2.39 & 3.83 & 6.51 & 8.51 & 2.86 & 3.28 & 5.22 & 8.68 & 10.38 \\
-5.99 & -6.72 & -5.58 & -3.24 & -2.61 & 1.50 & -0.85 & -0.22 & -0.07 & 13.89 & 10.54 & 4.98 & 3.15 & 2.86 & 21.39 & 15.72 & 7.30 & 4.40 & 3.93 \\
-5.69 & -5.84 & -4.51 & -3.12 & -2.79 & 0.67 & -0.03 & 0.01 & -0.01 & 10.66 & 9.09 & 5.75 & 3.75 & 3.28 & 15.72 & 13.81 & 8.17 & 5.17 & 4.53 \\
-4.72 & -4.11 & -2.97 & -3.32 & -3.45 & -0.58 & 1.21 & 0.54 & 0.39 & 5.00 & 5.75 & 7.13 & 5.91 & 5.22 & 7.30 & 8.17 & 10.33 & 8.14 & 7.17 \\
-3.36 & -3.04 & -2.96 & -3.82 & -3.86 & -0.44 & 0.94 & 0.90 & 1.33 & 3.06 & 3.74 & 6.01 & 8.15 & 8.68 & 4.40 & 5.17 & 8.14 & 11.91 & 12.07 \\
-2.88 & -2.78 & -3.15 & -4.01 & -3.95 & -0.25 & 0.62 & 1.00 & 1.71 & 2.79 & 3.28 & 5.30 & 8.63 & 10.38 & 3.93 & 4.53 & 7.17 & 12.07 & 15.63
\end{bmatrix}
$$

Flexibility matrix $[m/kN](\times 10^{-3})$

$$
M = \begin{bmatrix}
0.583 & 0 & 0 & 0 & 0 & 0 & 0 & 0 & 0 & 0 & 0 & 0 & 0 & 0 & 0 & 0 & 0 & 0 & 0 & 0 & 0 \\
0 & 2.04 & 0 & 0 & 0 & 0 & 0 & 0 & 0 & 0 & 0 & 0 & 0 & 0 & 0 & 0 & 0 & 0 & 0 & 0 & 0 \\
0 & 0 & 2.914 & 0 & 2.623 & 0 & 1.166 & 0 & 1.457 & 0 & 7.285 & 0 & 6.557 & 0 & 2.914 & 0 & 1.748 & 0 & 6.120 & 0 & 8.742 \\
0 & 0 & 0 & 2.914 & 0 & 2.623 & 0 & 1.166 & 0 & 1.457 & 0 & 7.285 & 0 & 6.557 & 0 & 2.914 & 0 & 1.748 & 0 & 6.120 & 0 \\
0 & 0 & 0 & 0 & 2.623 & 0 & 1.166 & 0 & 1.457 & 0 & 7.285 & 0 & 6.557 & 0 & 2.914 & 0 & 1.748 & 0 & 6.120 & 0 & 8.742 \\
0 & 0 & 0 & 0 & 0 & 2.623 & 0 & 1.166 & 0 & 1.457 & 0 & 7.285 & 0 & 6.557 & 0 & 2.914 & 0 & 1.748 & 0 & 6.120 & 0 \\
0 & 0 & 0 & 0 & 0 & 0 & 1.166 & 0 & 1.457 & 0 & 7.285 & 0 & 6.557 & 0 & 2.914 & 0 & 1.748 & 0 & 6.120 & 0 & 7.868 \\
0 & 0 & 0 & 0 & 0 & 0 & 0 & 1.166 & 0 & 1.457 & 0 & 7.285 & 0 & 6.557 & 0 & 2.914 & 0 & 1.748 & 0 & 6.120 & 0 \\
0 & 0 & 0 & 0 & 0 & 0 & 0 & 0 & 1.457 & 0 & 7.285 & 0 & 6.557 & 0 & 2.914 & 0 & 1.748 & 0 & 6.120 & 0 & 3.497 \\
0 & 0 & 0 & 0 & 0 & 0 & 0 & 0 & 0 & 1.457 & 0 & 7.285 & 0 & 6.557 & 0 & 2.914 & 0 & 1.748 & 0 & 6.120 & 0 \\
0 & 0 & 0 & 0 & 0 & 0 & 0 & 0 & 0 & 0 & 7.285 & 0 & 6.557 & 0 & 2.914 & 0 & 1.748 & 0 & 6.120 & 0 & 0.874 \\
0 & 0 & 0 & 0 & 0 & 0 & 0 & 0 & 0 & 0 & 0 & 7.285 & 0 & 6.557 & 0 & 2.914 & 0 & 1.748 & 0 & 6.120 & 0 \\
0 & 0 & 0 & 0 & 0 & 0 & 0 & 0 & 0 & 0 & 0 & 0 & 6.557 & 0 & 2.914 & 0 & 1.748 & 0 & 6.120 & 0 & 3.060 \\
0 & 0 & 0 & 0 & 0 & 0 & 0 & 0 & 0 & 0 & 0 & 0 & 0 & 6.557 & 0 & 2.914 & 0 & 1.748 & 0 & 6.120 & 0 \\
0 & 0 & 0 & 0 & 0 & 0 & 0 & 0 & 0 & 0 & 0 & 0 & 0 & 0 & 2.914 & 0 & 1.748 & 0 & 6.120 & 0 & 4.371 \\
0 & 0 & 0 & 0 & 0 & 0 & 0 & 0 & 0 & 0 & 0 & 0 & 0 & 0 & 0 & 2.914 & 0 & 1.748 & 0 & 6.120 & 0 \\
0 & 0 & 0 & 0 & 0 & 0 & 0 & 0 & 0 & 0 & 0 & 0 & 0 & 0 & 0 & 0 & 1.748 & 0 & 6.120 & 0 & 3.934 \\
0 & 0 & 0 & 0 & 0 & 0 & 0 & 0 & 0 & 0 & 0 & 0 & 0 & 0 & 0 & 0 & 0 & 1.748 & 0 & 6.120 & 0 \\
0 & 0 & 0 & 0 & 0 & 0 & 0 & 0 & 0 & 0 & 0 & 0 & 0 & 0 & 0 & 0 & 0 & 0 & 1.748 & 0 & 1.748
\end{bmatrix}
$$

Mass matrix $[kg]$

## Appendix B.

$$
D = \left[\begin{array}{cccccccccccccccccccc}
4.86 & 10.29 & 4.10 & 3.89 & 1.88 & 2.33 & -7.23 & -1.54 & -0.13 & -7.56 & -26.74 & -32.89 & -19.54 & -7.24 & -5.23 & -17.40 & -20.63 & -13.22 & -5.04 \\
2.94 & 10.94 & 9.42 & 4.92 & 1.83 & -0.39 & 2.36 & 0.08 & -0.22 & -9.18 & -27.51 & -26.02 & -17.33 & -7.13 & -5.87 & -17.87 & -17.95 & -11.97 & -4.87 \\
0.82 & 6.60 & 19.74 & 8.62 & 2.30 & -2.24 & 18.13 & 4.02 & -0.14 & -7.97 & -20.55 & -14.47 & -16.07 & -8.26 & -4.87 & -13.81 & -12.97 & -11.63 & -5.51 \\
0.87 & 3.82 & 9.58 & 14.47 & 6.10 & -0.45 & 5.04 & 6.75 & 3.89 & -4.25 & -13.84 & -20.01 & -21.16 & -9.60 & -2.83 & -9.56 & -14.51 & -15.02 & -7.01 \\
0.94 & 3.19 & 5.74 & 13.73 & 10.87 & 0.12 & -0.75 & 7.40 & 8.68 & -3.22 & -12.28 & -22.41 & -20.88 & -8.55 & -2.28 & -8.54 & -15.07 & -15.19 & -6.91 \\
0.93 & -0.55 & -4.48 & -0.80 & 0.10 & 3.29 & -8.70 & -1.58 & 0.00 & 2.94 & 3.35 & -6.72 & -2.91 & -0.52 & 1.32 & 2.05 & -2.53 & -1.74 & -0.44 \\
-0.58 & 0.66 & 7.25 & 1.81 & -0.12 & -1.74 & 16.95 & 3.82 & 0.24 & -1.75 & -0.12 & 13.35 & 6.64 & 1.43 & -0.74 & -0.08 & 5.29 & 3.68 & 1.08 \\
-0.14 & 0.02 & 1.78 & 2.70 & 1.32 & -0.35 & 4.24 & 6.44 & 3.13 & -0.40 & 0.03 & 4.82 & 7.27 & 3.57 & -0.19 & 0.03 & 2.36 & 3.55 & 1.75 \\
-0.03 & -0.15 & -0.14 & 3.50 & 3.47 & 0.00 & 0.59 & 7.04 & 8.91 & -0.06 & 0.01 & 2.36 & 10.20 & 7.20 & -0.06 & -0.03 & 1.71 & 5.22 & 2.99 \\
-2.52 & -10.71 & -13.29 & -6.37 & -2.15 & 2.45 & -7.31 & -1.50 & -0.10 & 19.26 & 47.48 & 28.62 & 17.13 & 7.18 & 12.14 & 32.62 & 21.87 & 12.03 & 4.89 \\
-2.55 & -9.17 & -9.78 & -5.93 & -2.34 & 0.80 & -0.14 & 0.03 & 0.01 & 13.57 & 41.36 & 35.79 & 21.27 & 8.35 & 9.22 & 27.81 & 25.14 & 14.70 & 5.74 \\
-2.19 & -6.07 & -4.82 & -6.00 & -2.99 & -1.12 & 11.12 & 3.62 & 0.79 & 5.72 & 25.05 & 50.58 & 35.01 & 13.38 & 4.35 & 17.61 & 31.15 & 23.65 & 9.26 \\
-1.45 & -4.49 & -5.95 & -7.05 & -3.09 & -0.54 & 6.15 & 6.06 & 3.78 & 3.81 & 16.55 & 38.90 & 49.90 & 22.76 & 2.76 & 11.48 & 25.85 & 32.05 & 15.09 \\
-1.21 & -4.16 & -6.89 & -7.20 & -2.85 & -0.22 & 2.98 & 6.69 & 6.00 & 3.59 & 14.60 & 33.44 & 51.21 & 29.75 & 2.50 & 10.04 & 22.83 & 34.17 & 18.15 \\
-3.49 & -13.70 & -16.25 & -8.49 & -3.04 & 2.19 & -6.20 & -1.44 & -0.21 & 24.28 & 64.53 & 43.53 & 24.81 & 10.01 & 18.70 & 48.11 & 31.89 & 17.30 & 6.87 \\
-3.31 & -11.91 & -13.16 & -8.19 & -3.25 & 0.98 & -0.19 & 0.07 & -0.03 & 18.64 & 55.62 & 50.31 & 29.52 & 11.47 & 13.74 & 42.26 & 35.69 & 20.33 & 7.91 \\
-2.75 & -8.38 & -8.64 & -8.71 & -4.02 & -0.84 & 8.82 & 3.55 & 1.14 & 8.75 & 35.20 & 62.30 & 46.54 & 18.26 & 6.38 & 24.99 & 45.14 & 32.03 & 12.54 \\
-1.96 & -6.21 & -8.61 & -10.01 & -4.50 & -0.64 & 6.81 & 5.92 & 3.87 & 5.35 & 22.86 & 52.55 & 64.10 & 30.37 & 3.84 & 15.81 & 35.59 & 46.85 & 21.10 \\
-1.68 & -5.68 & -9.18 & -10.51 & -4.61 & -0.36 & 4.49 & 6.56 & 4.98 & 4.89 & 20.10 & 46.32 & 67.91 & 36.30 & 3.43 & 13.85 & 31.34 & 47.49 & 27.34
\end{array}\right]
$$

Dynamic matrix ($\times 10^{-6}$)

# Appendix C

## C.1 Proportional control

Considering only proportional control, the proportional gain that corresponds to the optimal control solution is 115. The system response to the proportional control is represented in figure C.1.

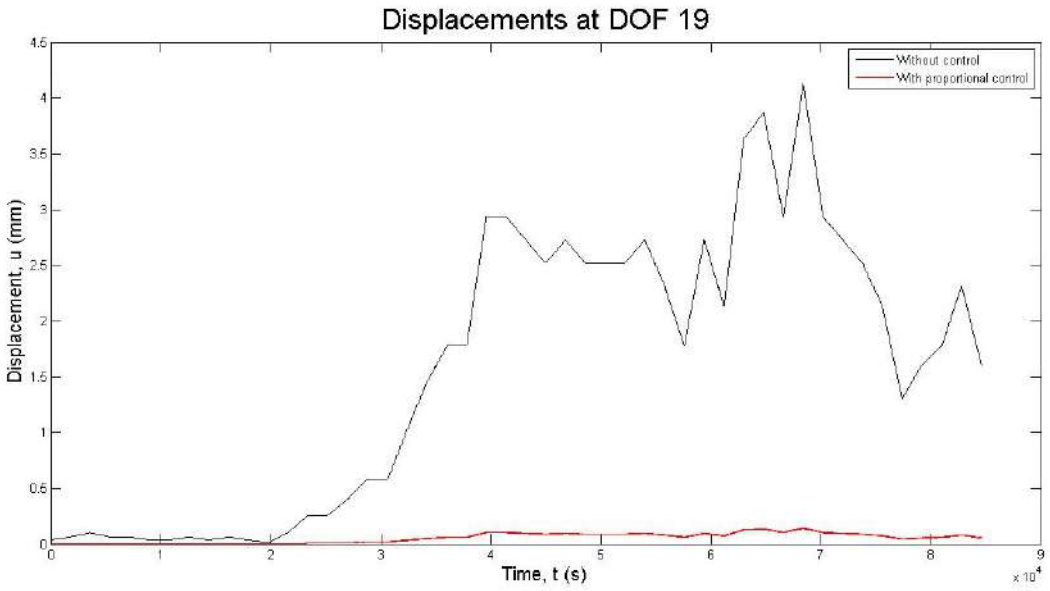


Figure C.1: Graphic of the displacements on the center of the glass pane, action of proportional control

## C.2 Proportional and integrative control

Combining both proportional and integrative control the system's response is improved. The gains considered were $K_p = 100$ and $K_i = 19$. The response obtained is represented in figure C.2.

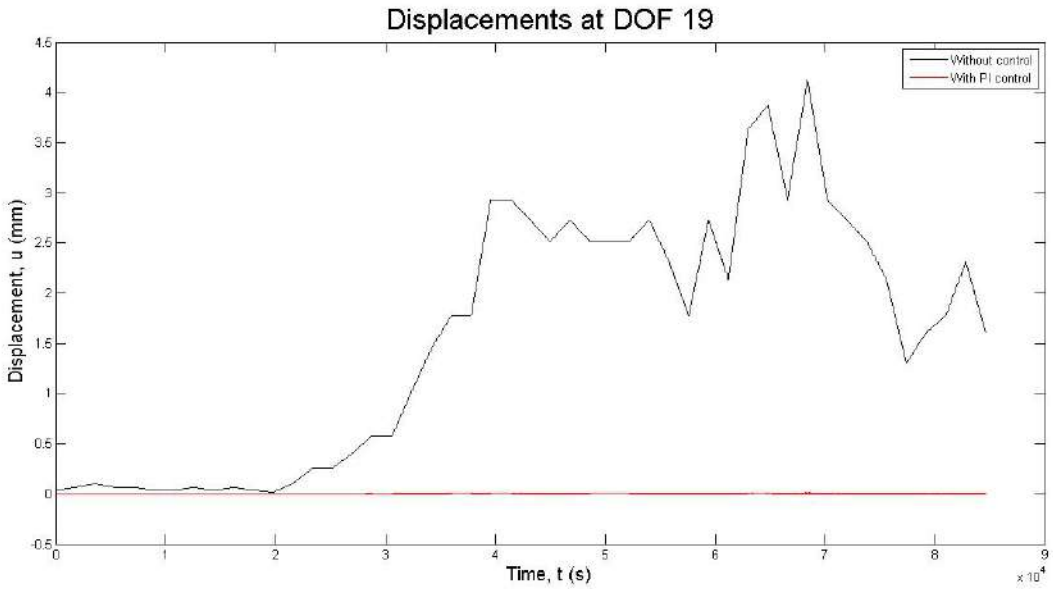


Figure C.2: Graphic of the displacements on the center of the glass pane, action of proportional and integral control

## C.3 Proportional, integrative and derivative control

Imposing the derivative parcel in the system, the gains were adjusted to $K_p = 100$, $K_i = 19$ and $K_d = 10$ and the obtained response can be interpreted with the graphic of the figure C.3.

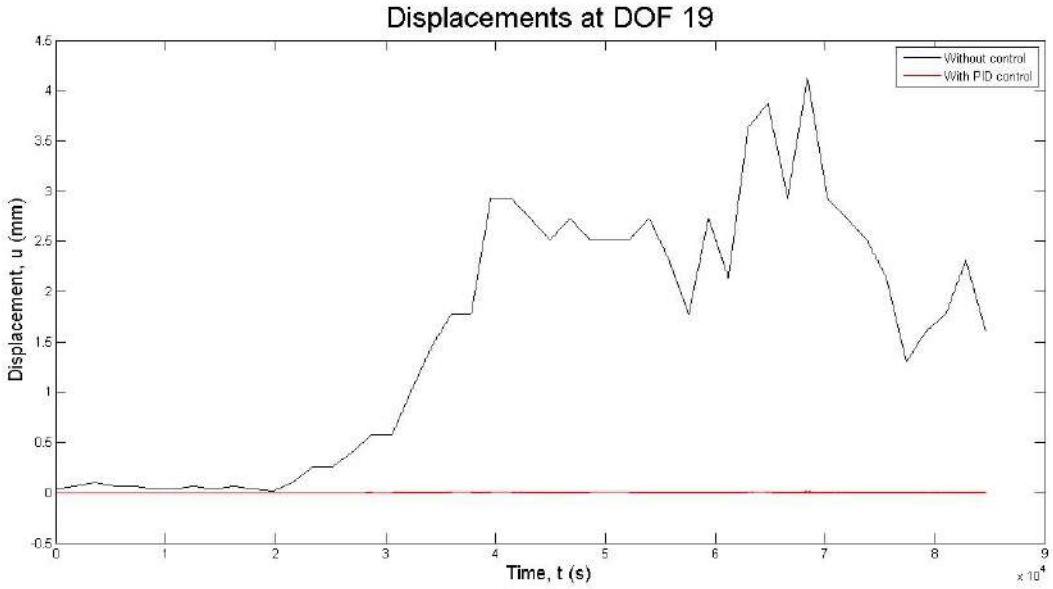


Figure C.3: Graphic of the displacements on the center of the glass pane, action of proportional, integral and derivative control

From the graphics obtained, it is easily observed the benefits of the control system. The displacements obtained in the central point decreased from 4mm at its highest value, to approximately zero.